



Impact and Penetration of Thin Aluminum 2024 Flat Panels at Oblique Angles of Incidence

*Charles R. Ruggeri, Duane M. Revilock, and J. Michael Pereira
Glenn Research Center, Cleveland, Ohio*

*William Emmerling
FAA William J. Hughes Technical Center, Atlantic City International Airport, New Jersey*

*Gilbert K. Queitzsch, Jr.
Federal Aviation Administration, Washington, DC*

NASA STI Program . . . in Profile

Since its founding, NASA has been dedicated to the advancement of aeronautics and space science. The NASA Scientific and Technical Information (STI) Program plays a key part in helping NASA maintain this important role.

The NASA STI Program operates under the auspices of the Agency Chief Information Officer. It collects, organizes, provides for archiving, and disseminates NASA's STI. The NASA STI Program provides access to the NASA Technical Report Server—Registered (NTRS Reg) and NASA Technical Report Server—Public (NTRS) thus providing one of the largest collections of aeronautical and space science STI in the world. Results are published in both non-NASA channels and by NASA in the NASA STI Report Series, which includes the following report types:

- **TECHNICAL PUBLICATION.** Reports of completed research or a major significant phase of research that present the results of NASA programs and include extensive data or theoretical analysis. Includes compilations of significant scientific and technical data and information deemed to be of continuing reference value. NASA counter-part of peer-reviewed formal professional papers, but has less stringent limitations on manuscript length and extent of graphic presentations.
- **TECHNICAL MEMORANDUM.** Scientific and technical findings that are preliminary or of specialized interest, e.g., “quick-release” reports, working papers, and bibliographies that contain minimal annotation. Does not contain extensive analysis.
- **CONTRACTOR REPORT.** Scientific and technical findings by NASA-sponsored contractors and grantees.
- **CONFERENCE PUBLICATION.** Collected papers from scientific and technical conferences, symposia, seminars, or other meetings sponsored or co-sponsored by NASA.
- **SPECIAL PUBLICATION.** Scientific, technical, or historical information from NASA programs, projects, and missions, often concerned with subjects having substantial public interest.
- **TECHNICAL TRANSLATION.** English-language translations of foreign scientific and technical material pertinent to NASA's mission.

For more information about the NASA STI program, see the following:

- Access the NASA STI program home page at <http://www.sti.nasa.gov>
- E-mail your question to help@sti.nasa.gov
- Fax your question to the NASA STI Information Desk at 757-864-6500
- Telephone the NASA STI Information Desk at 757-864-9658
- Write to:
NASA STI Program
Mail Stop 148
NASA Langley Research Center
Hampton, VA 23681-2199



Impact and Penetration of Thin Aluminum 2024 Flat Panels at Oblique Angles of Incidence

*Charles R. Ruggeri, Duane M. Revilock, and J. Michael Pereira
Glenn Research Center, Cleveland, Ohio*

*William Emmerling
FAA William J. Hughes Technical Center, Atlantic City International Airport, New Jersey*

*Gilbert K. Queitzsch, Jr.
Federal Aviation Administration, Washington, DC*

National Aeronautics and
Space Administration

Glenn Research Center
Cleveland, Ohio 44135

Trade names and trademarks are used in this report for identification only. Their usage does not constitute an official endorsement, either expressed or implied, by the National Aeronautics and Space Administration.

Level of Review: This material has been technically reviewed by technical management.

Available from

NASA STI Program
Mail Stop 148
NASA Langley Research Center
Hampton, VA 23681-2199

National Technical Information Service
5285 Port Royal Road
Springfield, VA 22161
703-605-6000

This report is available in electronic form at <http://www.sti.nasa.gov/> and <http://ntrs.nasa.gov/>

Impact and Penetration of Thin Aluminum 2024 Flat Panels at Oblique Angles of Incidence

Charles R. Ruggeri, Duane M. Revilock, and J. Michael Pereira
National Aeronautics and Space Administration
Glenn Research Center
Cleveland, Ohio 44135

William Emmerling
FAA William J. Hughes Technical Center
Atlantic City International Airport, New Jersey 08405

Gilbert K. Queitzsch, Jr.
Federal Aviation Administration
950 L'Enfant Plaza North, S.W.
Washington, DC 20024

Introduction

The U.S. Federal Aviation Administration (FAA) and the National Aeronautics and Space Administration (NASA) are actively involved in improving the predictive capabilities of transient finite element computational methods for application to safety issues involving unintended impacts on aircraft and aircraft engine structures. One aspect of this work involves the development of an improved deformation and failure model for metallic materials, known as the Tabulated Johnson-Cook model, or MAT224, which has been implemented in the LS-DYNA commercial transient finite element analysis code (LSTC Corp., Livermore, CA) (Ref. 1). In this model the yield stress is a function of strain, strain rate and temperature and the plastic failure strain is a function of the state of stress, temperature and strain rate. The failure criterion is based on the accumulation of plastic strain in an element. The model also incorporates a regularization scheme to account for the dependency of plastic failure strain on mesh size.

For a given material the model requires a significant amount of testing to determine the yield stress and failure strain as a function of the three-dimensional state of stress, strain rate and temperature. In addition, experiments are required to validate the model. Currently the model has been developed for Aluminum 2024 and validated against a series of ballistic impact tests on flat plates of various thicknesses (Refs. 1 to 3). Full development of the model for Titanium 6Al-4V is being completed, and mechanical testing for Inconel 718 has begun.

The validation testing for the models involves ballistic impact tests using cylindrical projectiles impacting flat plates at a normal incidence (Ref. 2). By varying the thickness of the plates, different stress states and resulting failure modes are induced, providing a range of conditions over which the model can be validated. The objective of the study reported here was to provide experimental data to evaluate the model under more extreme conditions, using a projectile with a more complex shape and sharp contacts, impacting flat panels at oblique angles of incidence.

Methods

Ballistic impact tests were conducted on flat AL2024-T3 sheet using a rectangular parallelepiped shaped projectile with sharp corners and edges. The roll angle (relative to the direction of the gun barrel) of the projectile and the pitch angle of the sheet were varied to produce different types of contacts between the projectile and the plate. For the purpose of defining the orientation of the projectile and the

test panel a laboratory coordinate system was established with the x direction parallel to the centerline of the gun barrel used to accelerate the projectiles. The z direction was vertically down and the y direction was to the right when facing the test panel from the direction of projectile travel.

Projectile

The projectile used for this study was a 55.88 mm (2.2 in.) long, by 31.75 mm (1.25 in.) high by 20.83 mm (0.82 in.) wide rectangular block of Inconel 718, heat treated to a hardness of 44 Rockwell C (Figs. 1 and 2). Three rectangular channels were machined through the center of the projectile in the length direction, as shown in Figures 1 and 2, to reduce the overall mass. The mass of the projectile ranged from 220.45 to 222.45 gm, with an average mass of 221.52 gm. It was accelerated toward the test panel with its long dimension parallel to the axis of flight. To define its orientation, a projectile coordinate system was established with the x direction along the length of the projectile, the y direction along the width and the z direction along the height, as shown in Figure 1. In the base orientation (zero roll, pitch and yaw angles) the projectile coordinate system was parallel to the laboratory coordinate system.

Gas Gun

The projectiles were accelerated with a helium filled gas gun connected to a vacuum chamber, shown in Figure 3. The gun barrel had a length of 3.7 m (12 ft) and a bore of 50.8 mm (2.0 in.). The pressure vessel was made up of sections as shown in Figure 4, with a total volume of 11.2 L (681 in.³). The projectile was carried down the gun barrel in a cylindrical polycarbonate sabot shown in Figure 5. The gun barrel protruded into the vacuum chamber which held the fixture for the specimens. The sabot was stopped at the end of the gun barrel by a stopper plate with a through-hole large enough to allow the projectile to pass through. This stopper system was designed such that the bottom of the sabot, which incorporated o-rings, remained in the gun barrel and formed a seal which prevented the gas pressure behind the sabot from affecting the pressure in the vacuum chamber.

Test Panels

The impact test panels were 30.48 cm (12 in.) wide by 53.34 cm (21 in.) long by 3.20 mm (0.126 in.) thick AL-2024-T3. This material is the identical material that was used to develop and validate the deformation and failure model for AL-2024 (Refs. 1 to 3). The panels were supported in a fixture that had accommodation for rotating about a horizontal axis to produce different angles of obliquity with the projectile (Figs. 6 and 7). The panels were sandwiched between 12.7 mm (0.5 in.) thick front and back frames with an aperture of 22.86 cm (9 in.) wide by 45.72 cm (18 in.) tall. The front frame had outer dimensions the same as the test panel. The panels were attached by twenty-eight through bolts connecting the front frame, panel and back frame. A drawing of the front frame is shown in Figure 8. In the base configuration the test panel was perpendicular to the direction of projectile flight, with the long dimension vertical and the center of the panel coincident with the gun barrel centerline.

Instrumentation

The projectile velocity and orientation were measured prior to impact using pair of high speed digital video cameras (Phantom V7.3, Vision Research Inc.) and a photogrammetry system (PONTOS, GOM mbH) that tracked the three-dimensional coordinates of a number of circular markers painted on the projectile. The positions of the markers were used to define the orientation of the projectile local coordinate system relative to a laboratory coordinate system. The velocity of the projectile after impact, if penetration occurred, was measured using a similar system mounted behind the panel. The framing rate for both the front and rear camera pair was 12,500 frames/sec.

Full field deformation measurements were made on the back side of the panel using a pair of high speed digital video cameras (Photron SA1-1, Photron USA, Inc.) and a digital image correlation system (ARAMIS, GOM mbH). These cameras viewed the full back side of the panel, including a portion of the support beams, using a frame rate of 27,000 frames/sec with a horizontal resolution of 384 pixels and a vertical resolution of 496 pixels.

Test Parameters

In this test program the parameters that were varied were the roll angle of the projectile, the tilt angle of the test panel, the projectile impact velocity and the impact location on the panel. The desired roll angles of the projectile were 0°, 30°, 60° or 90° measured about the projectile local coordinate system x-axis. The test panel was either in the vertical position (normal impact orientation, 90° angle of incidence), tilted 30° toward the gun (60° angle of incidence) or 45° toward the gun. Adjustment for the panel tilt is shown in Figure 6. The test velocities were selected so that for each configuration there was at least one test in which the projectile completely penetrated the panel and one that did not. A total of 34 impact tests were conducted. In most cases the impact location was in the center of the top half of the test panel (along the centerline of the width, 3/4 of the distance from the bottom of the test panel to the top). Four of the tests were conducted with the target point at the center of the panel.

Results

For the purposes of this report, the term “penetration” refers to the situation in which the projectile travels fully through the panel and exits the other side. The term non-penetration refers to situations in which the projectile either ricochets away from the panel with no fracture, fractures the panel without fully exiting the back side, or gets lodged in the panel. Table 1 lists the desired test parameters for each of the tests, as well as the actual measured values of projectile velocity and orientation. In the table the panel tilt angle is the angle from the vertical, with the top of the panel tilting toward the gun barrel about the laboratory Y axis. This corresponds to a negative rotation about the laboratory Y axis. The intended pitch and yaw angles of the projectile were zero. The penetration results for tests in which the projectile impacted the center of the upper half of the panel (tests DB196 to DB225) are shown in Figure 9. The solid lines on the graph indicate the lowest velocity at which penetration occurred and the highest velocity at which no penetration occurred for each combination of panel tilt angle and projectile roll angle. As would be expected, there is a large difference in the penetration velocity between the various combinations. The normal impact case has the highest penetration velocity and the 30° panel tilt combinations show the lowest penetration velocity, with the 45° panel tilt combinations intermediate between the two.

Photographs of the front and back side of the impacted panel from each test are shown in Appendix A, as well as results from digital image correlation (DIC) analysis for tests in which a solution was possible. Of the 34 tests, DIC results are not available for five of the tests, DB196, DB198, DB200, DB214, and DB218. In some cases the painted spray pattern dislodged from the backside of the panel upon impact. In the case of DB196 there was a camera malfunction. The results show a representative deformation map for each test and the displacement profile along a line for several time steps up to the time of maximum deformation or when failure occurred. In some cases, a post test deformation map is shown that indicates the permanent plastic deformation in the panel and the time history of the displacement of an indicated point.

Summary

A test program was conducted to provide data on the deformation and failure of Al2024 panels when impacted by hardened Inconel 718 (Special Metals Corporation, New Hartford, NY) rectangular parallelepiped projectiles at oblique angles. These results provide validation data for the development of new transient dynamic models.

TABLE 1.—IMPACT TEST RESULTS

Test	Test ID	Desired Panel Tilt Angle (deg)	Desired Proj. Roll Angle (deg)	Desired Impact Velocity (ft/sec)	Proj. Mass (gm)	Measured Panel Tilt Angle (deg)	Measured Impact Velocity (ft/sec)	Measured Exit Velocity (ft/sec)	Measured proj. Roll Angle (deg)	Measured proj. Pitch Angle (deg)	Measured proj. Yaw Angle (deg)	Comments
1	DB196	0	0	210	221.58	0	209.5	N/A	1.815	0.11	0.941	No Penetration
2	DB197	0	0	210	221.35	0	211.5	N/A	2.891	-0.648	-0.428	No Penetration
3	DB198	0	0	270	221.35	0	270.9	N/A	-0.327	2.274	-2.08	No Penetration. Crack.
4	DB199	0	0	340	221.36	0	342	167	-0.008	-1.531	-2.832	Penetration
5	DB200	0	0	320	221.35	0	319	N/A	-2.9	1.695	1.046	Proj. lodged in panel
6	DB201	45	30	318	221.35	44.8	319.5	213.7	30.22	0.613	-1.378	Penetration
7	DB202	45	30	270	220.45	44.8	270.6	132.7	29.128	4.102	0.771	Penetration
8	DB203	45	30	210	220.5	44.8	228	68.9	30.263	4.21	-1.225	Penetration
9	DB204	45	30	150	221.42	44.8	159.9	N/A	33.061	0.987	0.742	No Penetration. Corner Petal.
10	DB205	45	0	270	220.52	44.8	274.8	86.7	2.048	3.134	-1.55	Penetration
11	DB206	45	90	270	221.36	44.8	277	N/A	90.761	-3.223	-1.275	No Penetration. Crack.
12	DB207	45	90	320	220.51	44.8	322.5	185	92.109	-3.386	-2.331	Penetration
13	DB208	45	60	270	222.27	44.8	270.4	151.6	55.945	2.451	-2.792	Penetration
14	DB209	45	60	210	221.62	44.8	200.6	N/A	64.846	-4.446	6.247	No Penetration. Hole.
15	DB210	45	60	325	221.38	44.8	317.4	216.4	60.854	-2.984	2.647	Penetration
16	DB211	45	60	175	221.39	44.8	161.7	N/A	60.241	3.378	-5.199	No Penetration
17	DB212	45	60	150	221.6	44.8	155	N/A	58.14	0.599	1.151	No Penetration
18	DB213	45	0	210	222.3	44.8	205.7	N/A	-0.026	-1.224	0.427	No Penetration. Flap.
19	DB214	45	0	325	222.24	44.8	318.7	Not Measured	Not Measured	Not Measured	Not Measured	Penetration
20	DB215	45	0	175	221.59	44.8	179.2	N/A	-4.491	-0.578	1.622	No Penetration
21	DB216	45	30	170	221.42	44.8	172.9	N/A	24.917	0.255	3.332	No Penetration. Corner Flap
22	DB217	30	0	270	222.26	30.6	269.6	169.9	1.781	1.034	3.889	Penetration
23	DB218	30	0	210	221.42	30.6	203.4	2.45	-1.014	-1.13	0.651	Penetration
24	DB219	30	0	150	221.6	30.6	146.4	N/A	-4.551	-1.243	1.995	No Penetration
25	DB220	30	60	270	221.6	30.6	268.3	191.45	61.315	-4.269	5.256	Penetration
26	DB221	30	60	210	221.87	30.6	200.3	77.9	59.494	-2.43	5.407	Penetration
27	DB222	30	60	150	222.45	30.6	145.9	N/A	61.502	-8.124	5.311	No Penetration. Perforation.
28	DB223	30	90	270	222.27	30.6	263.8	162.5	94.794	2.787	0.226	Penetration
29	DB224	30	90	210	221.6	30.6	208.4	Negligable.	88.614	2.582	1.904	Projectile Exited Vertically
30	DB225	30	90	150	221.68	30.6	143.2	N/A	87.945	0.143	-1.406	No Penetration
31	DB226	0	0	270	221.53	0.5	262.5	N/A	-3.009	2.019	1.197	No Penetration
32	DB227	0	0	325	221.53	0.5	310.2	20	Not Measured	Not Measured	Not Measured	Penetration. Large Flap
33	DB228	0	60	270	221.89	0.5	266.1	N/A	62.551	-1.066	2.585	No Penetration
34	DB229	0	60	325	221.63	0.5	312.1	134.4	67.622	-14.362	14.021	Penetration

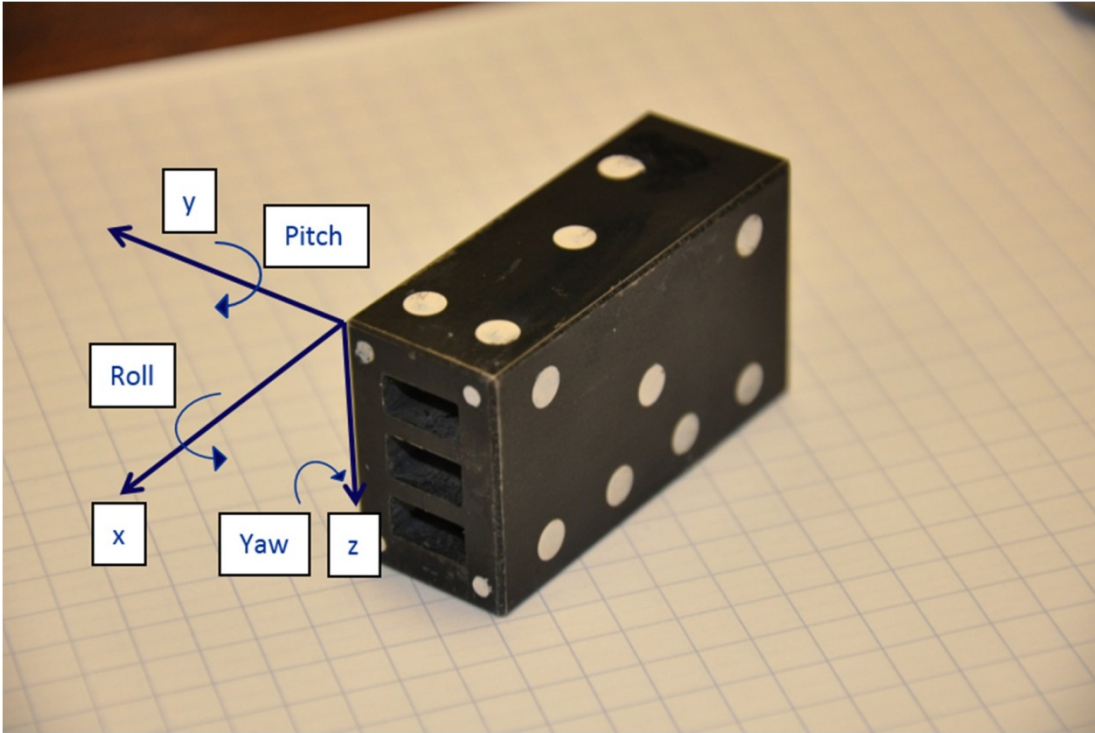


Figure 1.—Hardened Inconel 718 Projectile. Rectangular channels are machined through the length to limit the overall mass. Projectile coordinate system shown. Orientation angles are defined in the local coordinate system by successive rotations of roll, pitch and yaw.

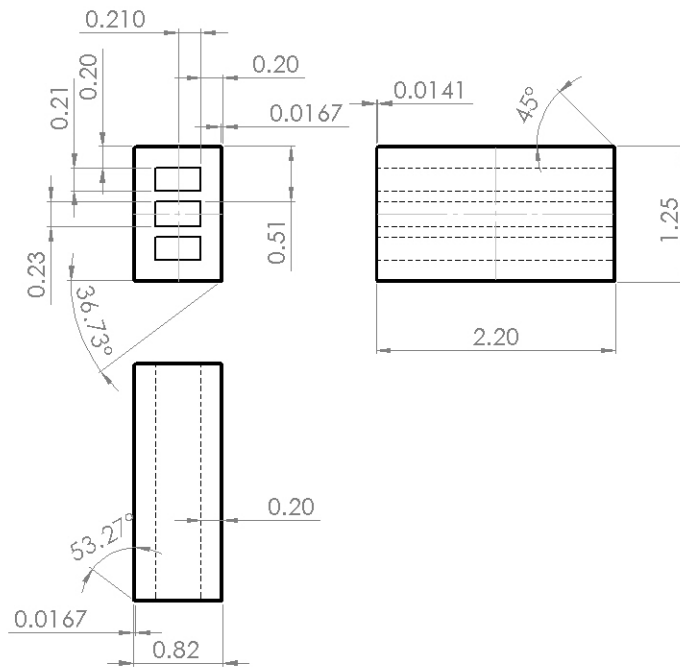


Figure 2.—Projectile drawing. Dimensions in inches.



Figure 3.—Gas gun connected to the vacuum chamber.

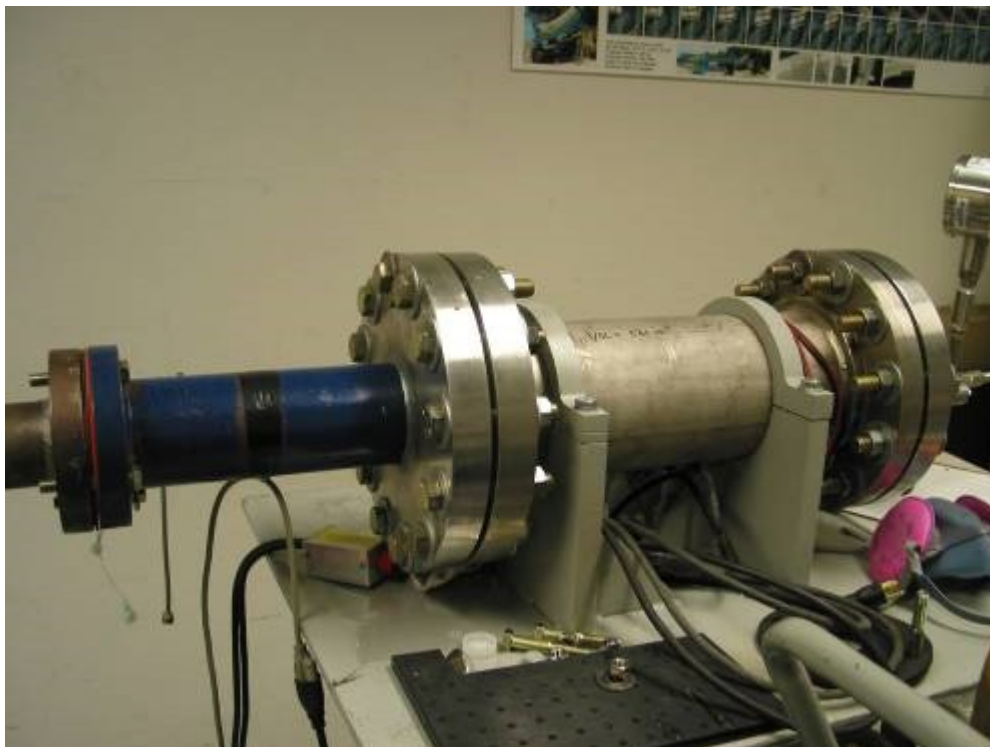


Figure 4.—Pressure vessel.



Figure 5.—Projectile in polycarbonate sabot.

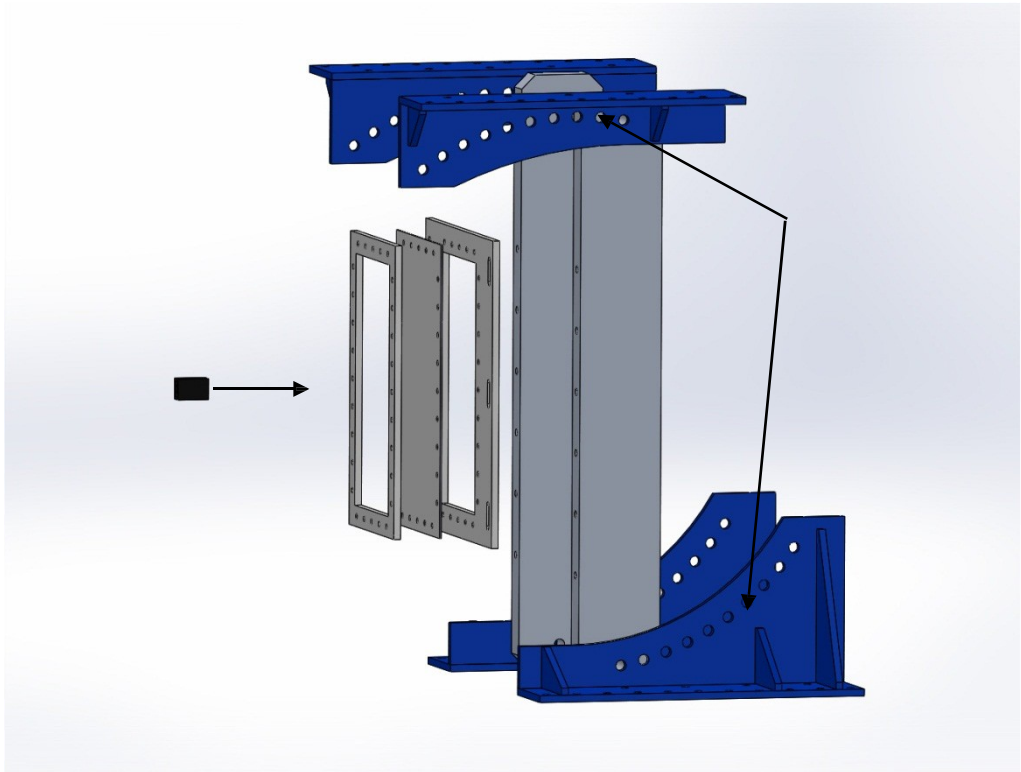


Figure 6.—Exploded view of test fixture in zero tilt position showing projectile, front plate, test panel, back plate and rotatable fixture supports.

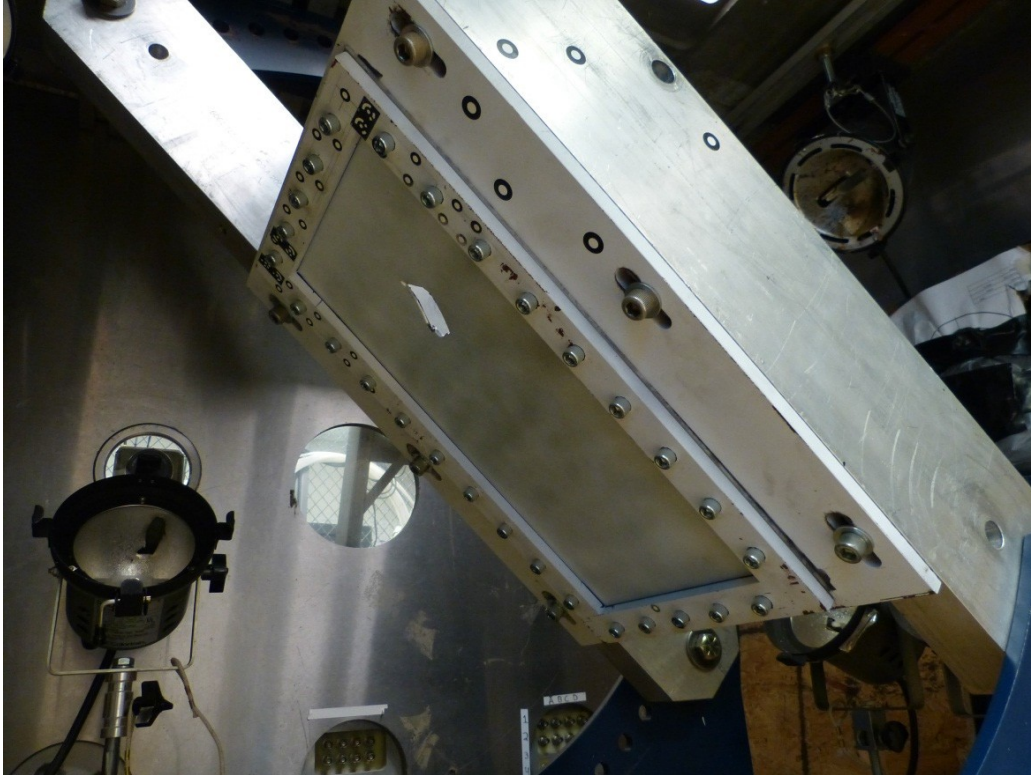


Figure 7.—Panel in fixture rotated to 45°.

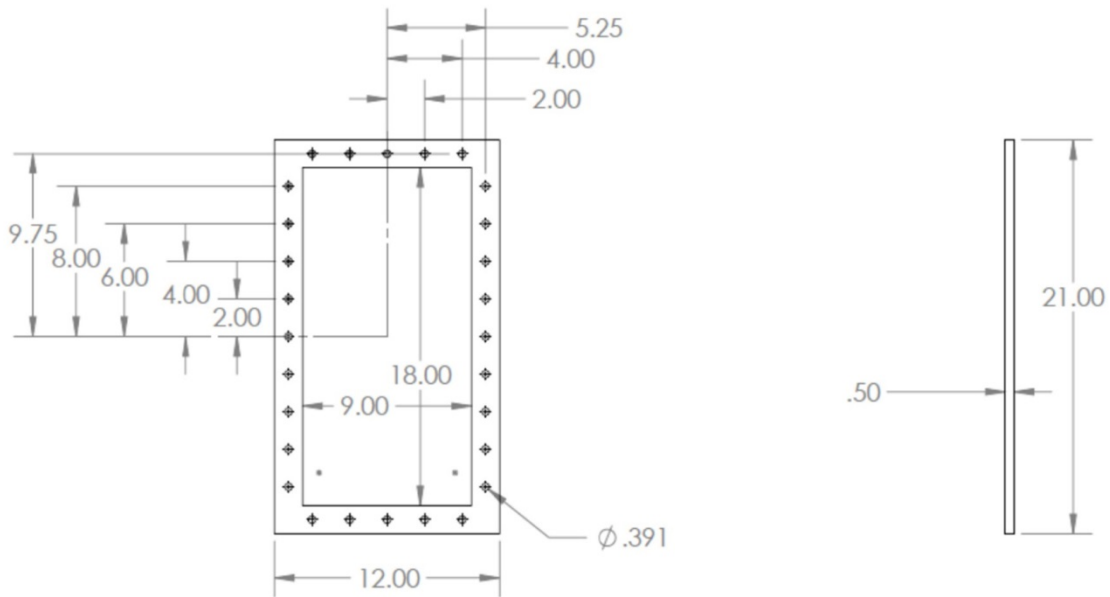


Figure 8.—Drawing of front plate. Dimensions in inches.

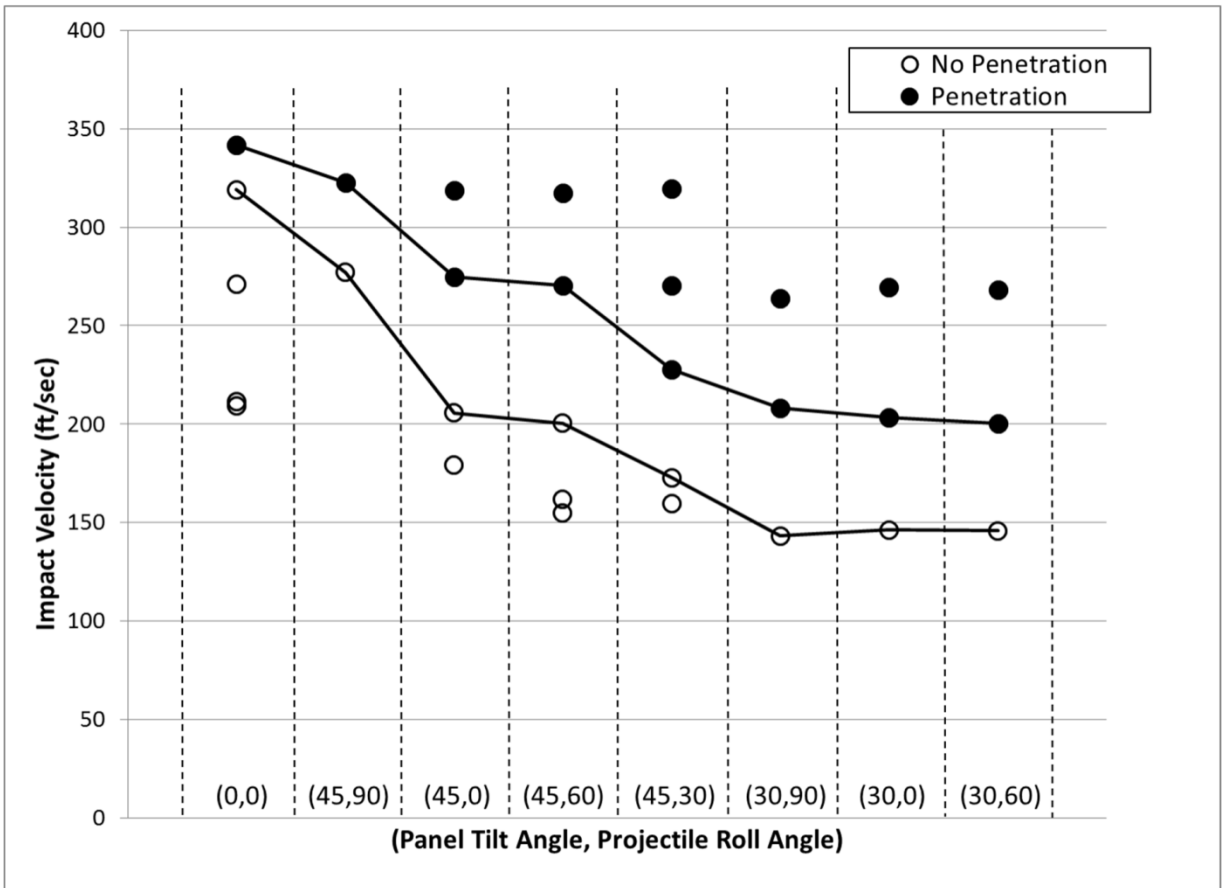


Figure 9.—Penetration Results for tests DB196-DB225, where the projectile impacted the upper half of the panel.

Appendix A.—Impact Test Results

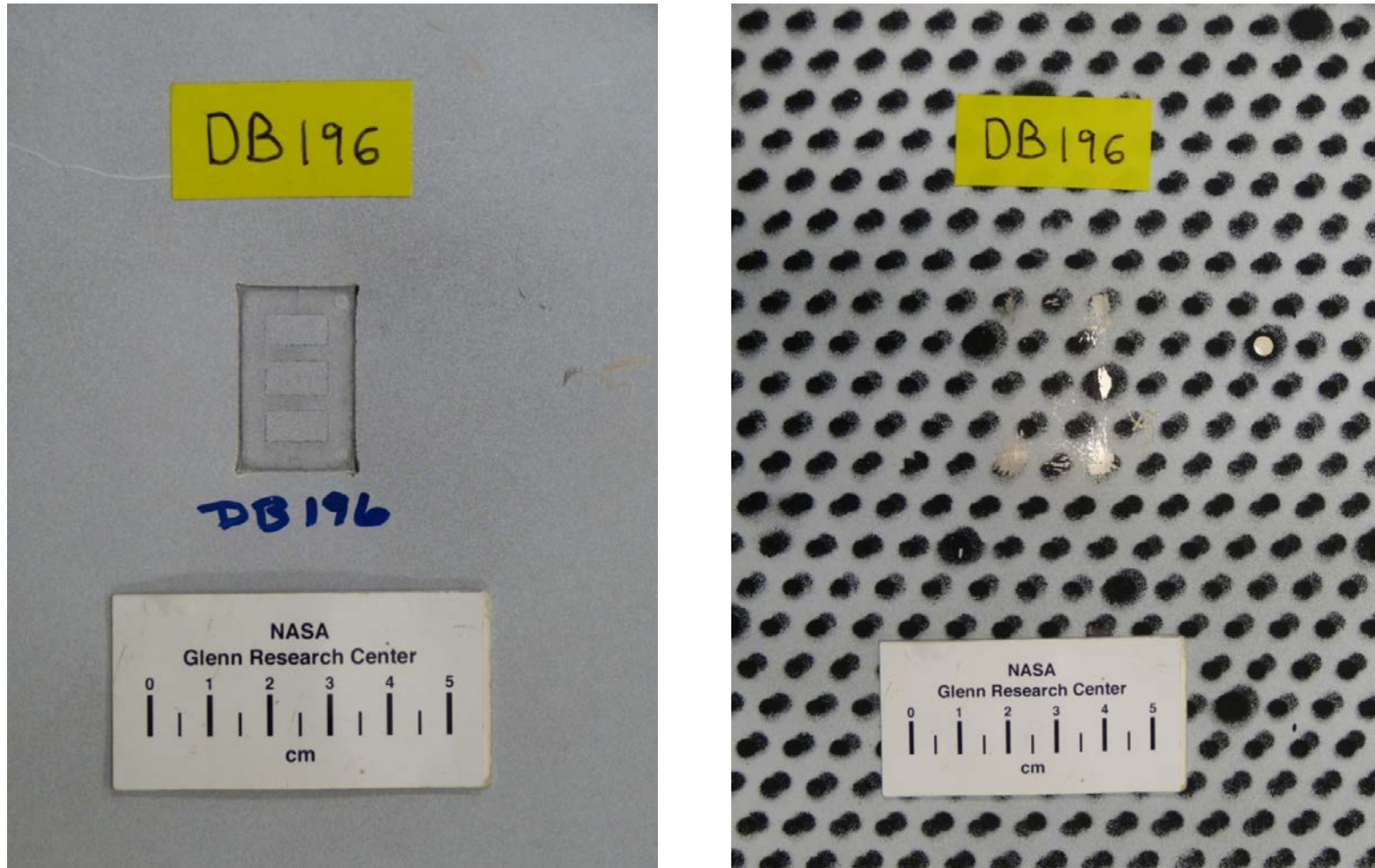


Figure A1.—Front (left) and back side views of impacted panel in test DB196.

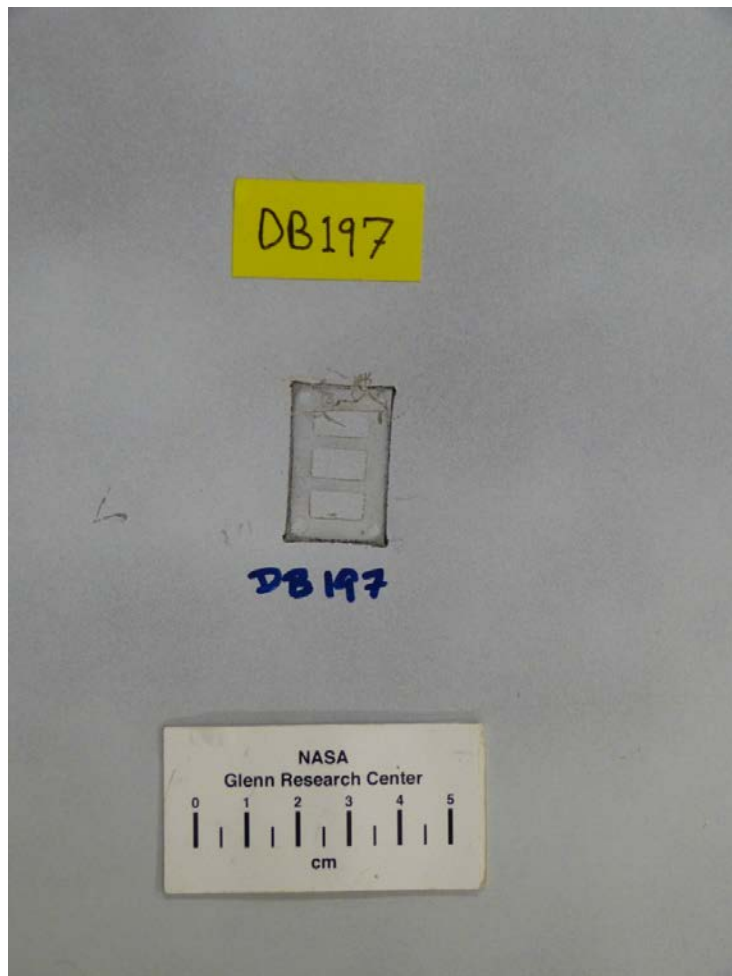


Figure A2.—Front (left) and back side views of impacted panel in test DB197.

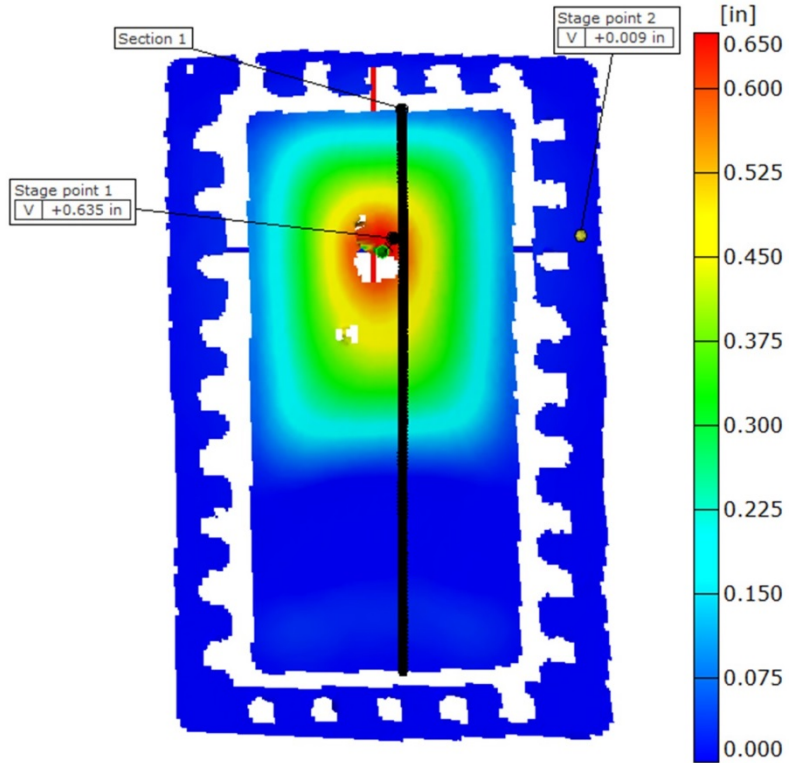


Figure A3.—Out-of-plane deformation map of panel in test DB197. Map of fixture deformation is also shown. No penetration occurred but loss of paint made some areas unsolvable.

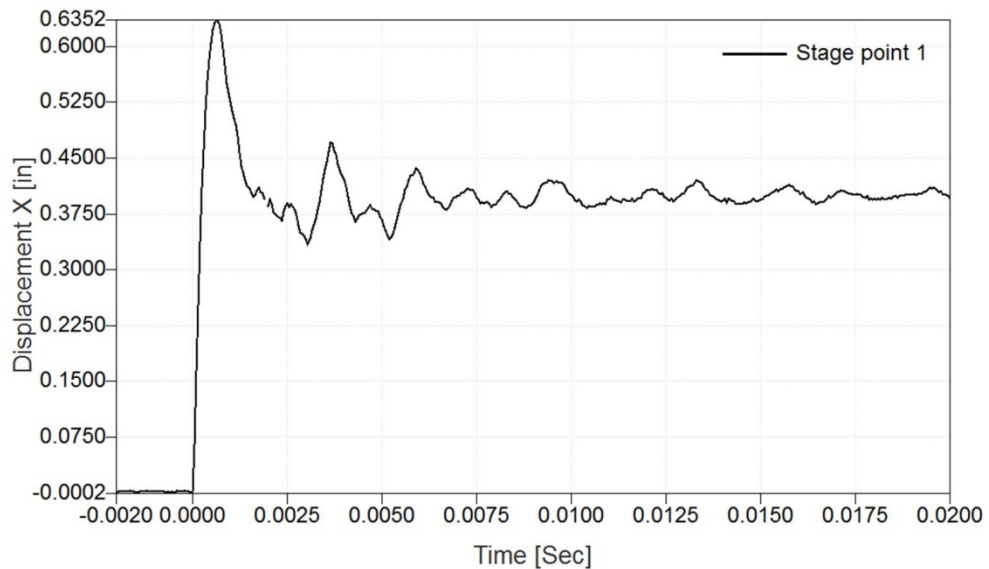


Figure A4.—Out-of-plane deformation as a function of time of point indicated in Figure A2 for test DB197.

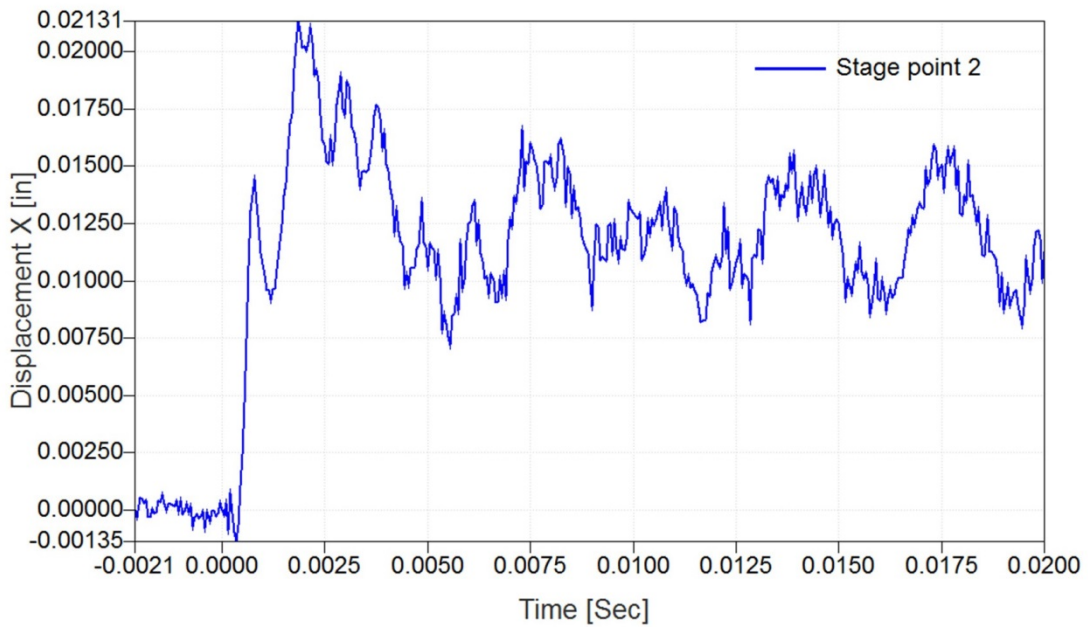


Figure A5.—Out-of-plane deformation as a function of time of point on test frame indicated in Figure A2 for test DB197.

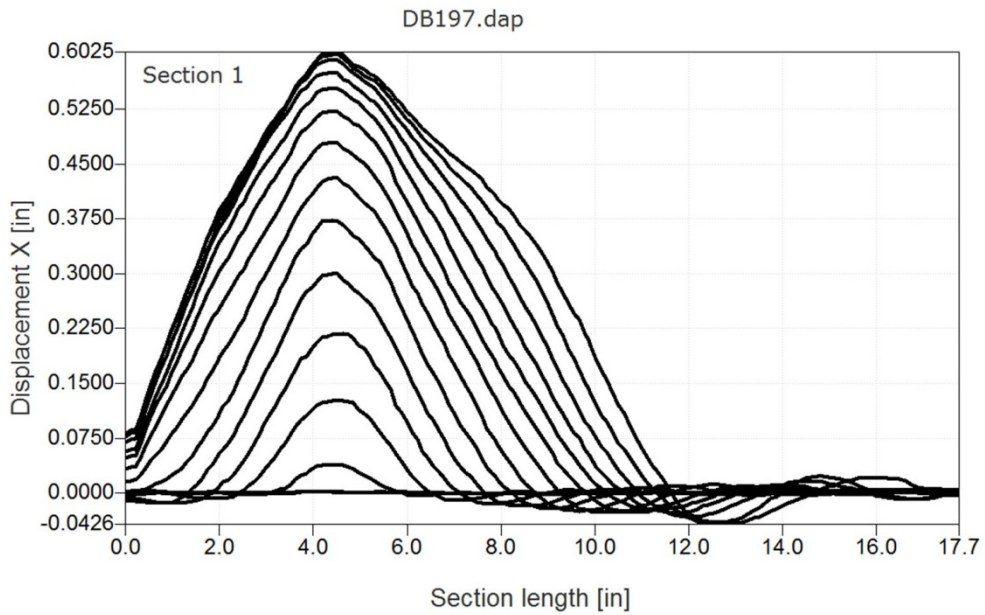


Figure A6.—Out-of-plane deformation along section line indicated in Figure A2 for a series of time steps up until the time of maximum deformation (frame rate 20000 frames/sec).



Figure A7.—Front (left) and back side views of impacted panel in test DB198.



Figure A8.—Front (left) and back side views of impacted panel in test DB199.

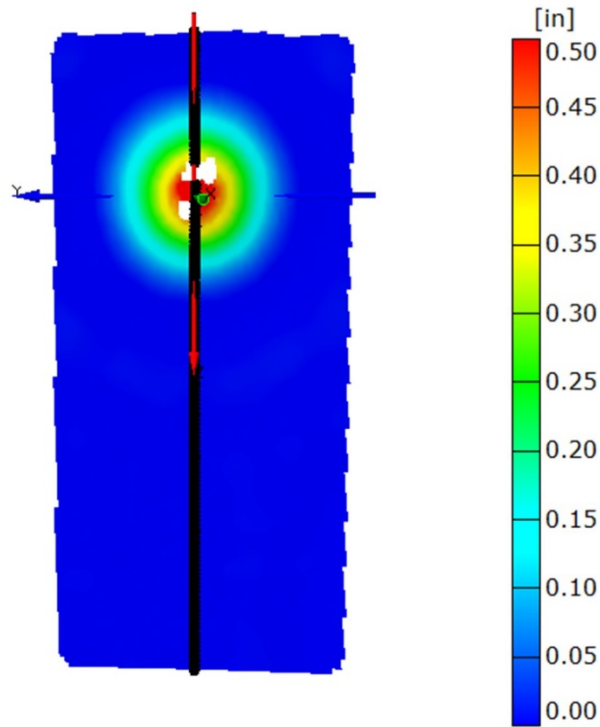


Figure A9.—Out-of-plane deformation map of panel in test DB199 just prior to initial failure.

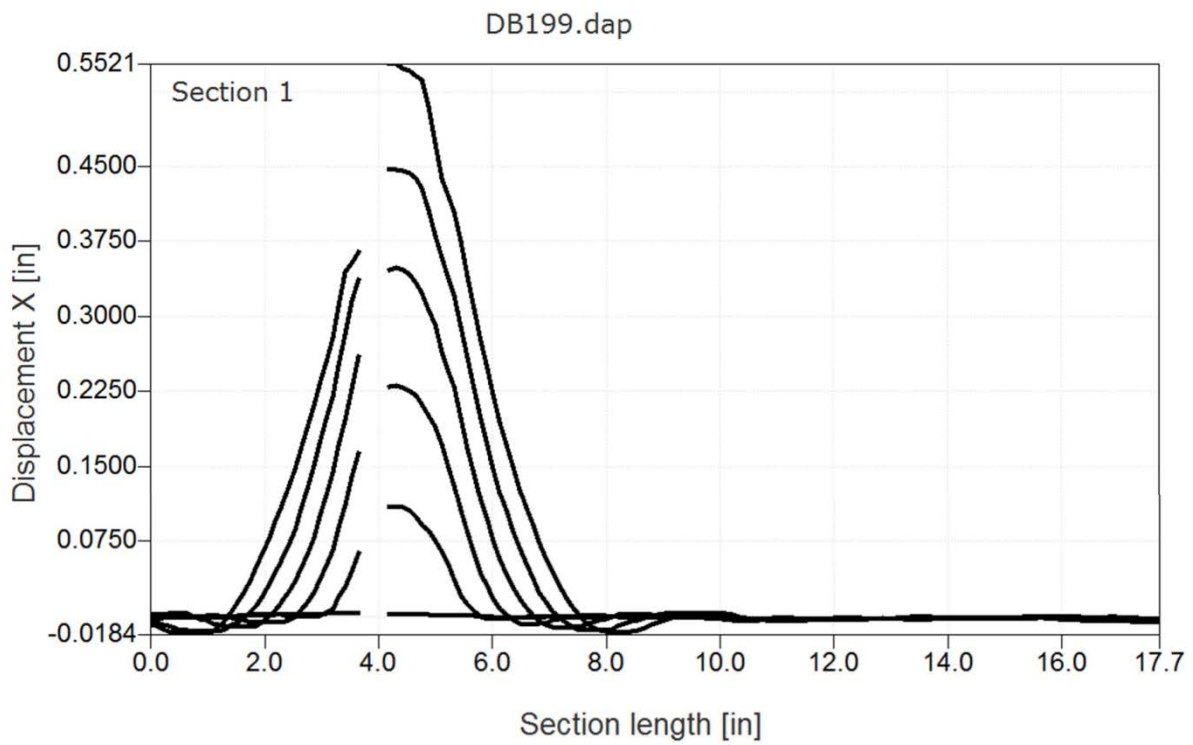


Figure A10.—Out-of-plane deformation along section line indicated in Figure A6 for a series of time steps up until the time of initial failure (frame rate 30000 frames/sec). Discontinuous line due to paint loss.



Figure A11.—Front (left) and back side views of impacted panel in test DB200.

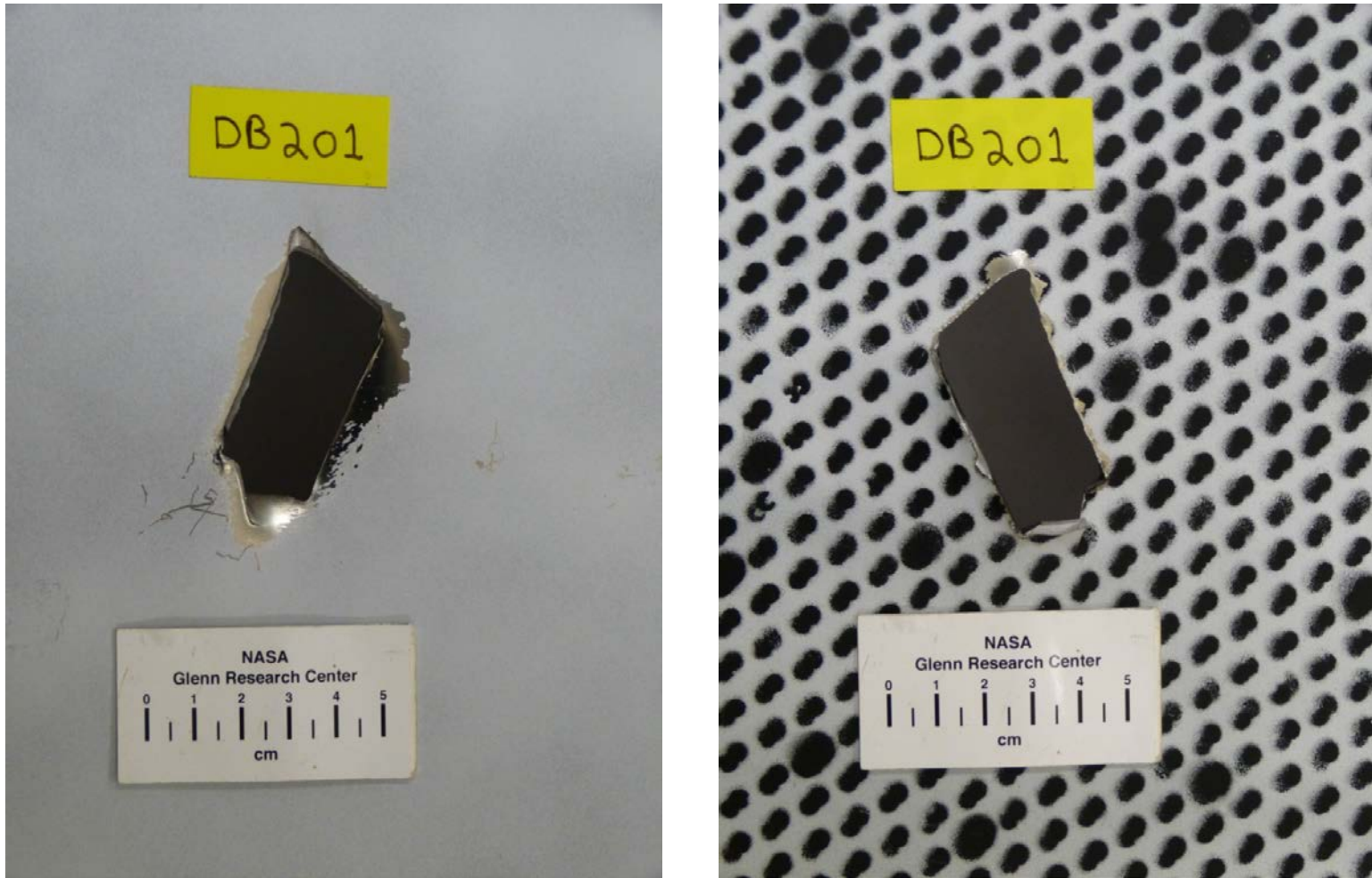


Figure A12.—Front (left) and back side views of impacted panel in test DB201.

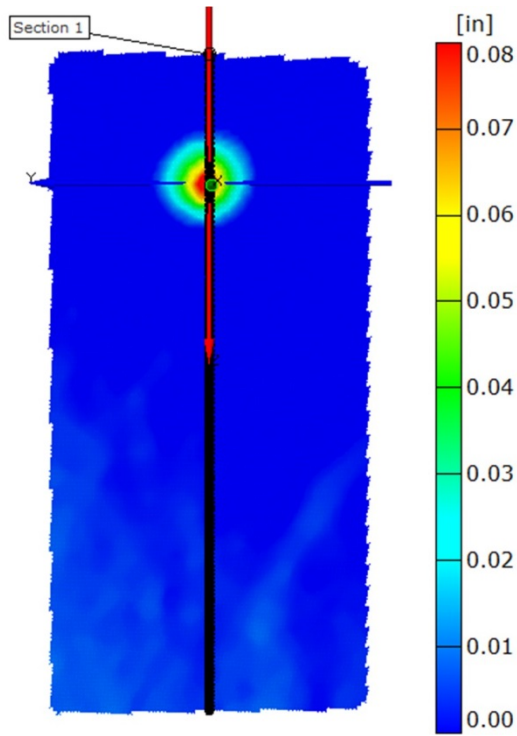


Figure A13.—Out-of-plane deformation map of panel in test DB201 just prior to initial failure.

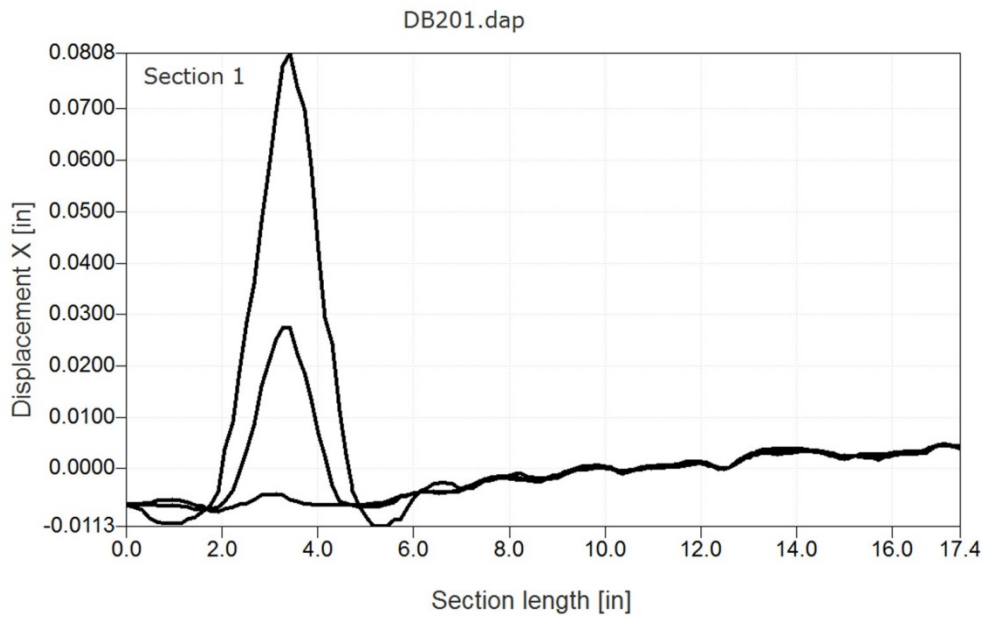


Figure A14.—Out-of-plane deformation along section line indicated in Figure A10 for a series of time steps up until the time of initial failure (frame rate 27000 frames/sec).

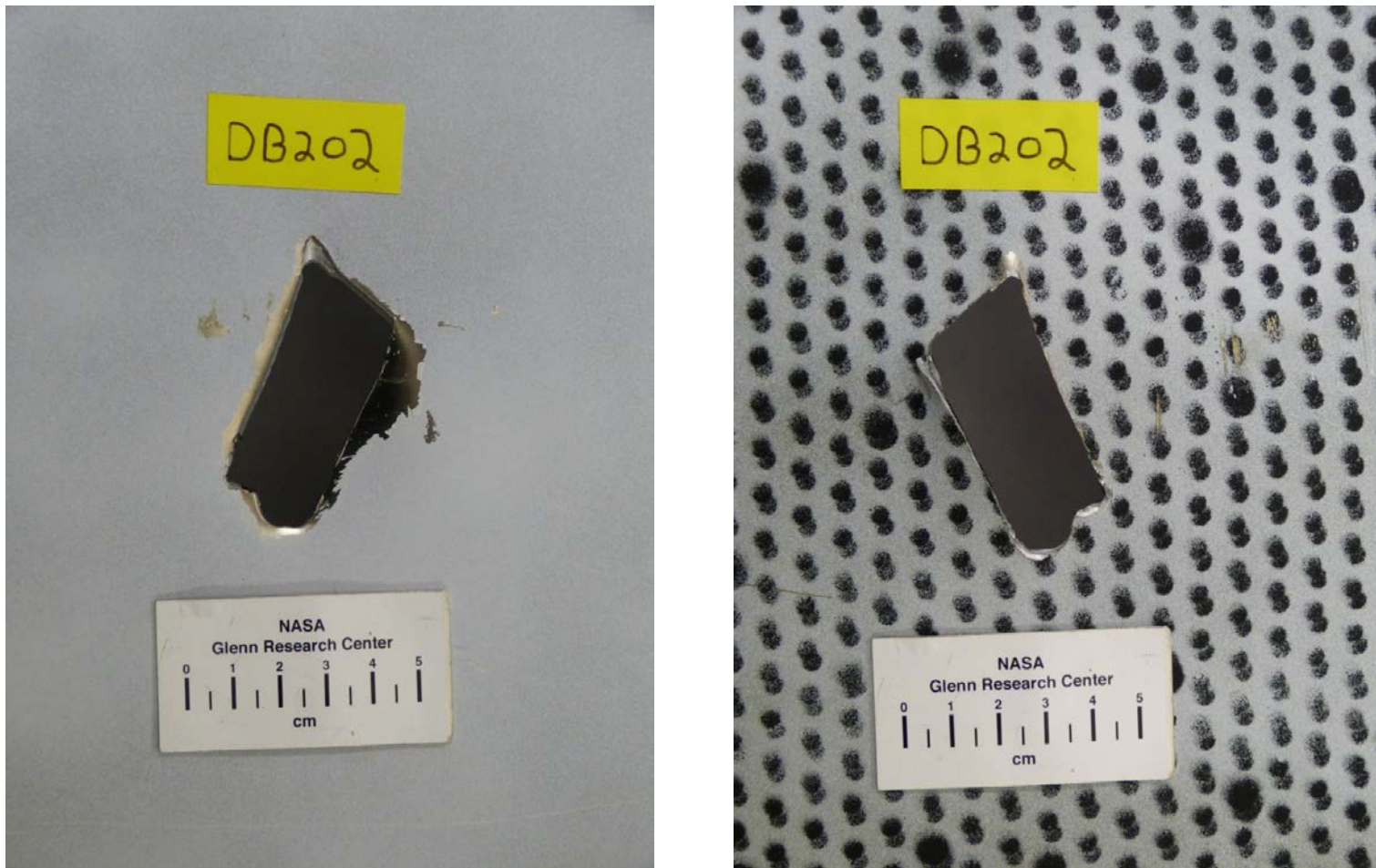


Figure A15.—Front (left) and back side views of impacted panel in test DB202.

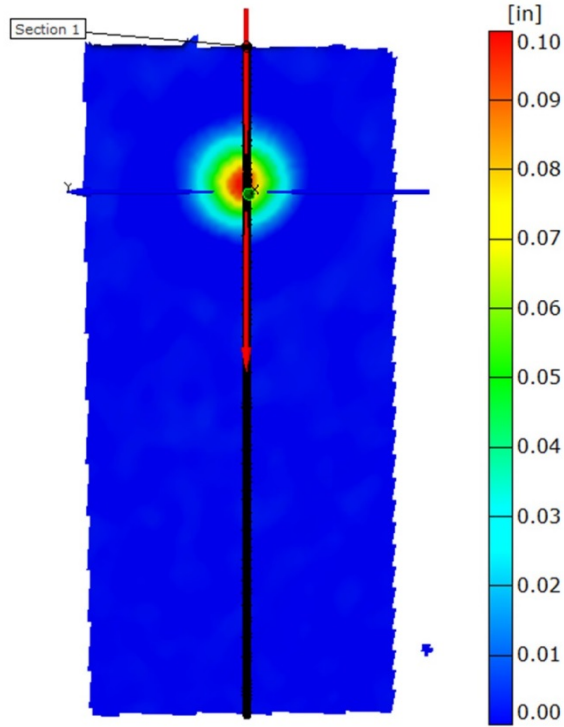


Figure A16.—Out-of-plane deformation map of panel in test DB202 just prior to initial failure.

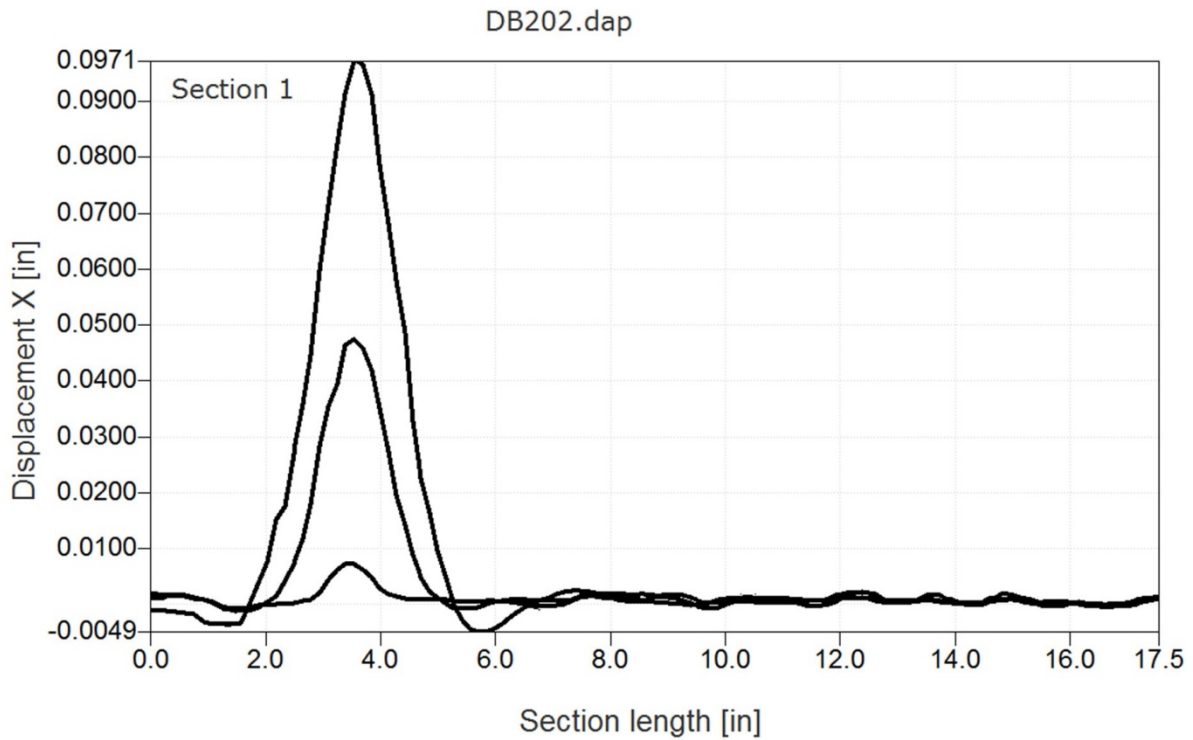


Figure A17.—Out-of-plane deformation along section line indicated in Figure A13 for a series of time steps up until the time of initial failure (frame rate 27000 frames/sec).

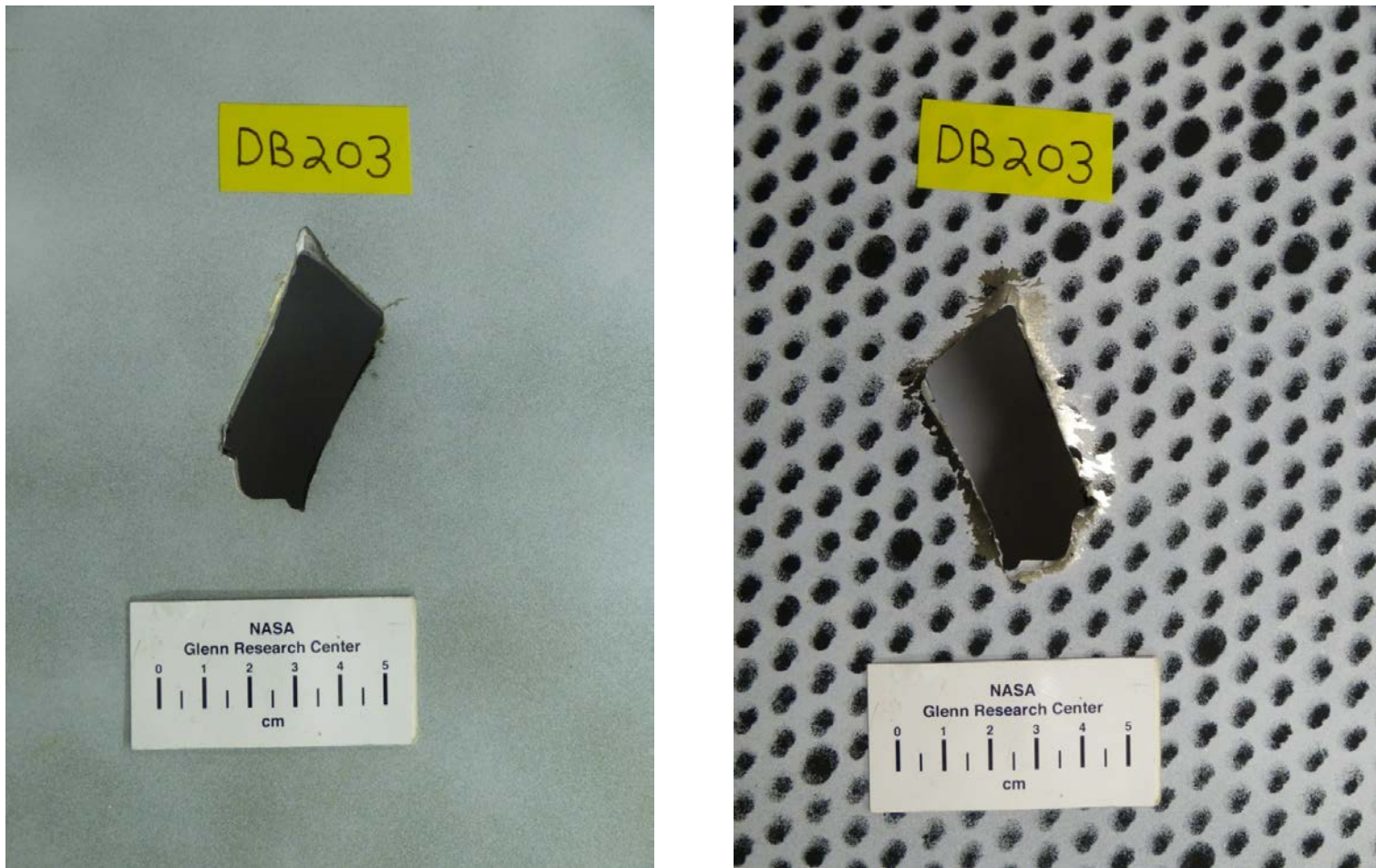


Figure A18.—Front (left) and back side views of impacted panel in test DB203.

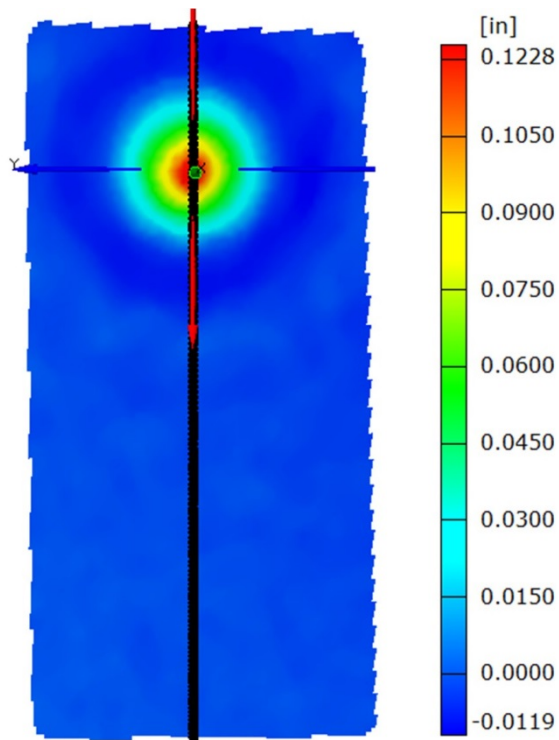


Figure A19.—Out-of-plane deformation map of panel in test DB203 just prior to initial failure.

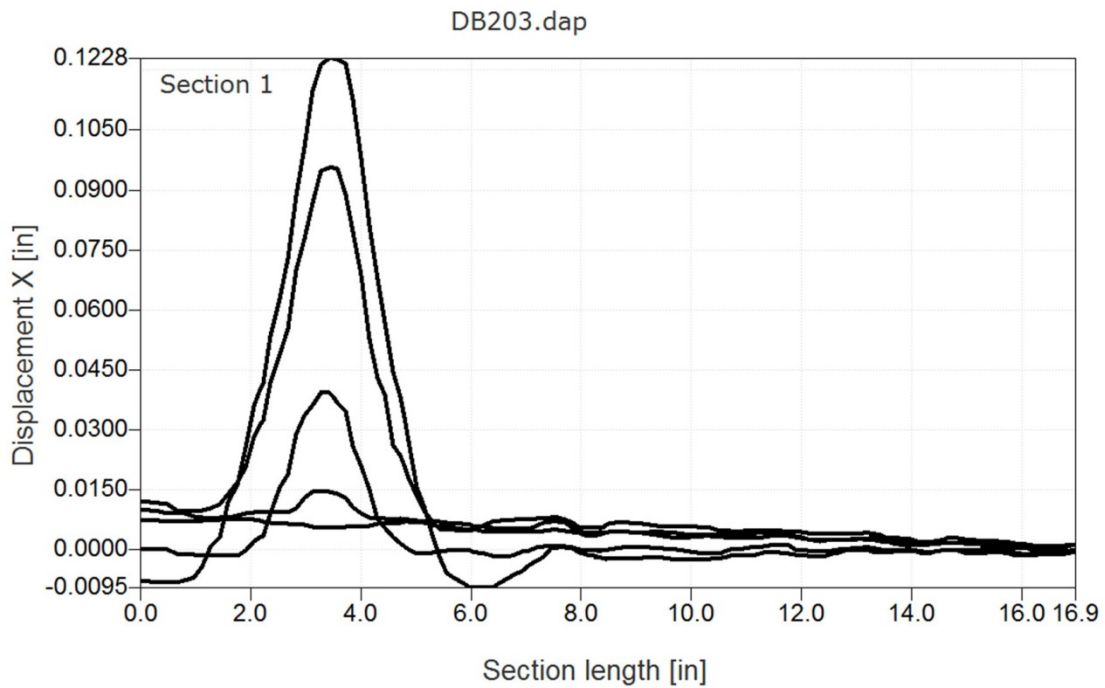


Figure A20.—Out-of-plane deformation along section line indicated in Figure A16 for a series of time steps up until the time of initial failure (frame rate 27000 frames/sec).

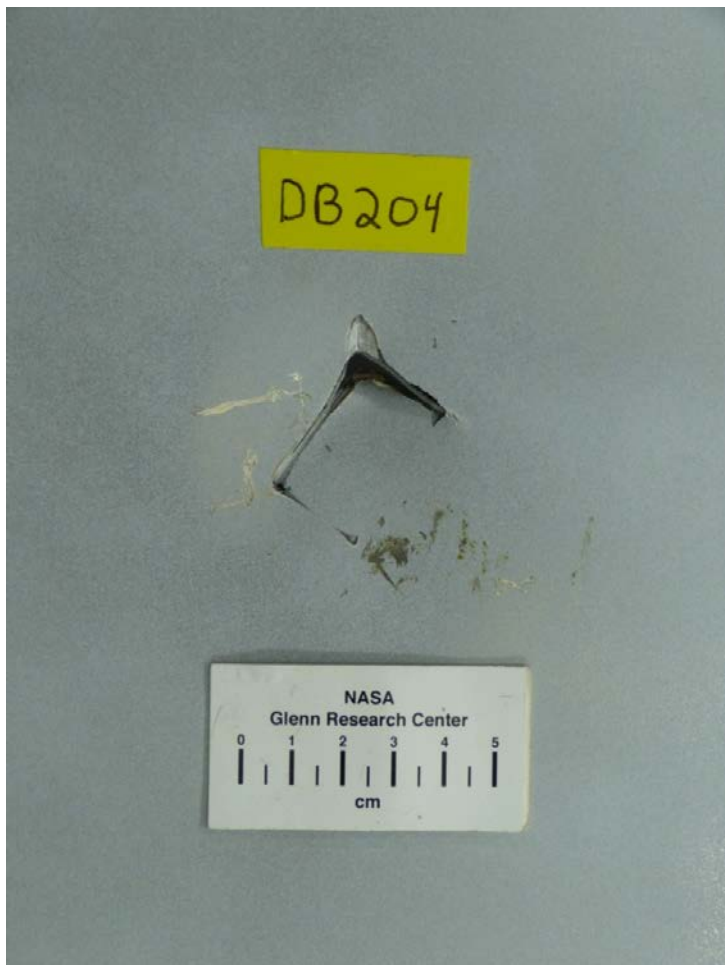


Figure A21.—Front (left) and back side views of impacted panel in test DB204.

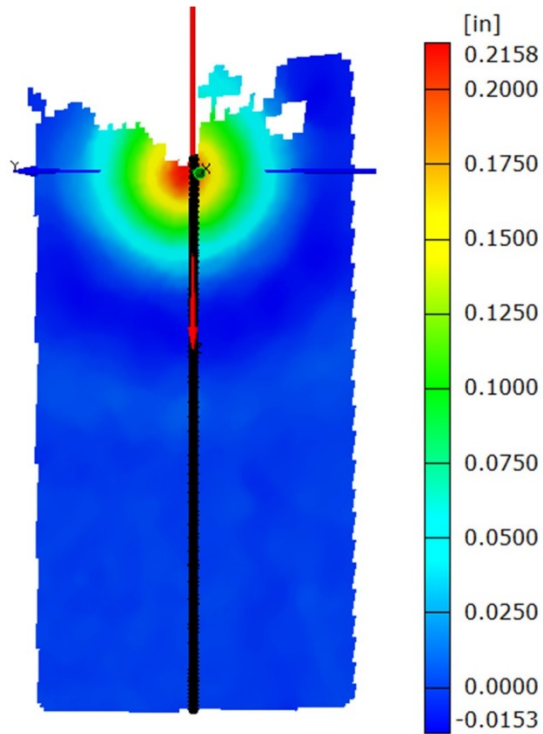


Figure A22.—Out-of-plane deformation map of panel in test DB204 just prior to initial failure.

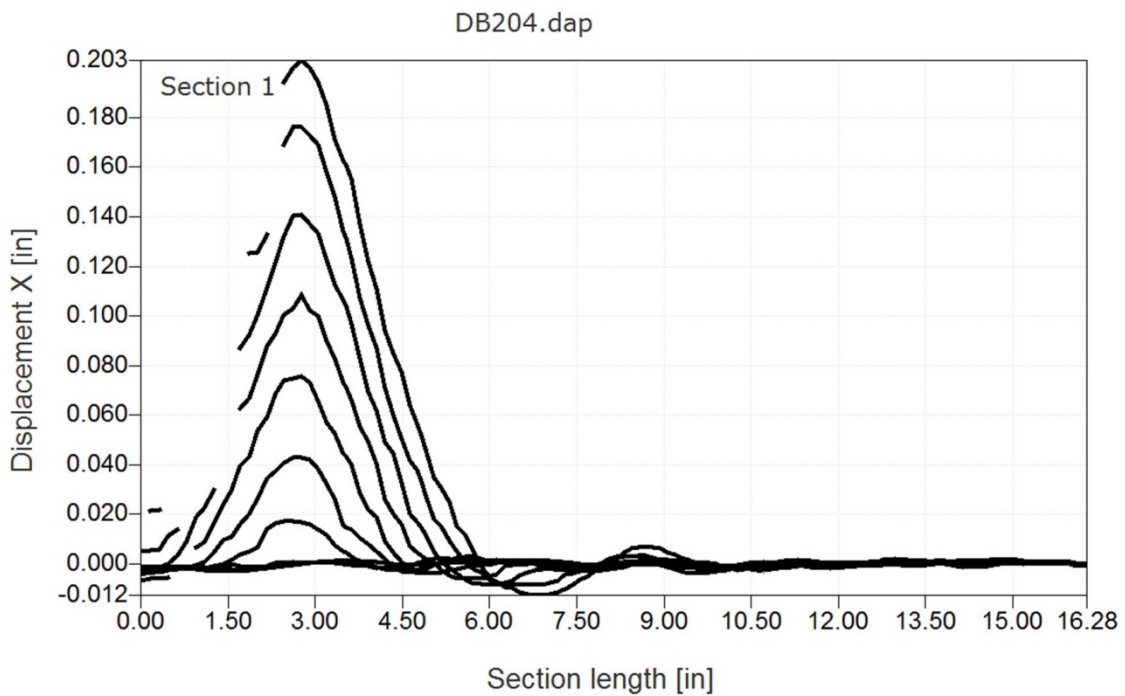


Figure A23.—Out-of-plane deformation along section line indicated in Figure A19 for a series of time steps up until the time of initial failure (frame rate 27000 frames/sec).

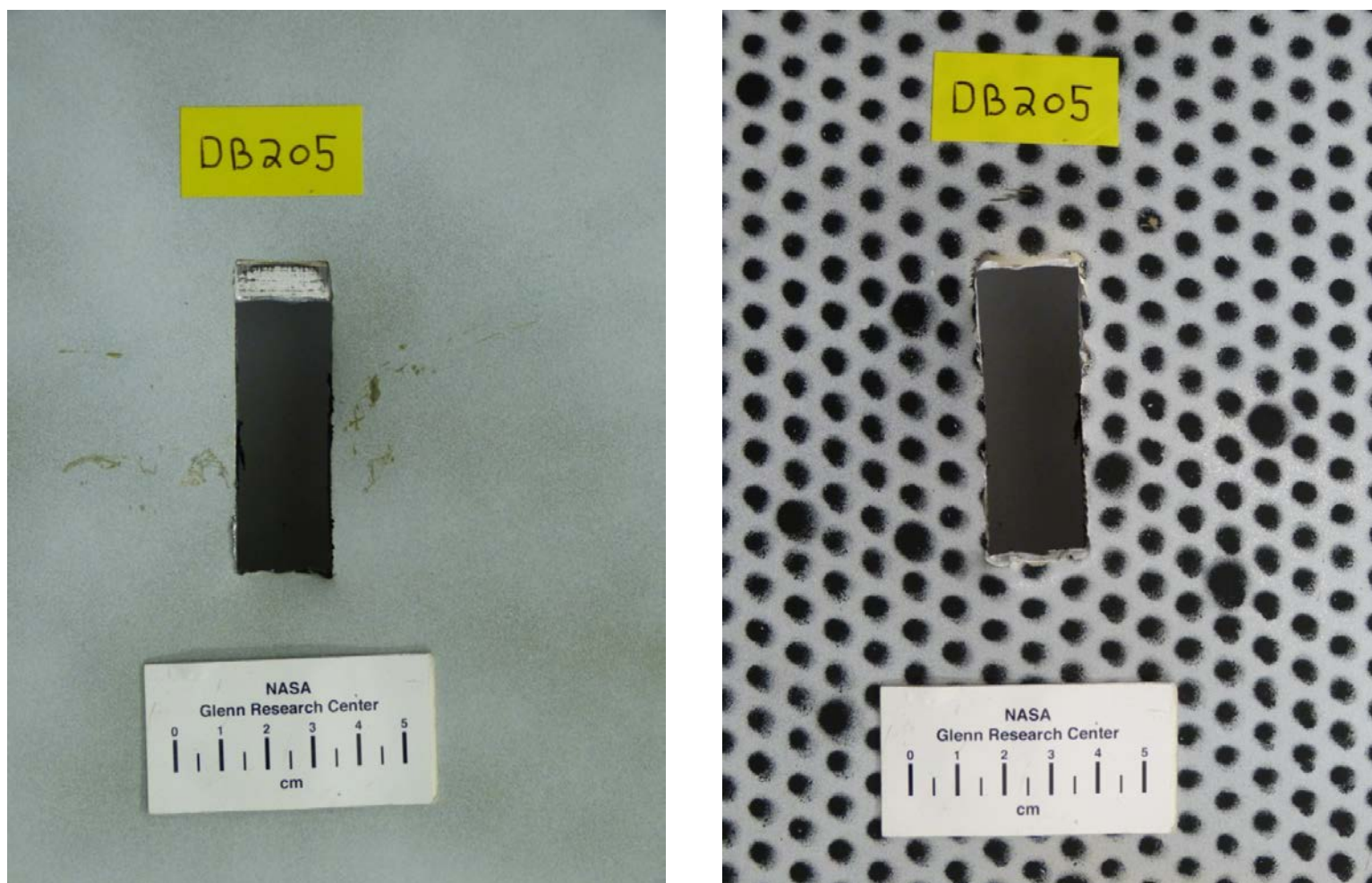


Figure A24.—Front (left) and back side views of impacted panel in test DB205.

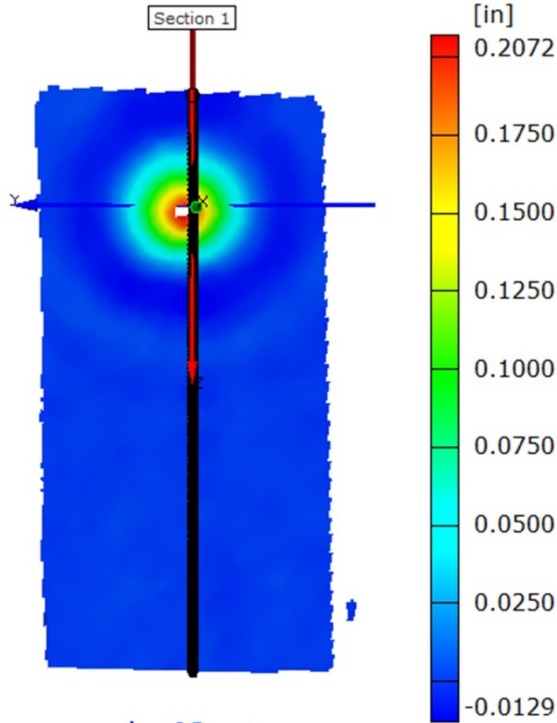


Figure A25.—Out-of-plane deformation map of panel in test DB205 just prior to initial failure.

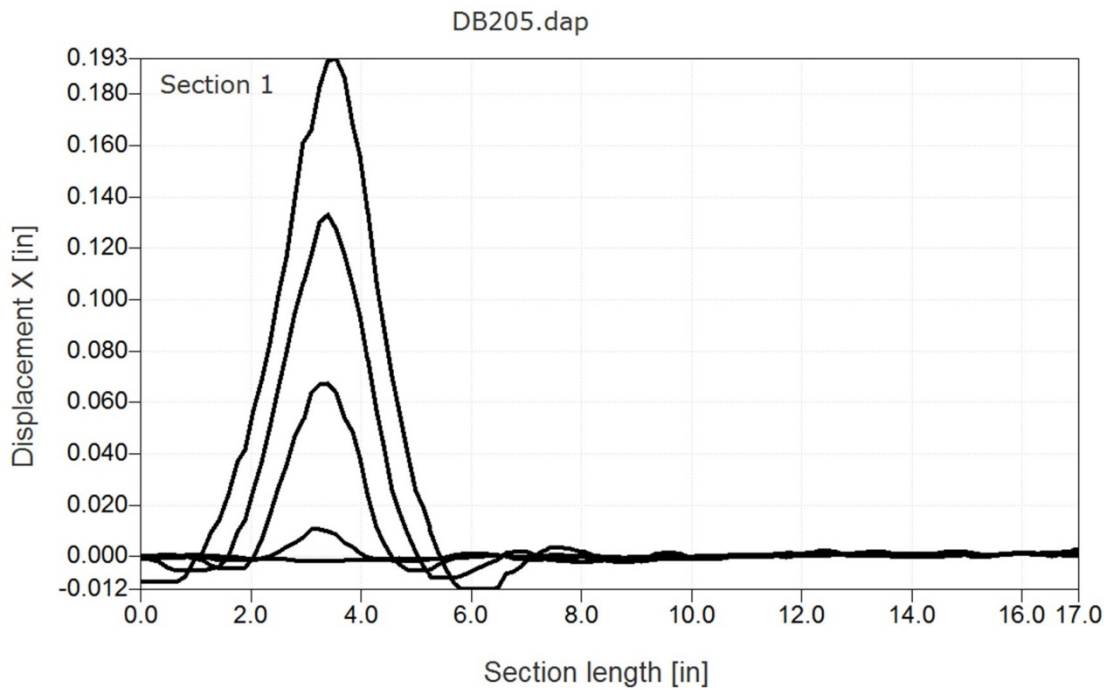


Figure A26.—Out-of-plane deformation along section line indicated in Figure A22 for a series of time steps up until the time of initial failure (frame rate 27000 frames/sec).

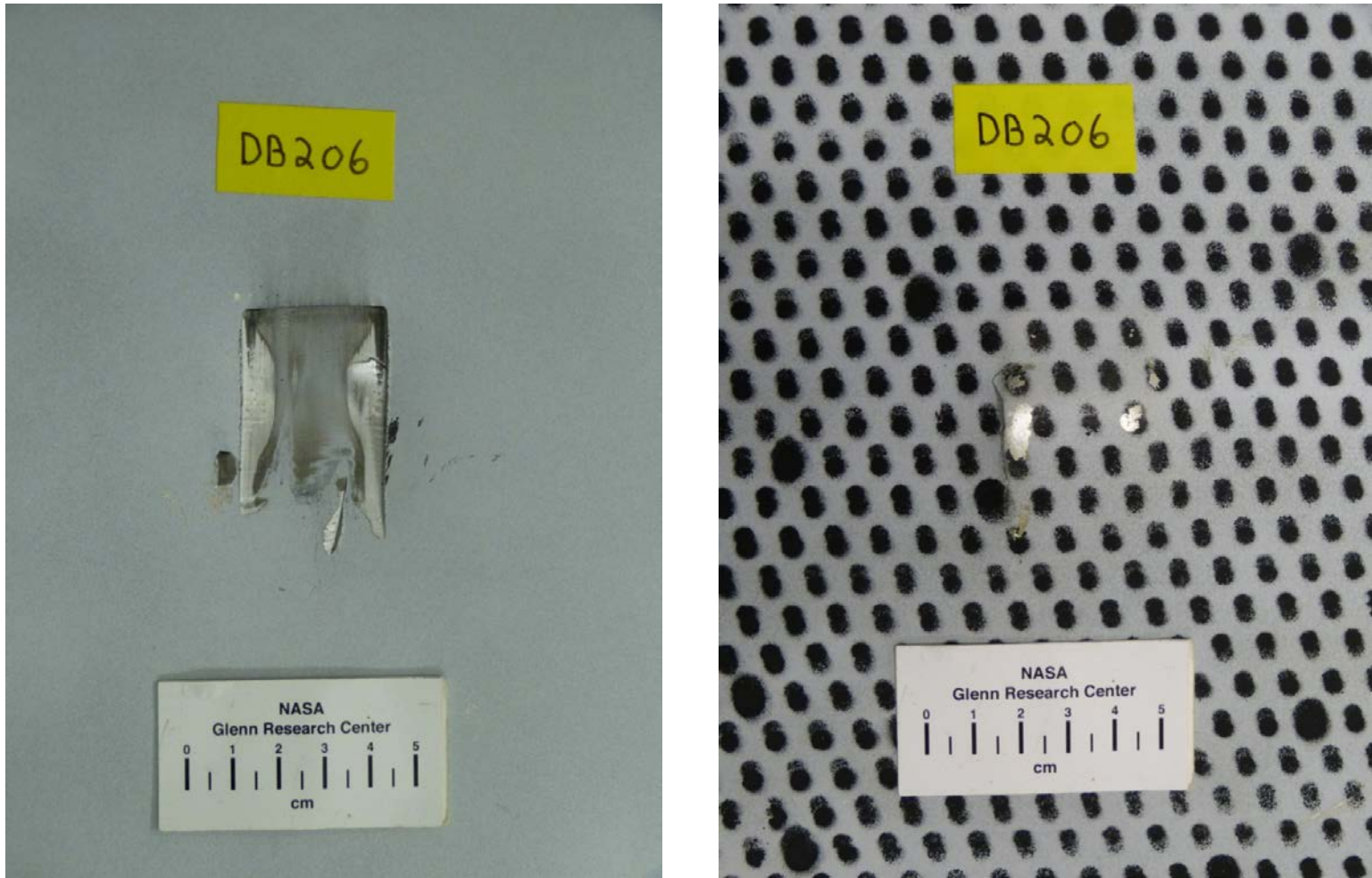


Figure A27.—Front (left) and back side views of impacted panel in test DB206.

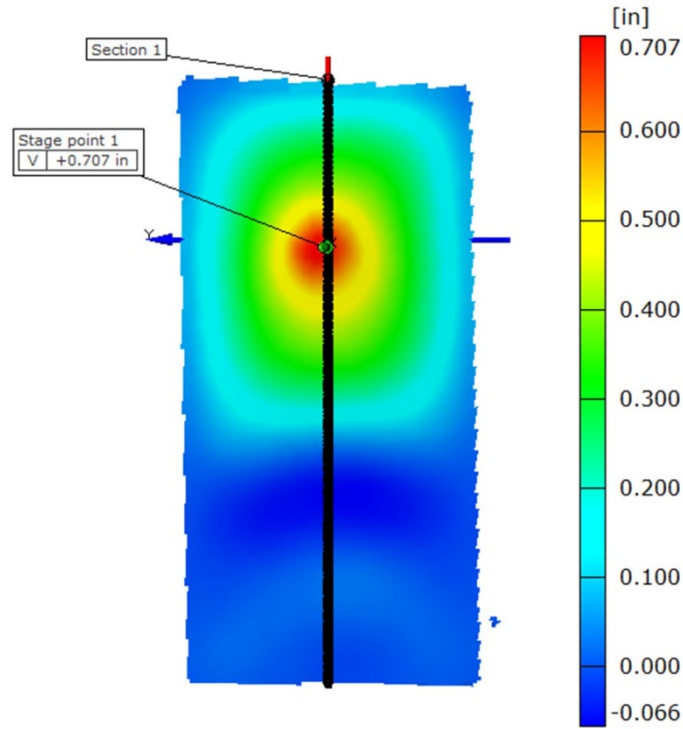


Figure A28.—Out-of-plane deformation map of panel in test DB206 at the point of maximum deformation.

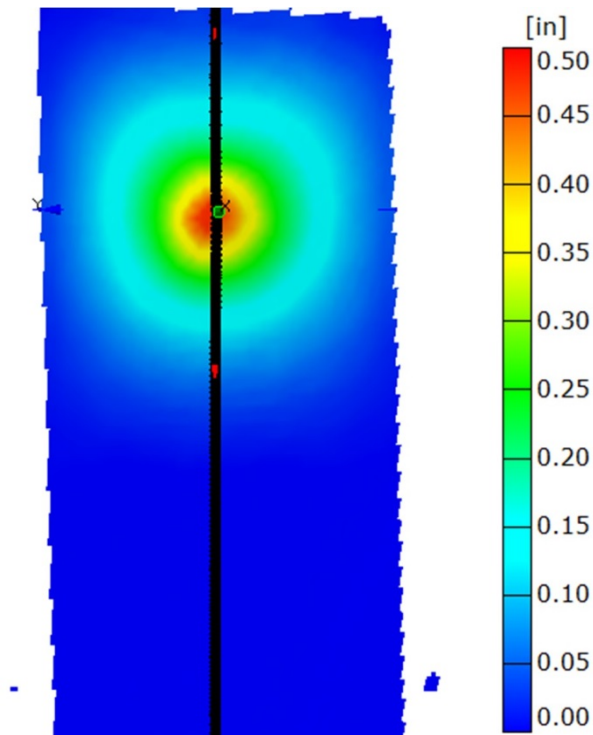


Figure A29.—Out-of-plane deformation map of panel in test DB206 after test is completed and all movement has stopped. This indicates the permanent deformation field.

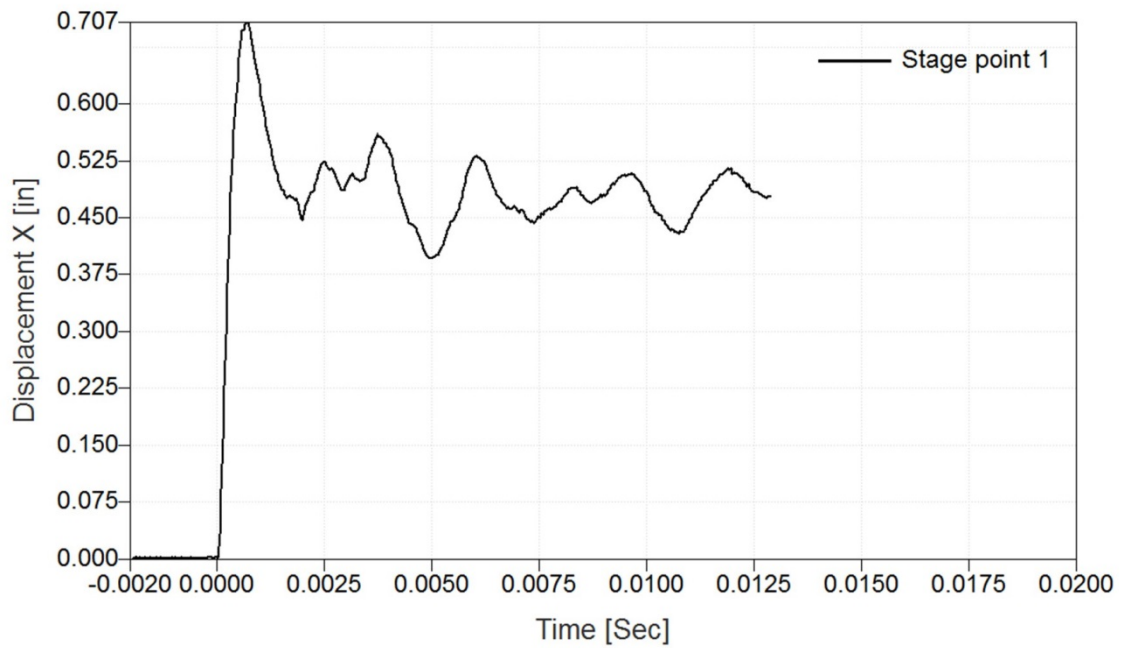


Figure A30.—Out-of-plane deformation as a function of time of point indicated in Figure A25 for test DB206.

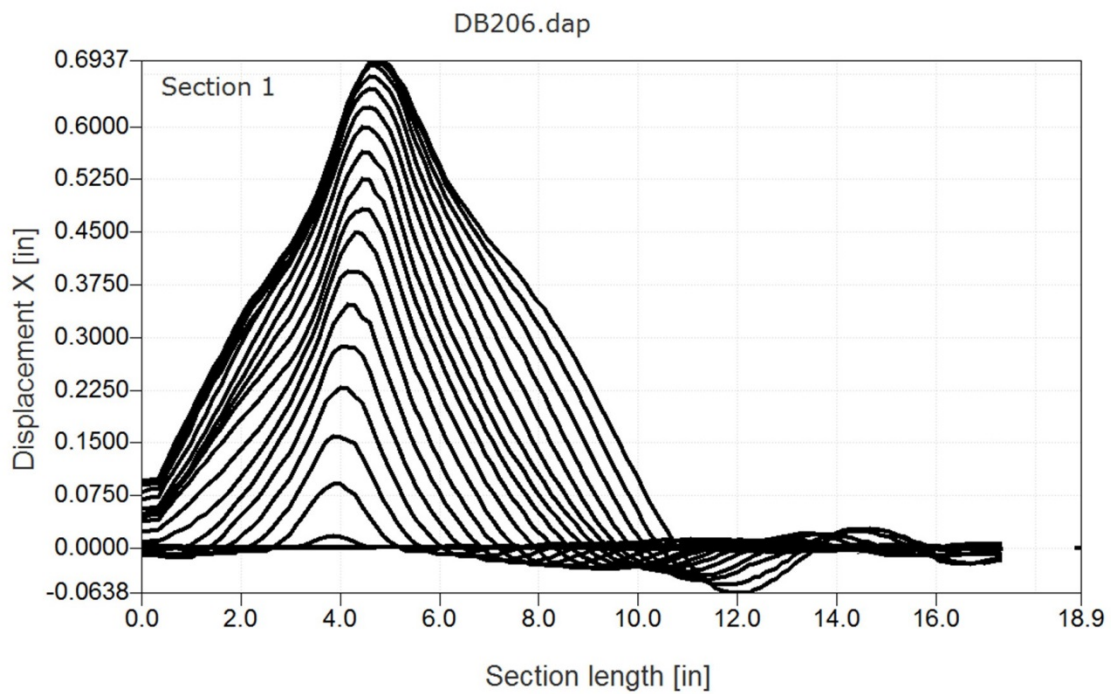


Figure A31.—Test DB206. Out-of-plane deformation along section line indicated in Figure A25 for a series of time steps up until the time of initial failure (frame rate 27000 frames/sec).

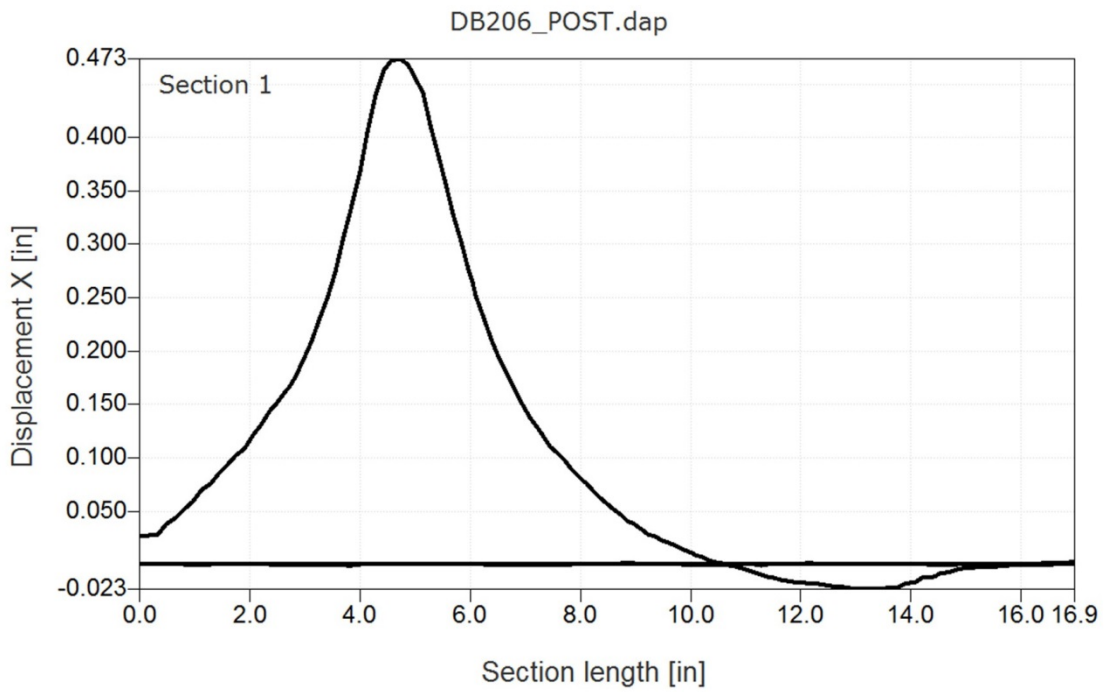


Figure A32.—Test DB206. Out-of-plane deformation along section line indicated in Figure A26. This indicates the plastic deformation along the section line after all movement has stopped.

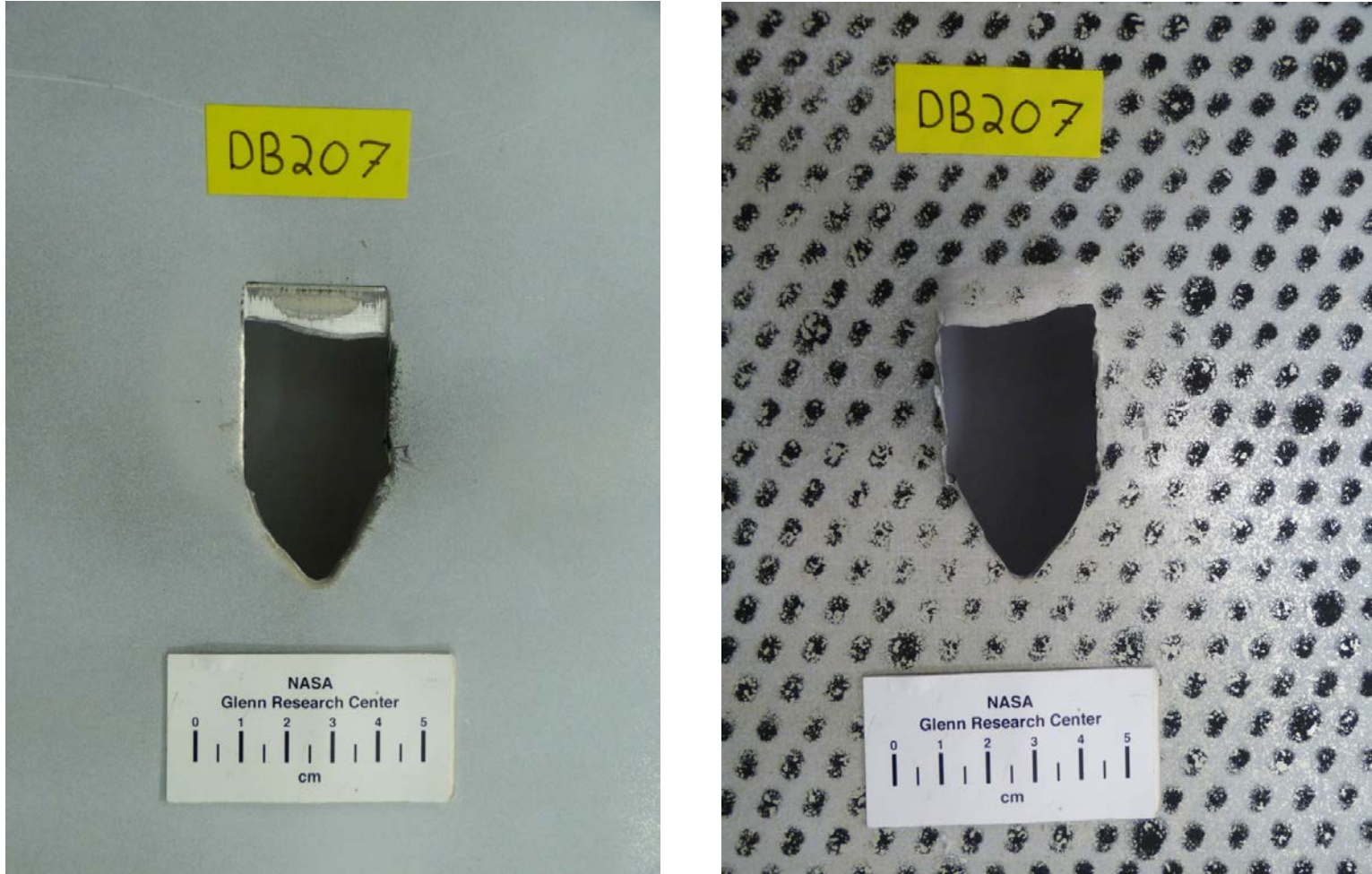


Figure A33.—Front (left) and back side views of impacted panel in test DB207.

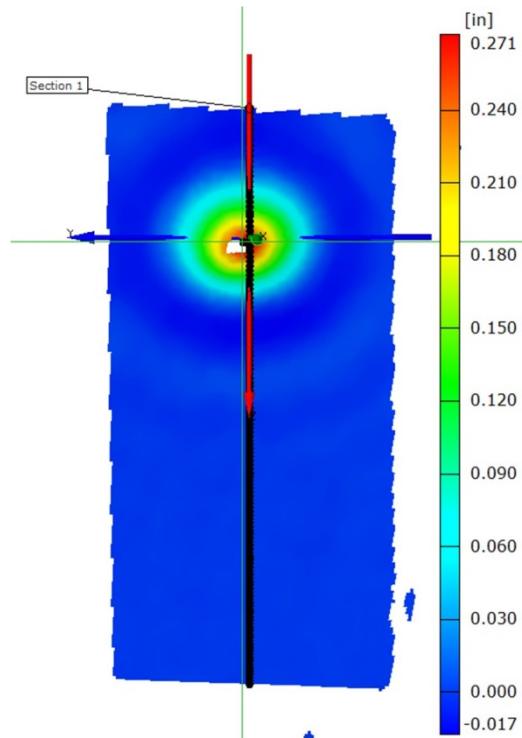


Figure A34.—Out-of-plane deformation map of panel in test DB207 just prior to initial failure.

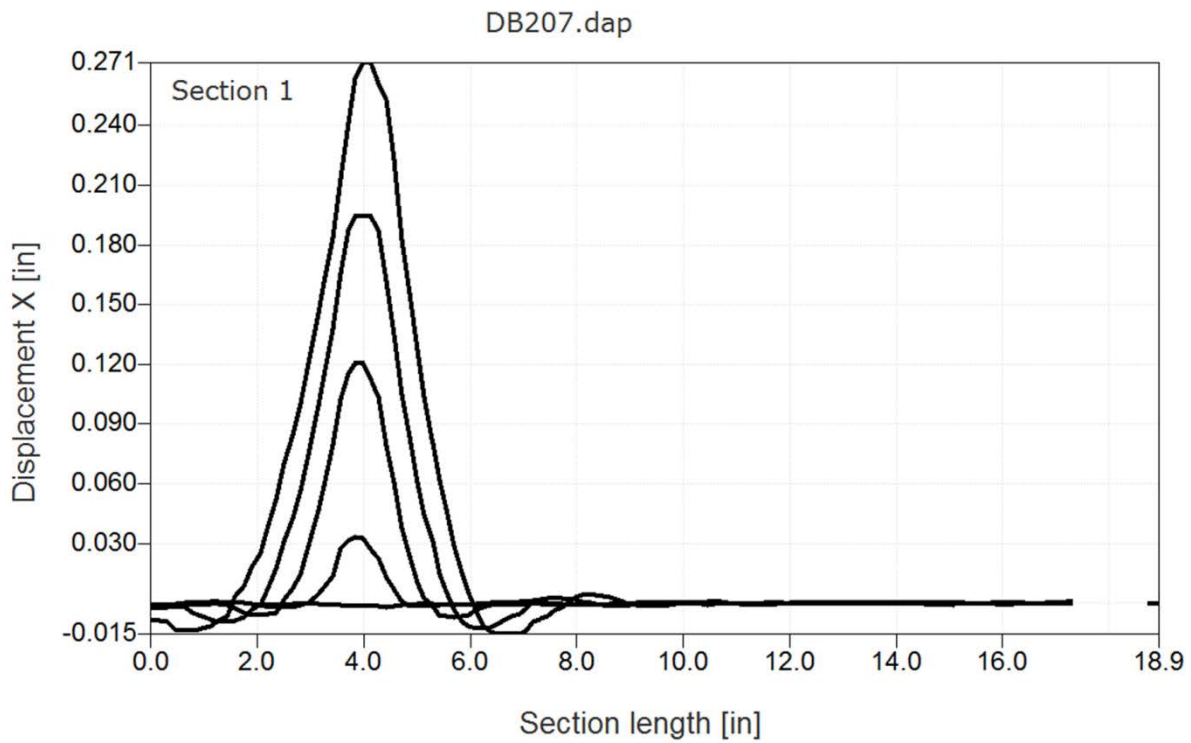


Figure A35.—Test DB207. Out-of-plane deformation along section line indicated in Figure A31 for a series of time steps up until the time of initial failure (frame rate 27000 frames/sec).

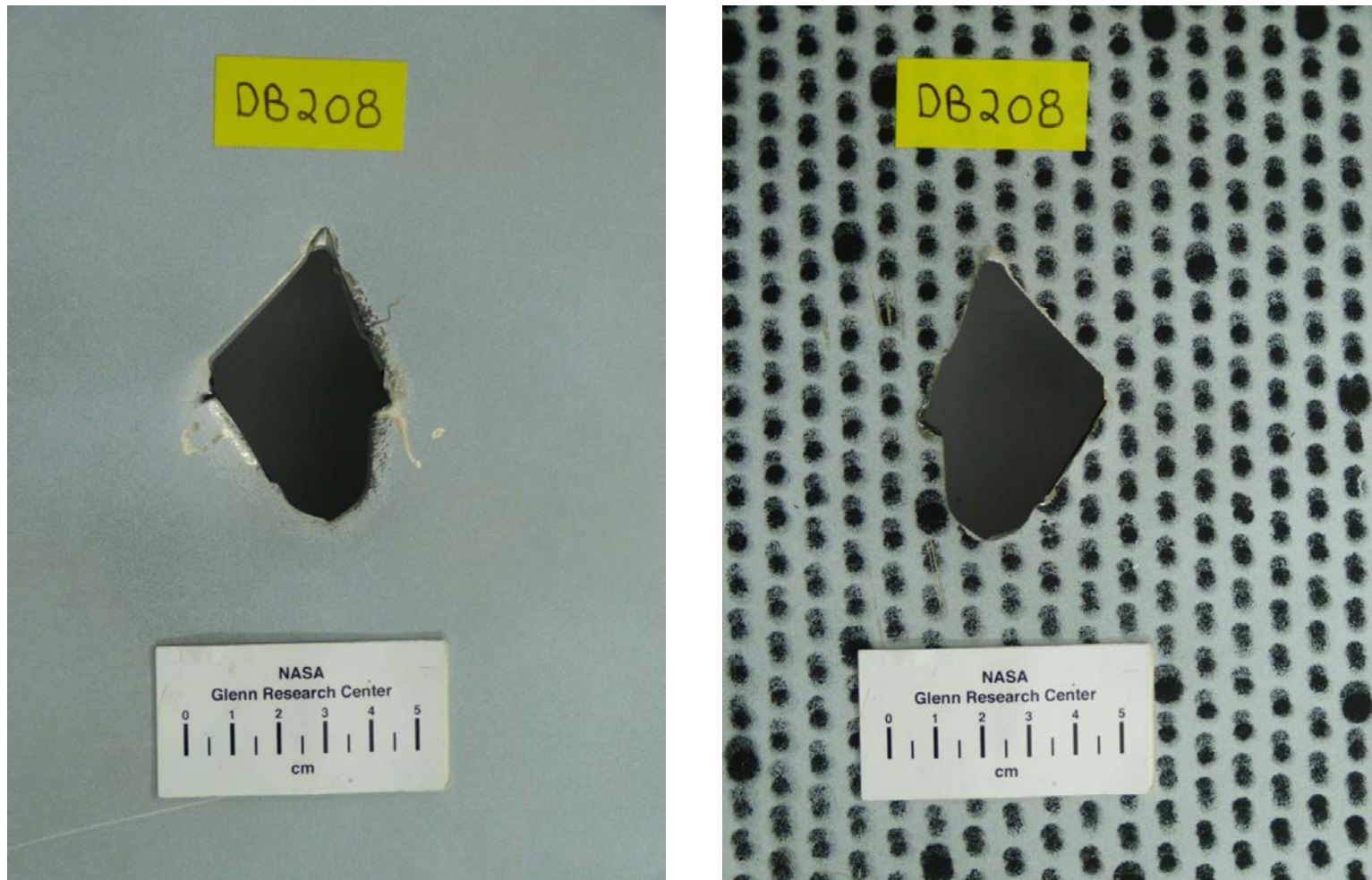


Figure A36.—Front (left) and back side views of impacted panel in test DB208.

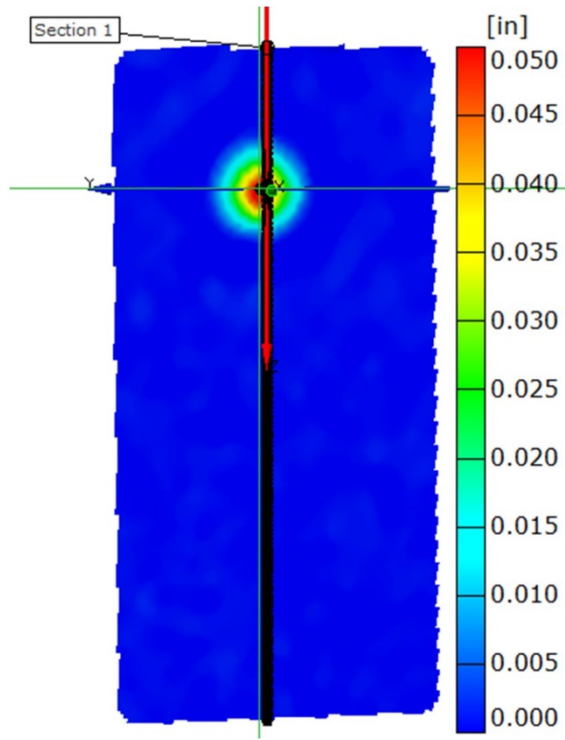


Figure A37.—Out-of-plane deformation map of panel in test DB208 just prior to initial failure.

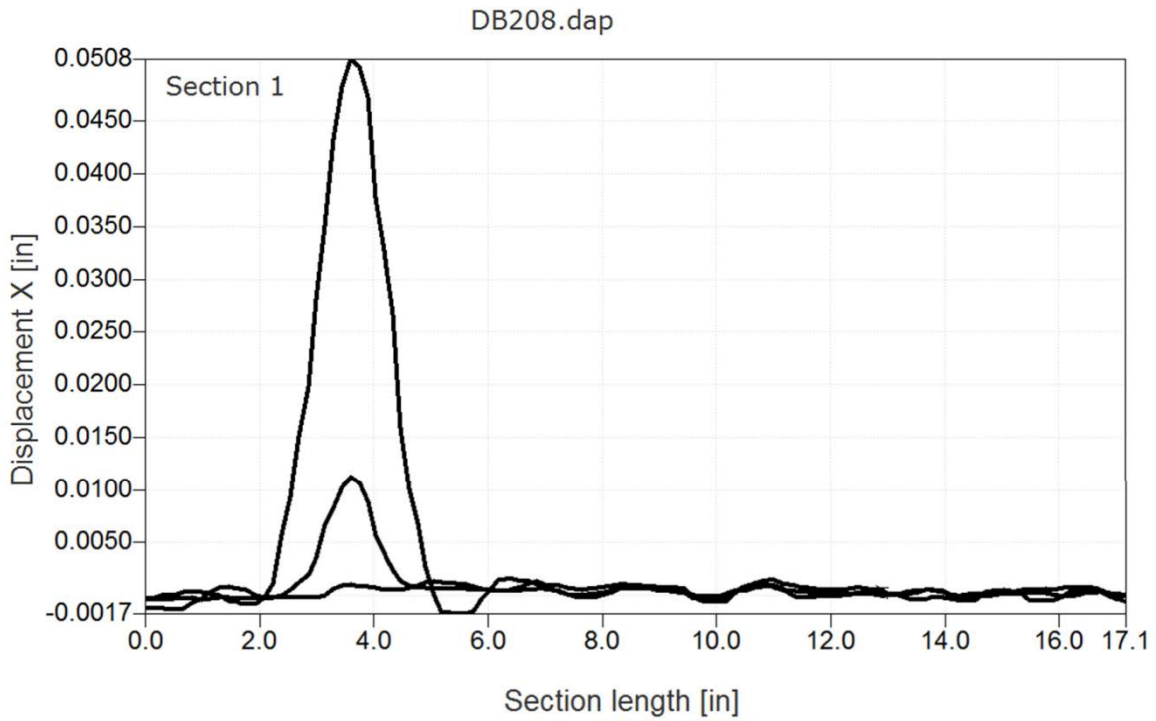


Figure A38.—Test DB208. Out-of-plane deformation along section line indicated in Figure A34 for a series of time steps up until the time of initial failure (frame rate 27000 frames/sec).

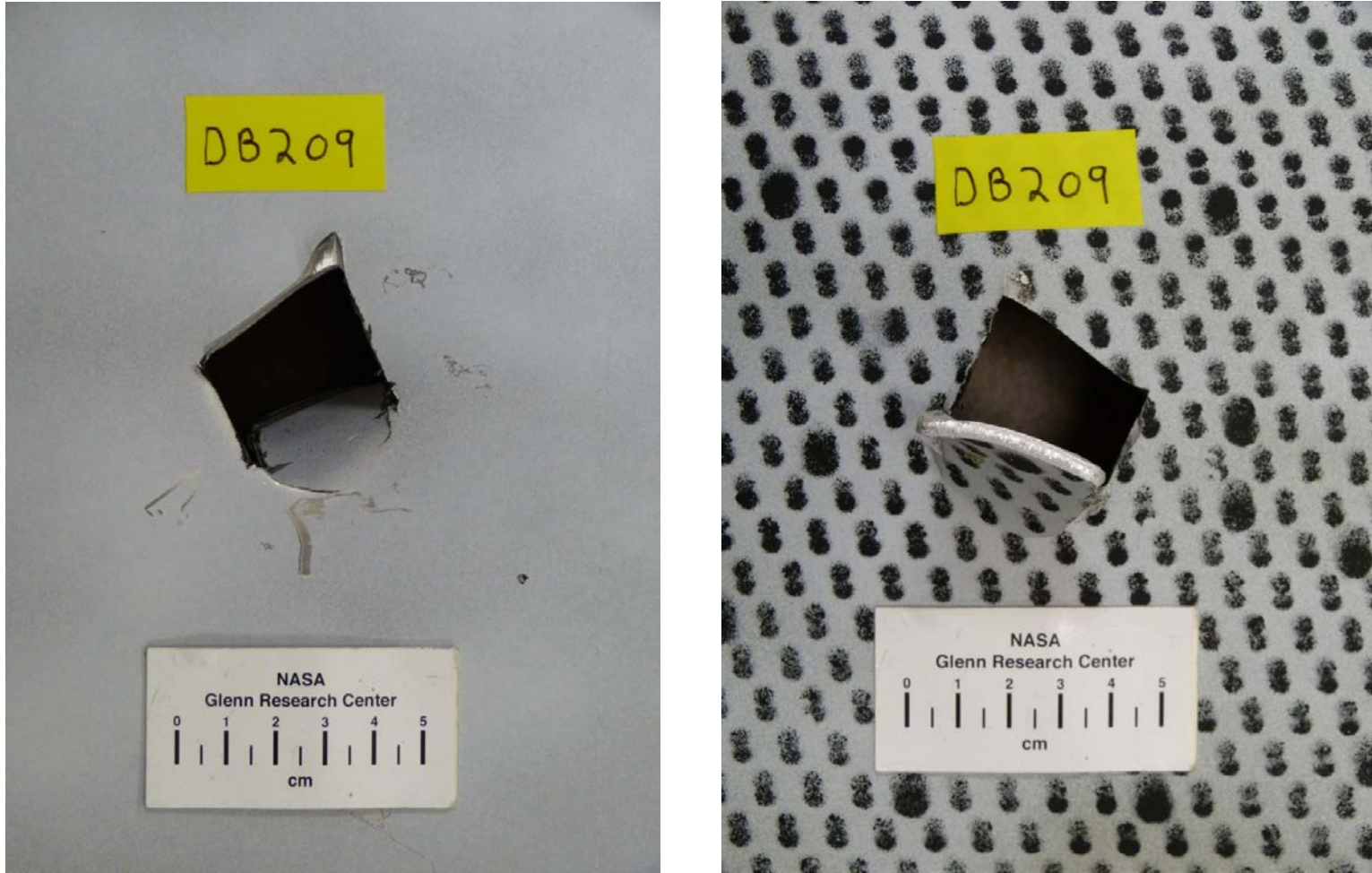


Figure A39.—Front (left) and back side views of impacted panel in test DB209.

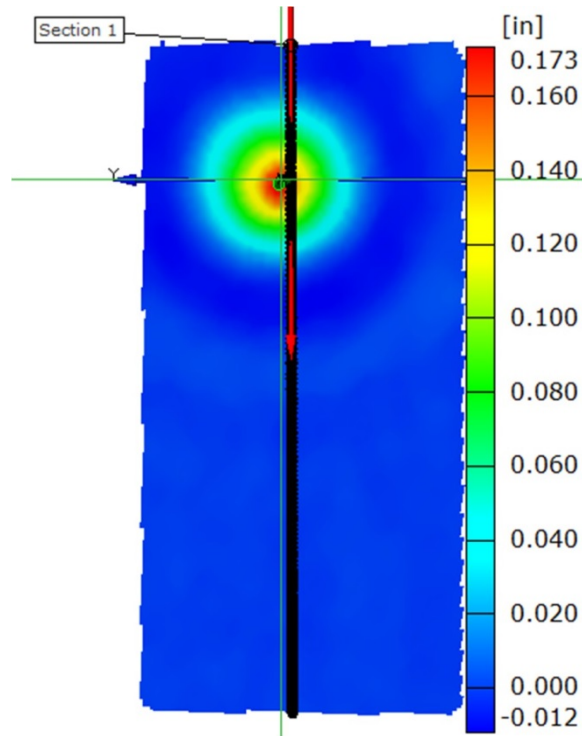


Figure A40.—Out-of-plane deformation map of panel in test DB209 just prior to initial failure.

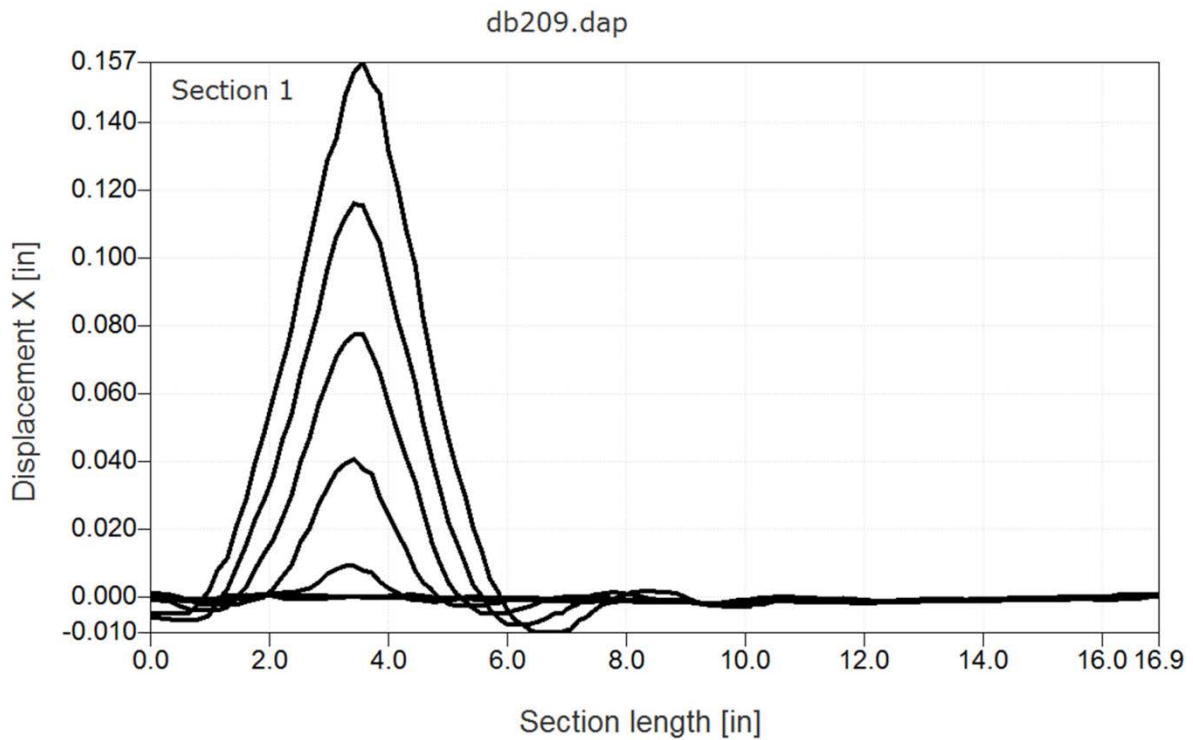


Figure A41.—Test DB209. Out-of-plane deformation along section line indicated in Figure A37 for a series of time steps up until the time of initial failure (frame rate 27000 frames/sec).

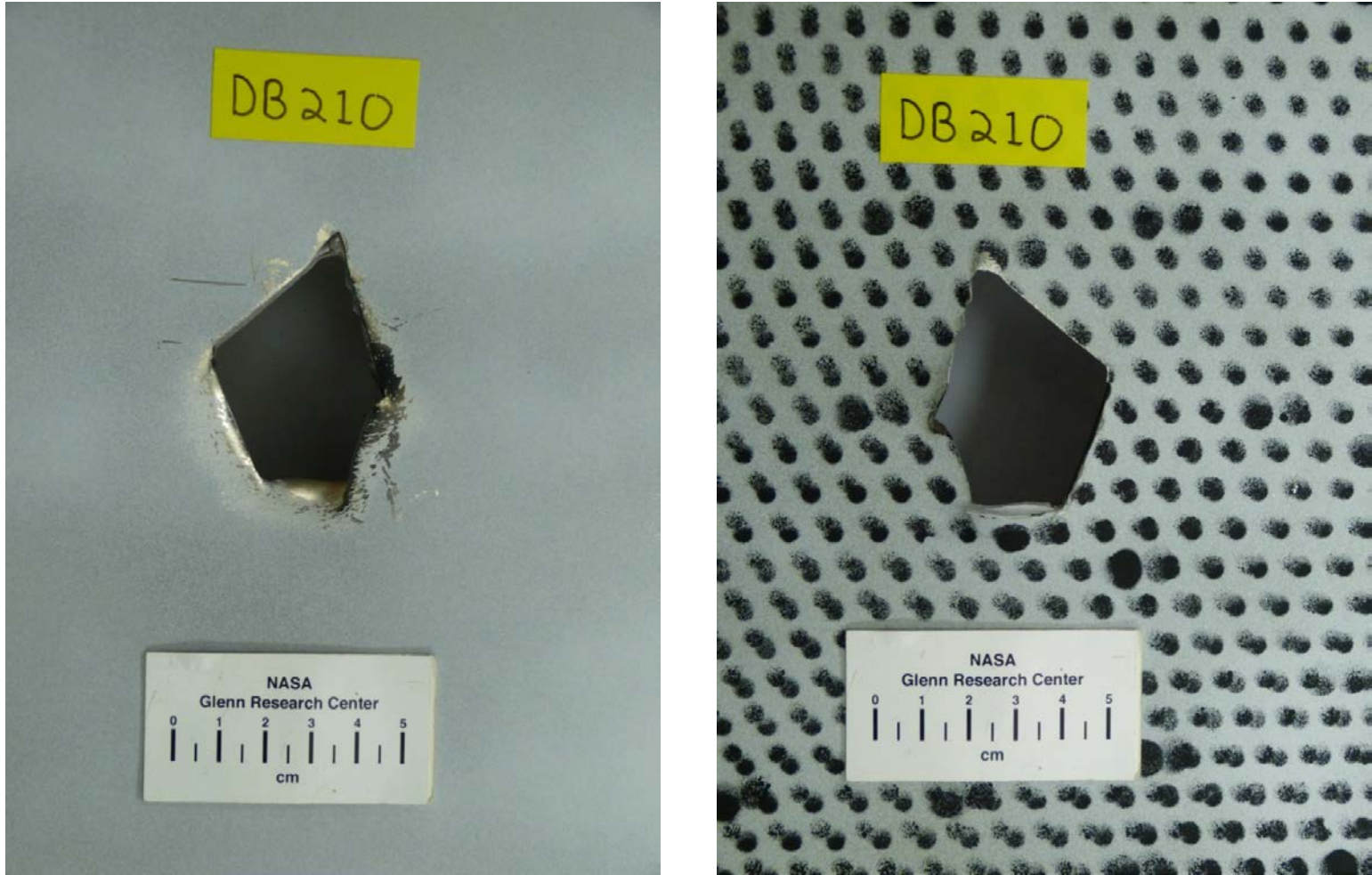


Figure A42.—Front (left) and back side views of impacted panel in test DB210.

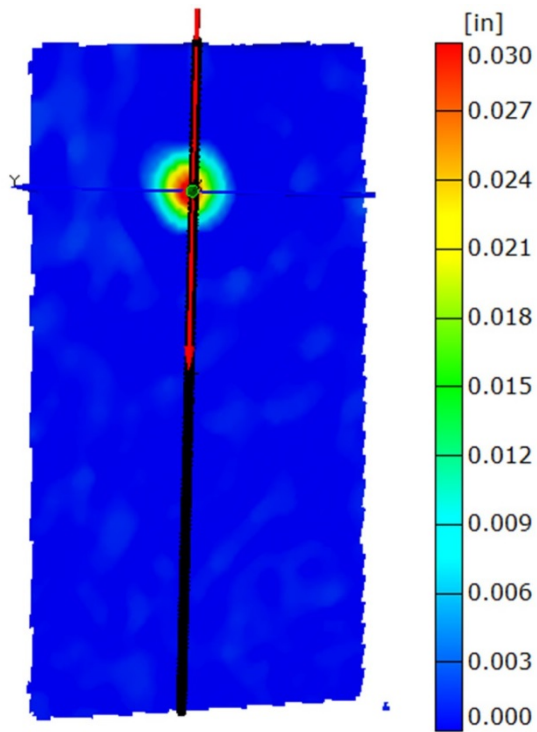


Figure A43.—Out-of-plane deformation map of panel in test DB210 just prior to initial failure.

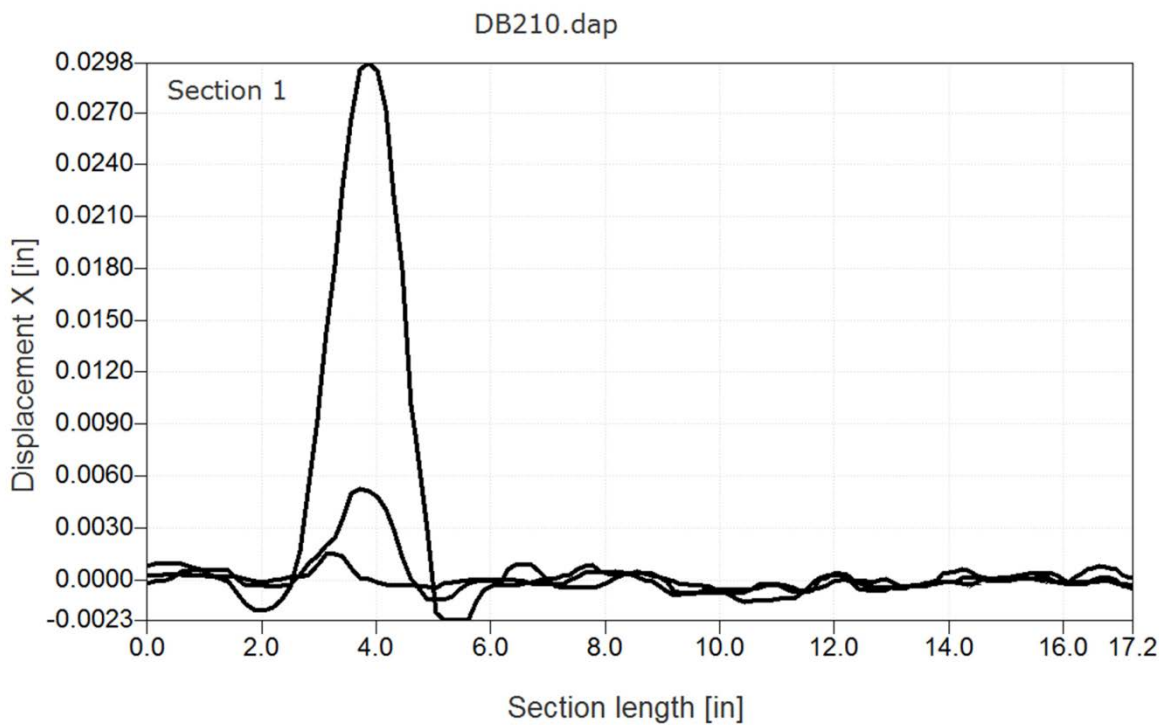


Figure A44.—Test DB210. Out-of-plane deformation along section line indicated in Figure A40 for a series of time steps up until the time of initial failure (frame rate 27000 frames/sec).

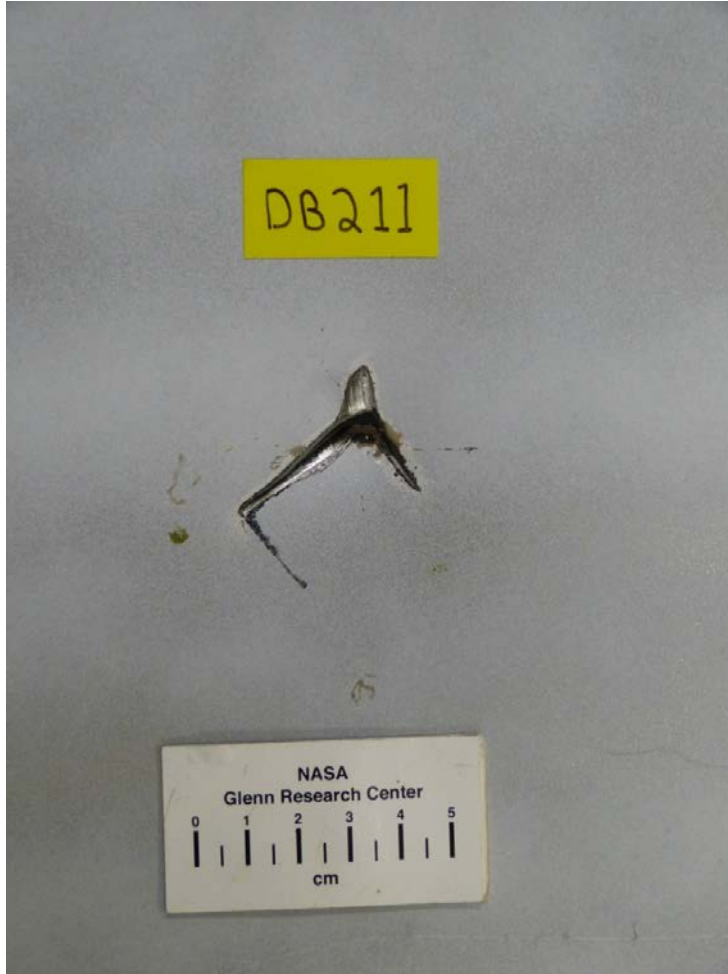


Figure A45.—Front (left) and back side views of impacted panel in test DB211.

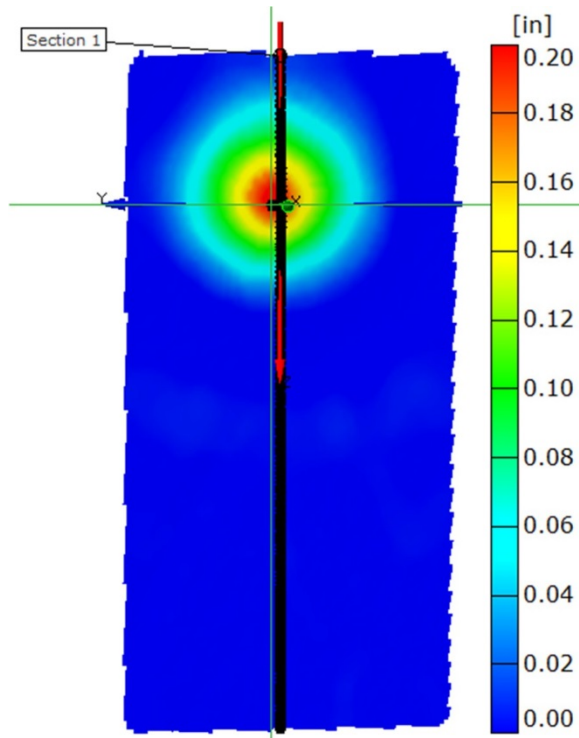


Figure A46.—Out-of-plane deformation map of panel in test DB211 just prior to initial failure.

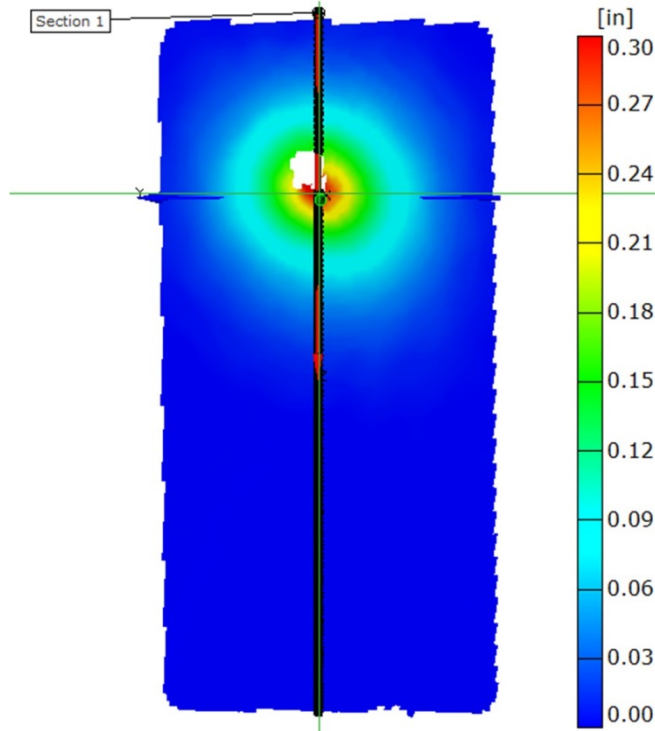


Figure A47.—Out-of-plane deformation map of panel in test DB211 after test is completed and all movement has stopped. This indicates the permanent deformation field.

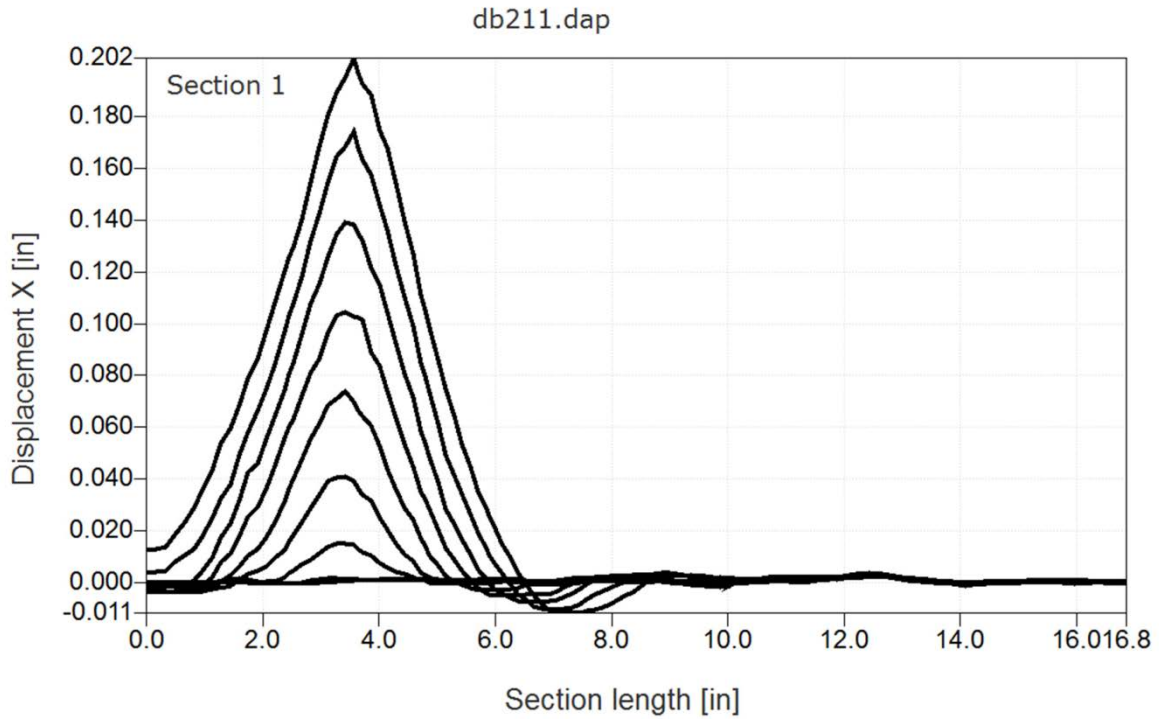


Figure A48.—Test DB211. Out-of-plane deformation along section line indicated in Figure A42 for a series of time steps up until the time of initial failure (frame rate 27000 frames/sec).

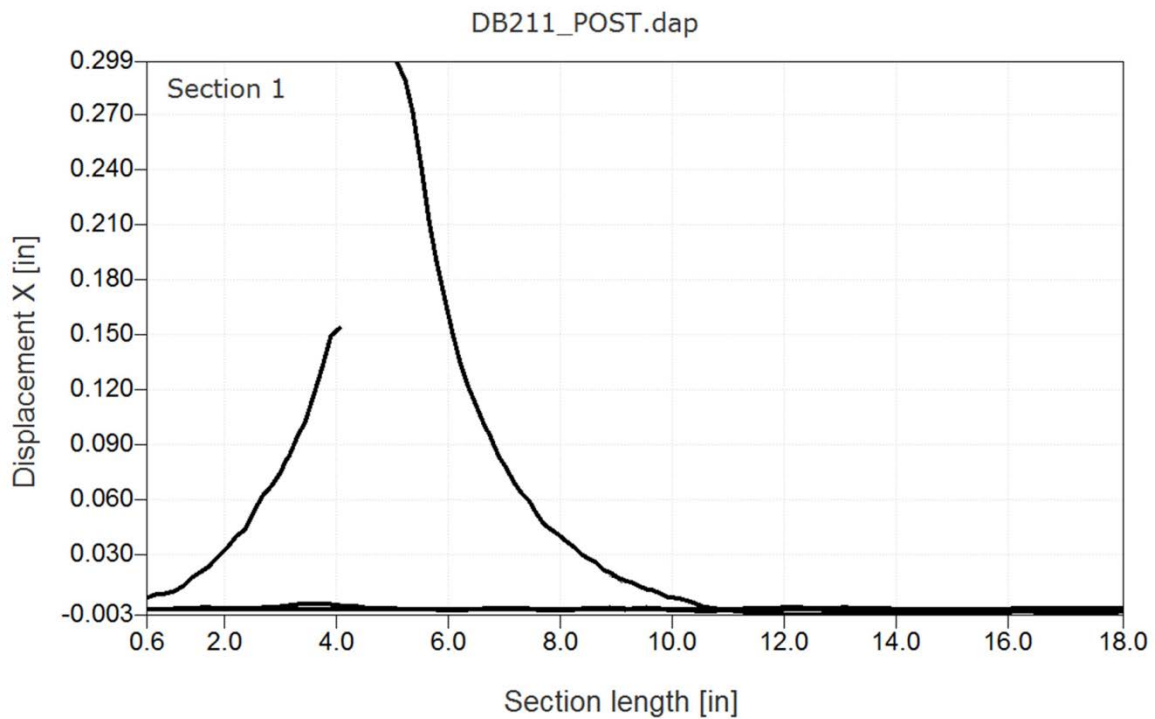


Figure A49.—Test DB211. Out-of-plane deformation along section line indicated in Figure A43. This indicates the plastic deformation along the section line after all movement has stopped.



Figure A50.—Front (left) and back side views of impacted panel in test DB212.

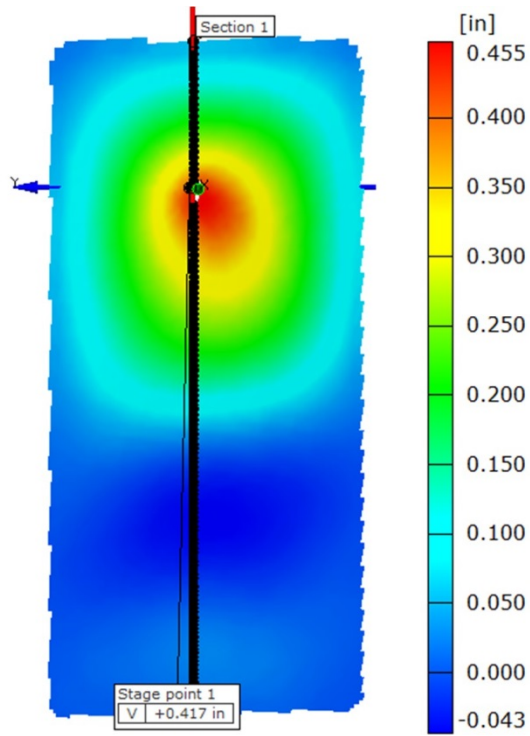


Figure A51.—Out-of-plane deformation map of panel in test DB212 at the point of maximum deflection.

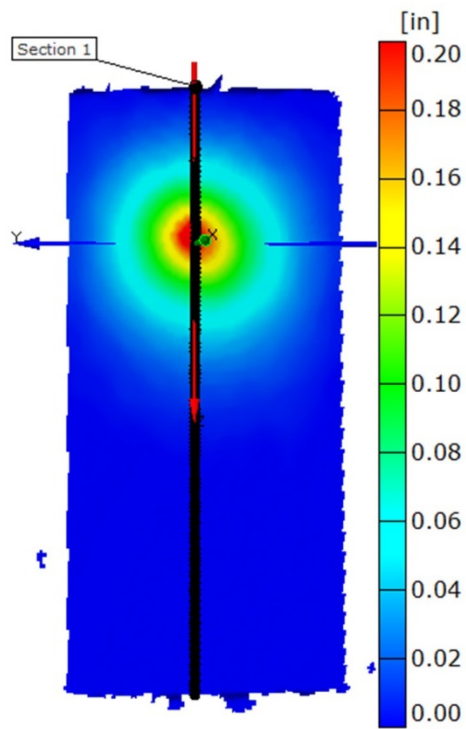


Figure A52.—Out-of-plane deformation map of panel in test DB212 after test is completed and all movement has stopped. This indicates the permanent deformation field.

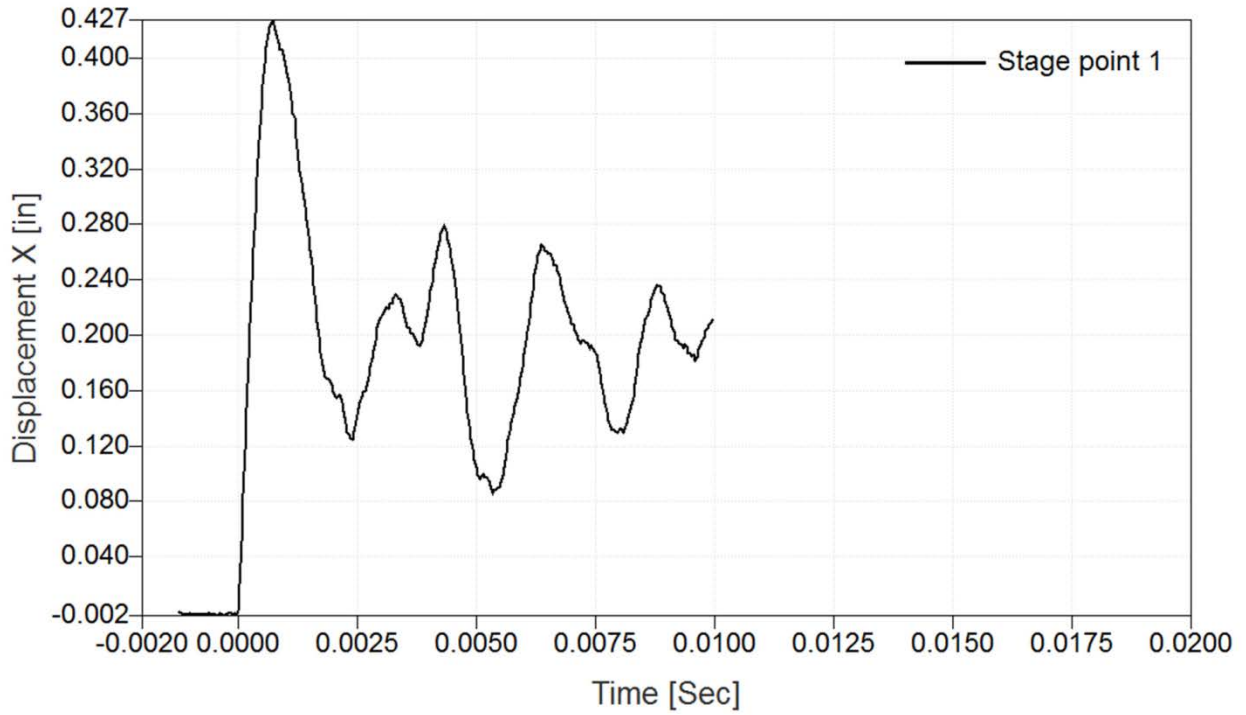


Figure A53.—Out-of-plane deformation as a function of time of point indicated in Figure A47 for test DB212.

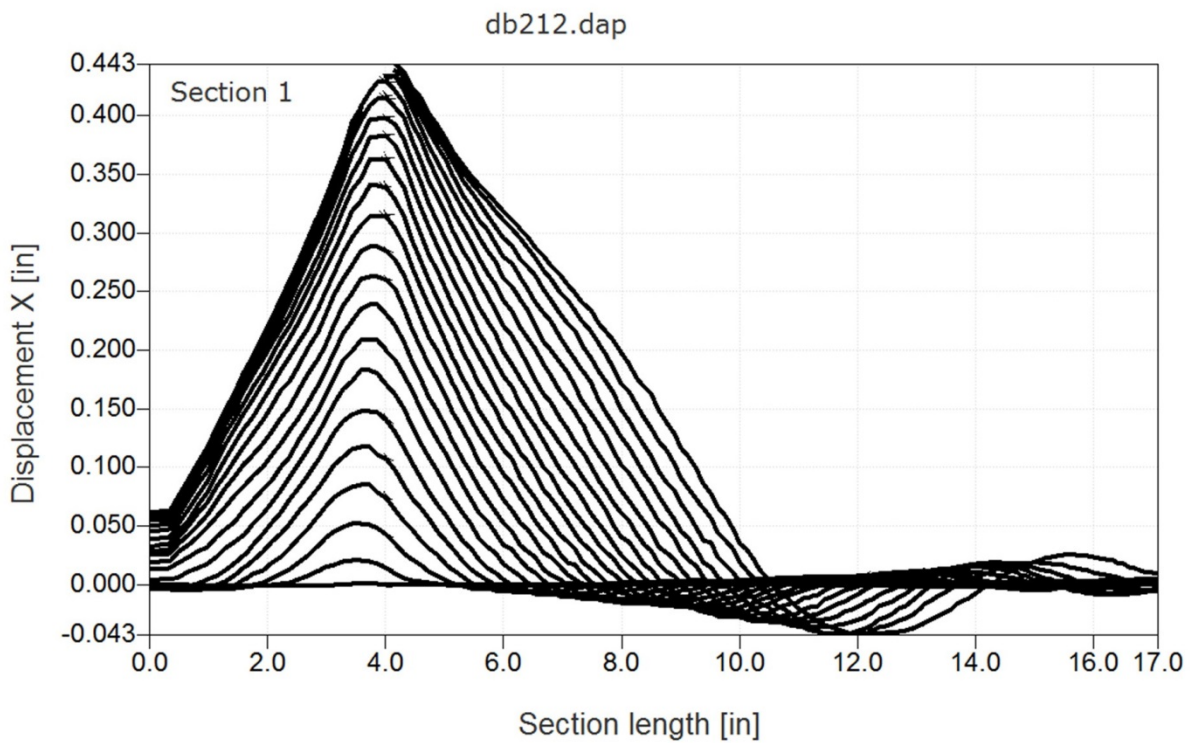


Figure A54.—Test DB212. Out-of-plane deformation along section line indicated in Figure A47 for a series of time steps up until the time of maximum deformation (frame rate 27000 frames/sec).

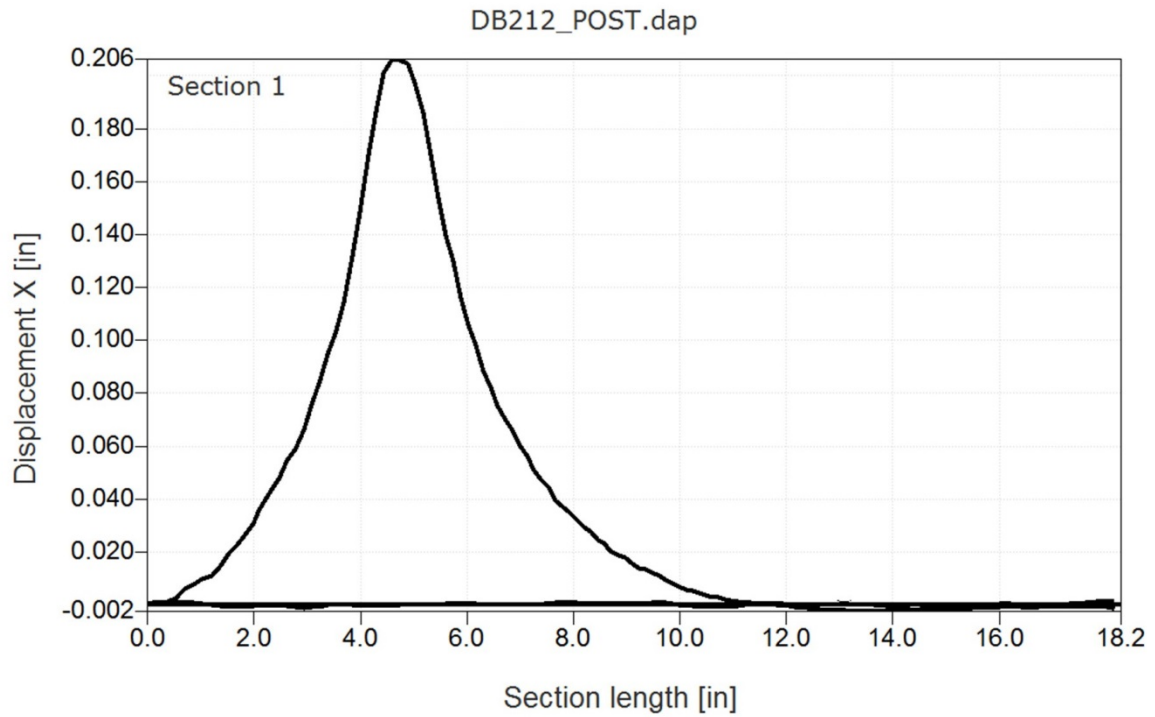


Figure A55.—Test DB212. Out-of-plane deformation along section line indicated in Figure A48. This indicates the plastic deformation along the section line after all movement has stopped.

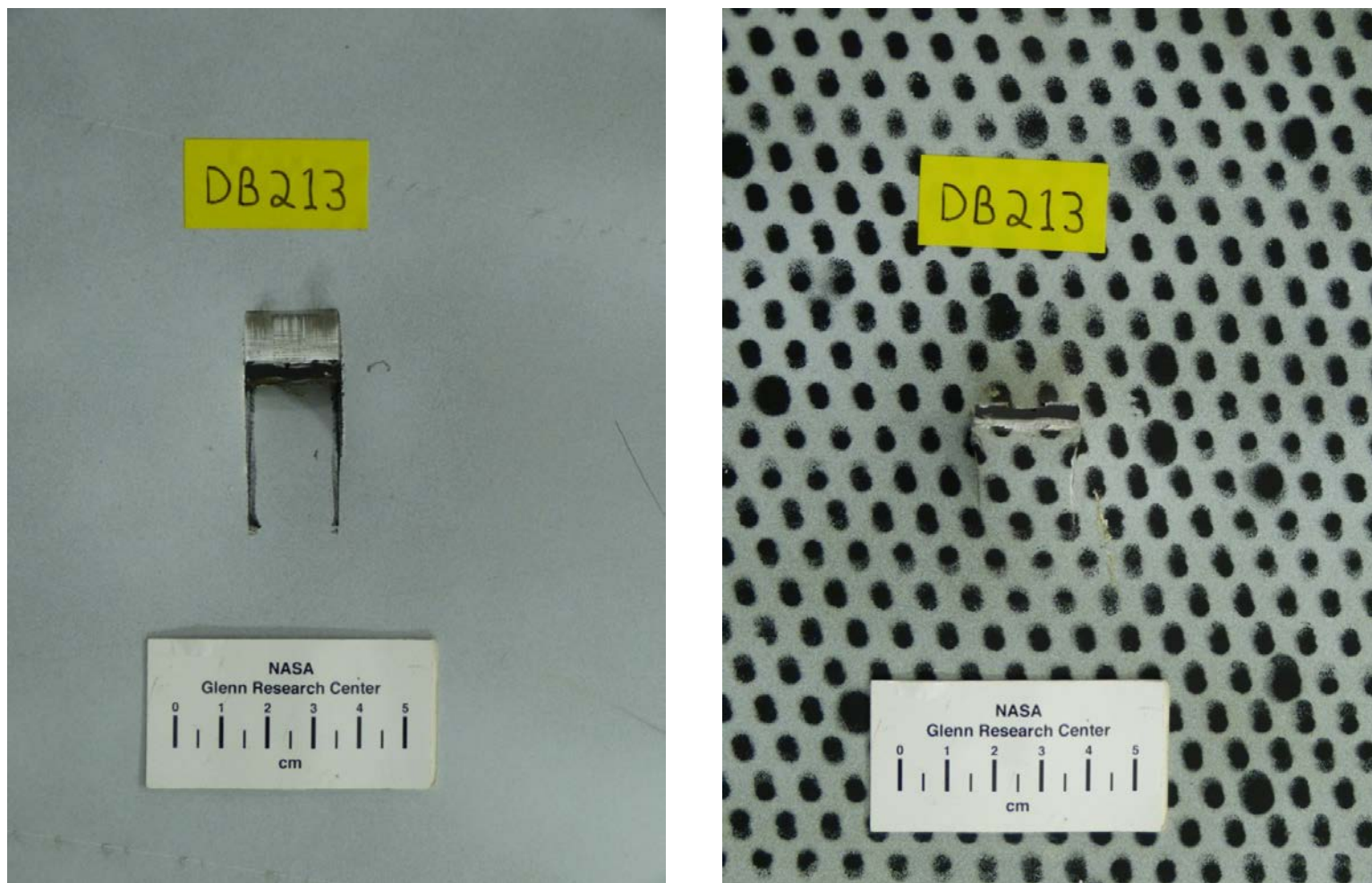


Figure A56.—Front (left) and back side views of impacted panel in test DB213.

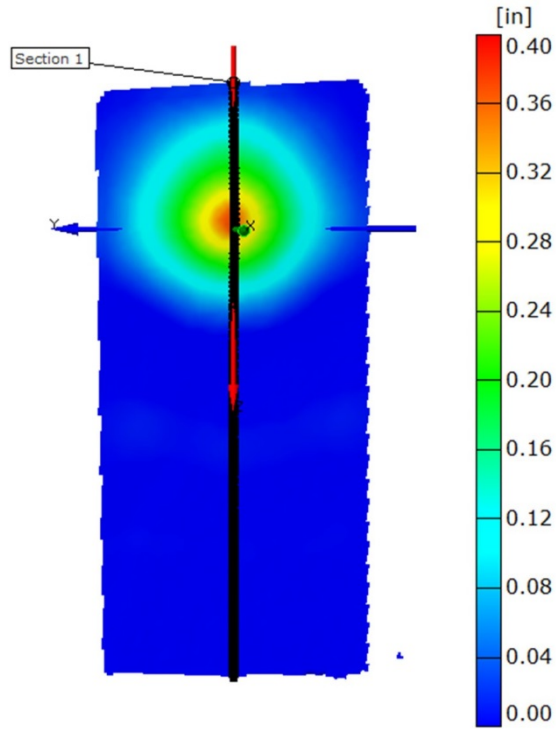


Figure A57.—Out-of-plane deformation map of panel in test DB213 just prior to initial failure.

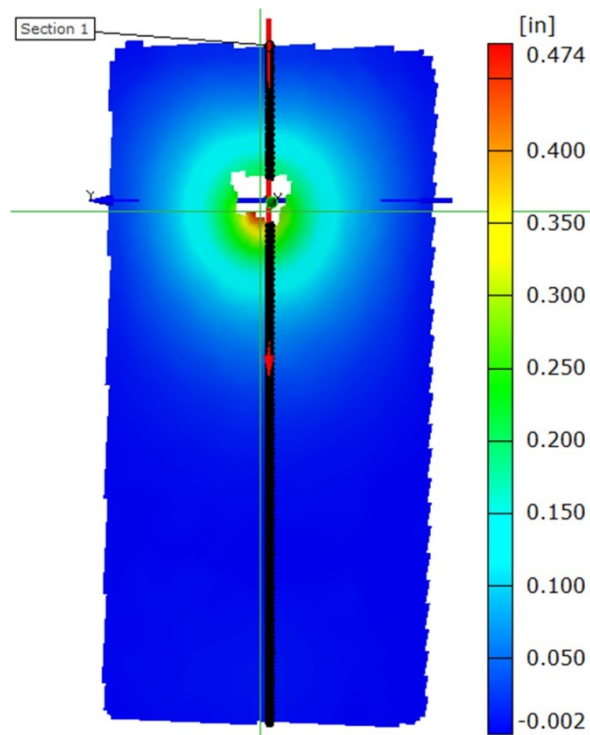


Figure A58.—Out-of-plane deformation map of panel in test DB213 after test is completed and all movement has stopped. This indicates the permanent deformation field.

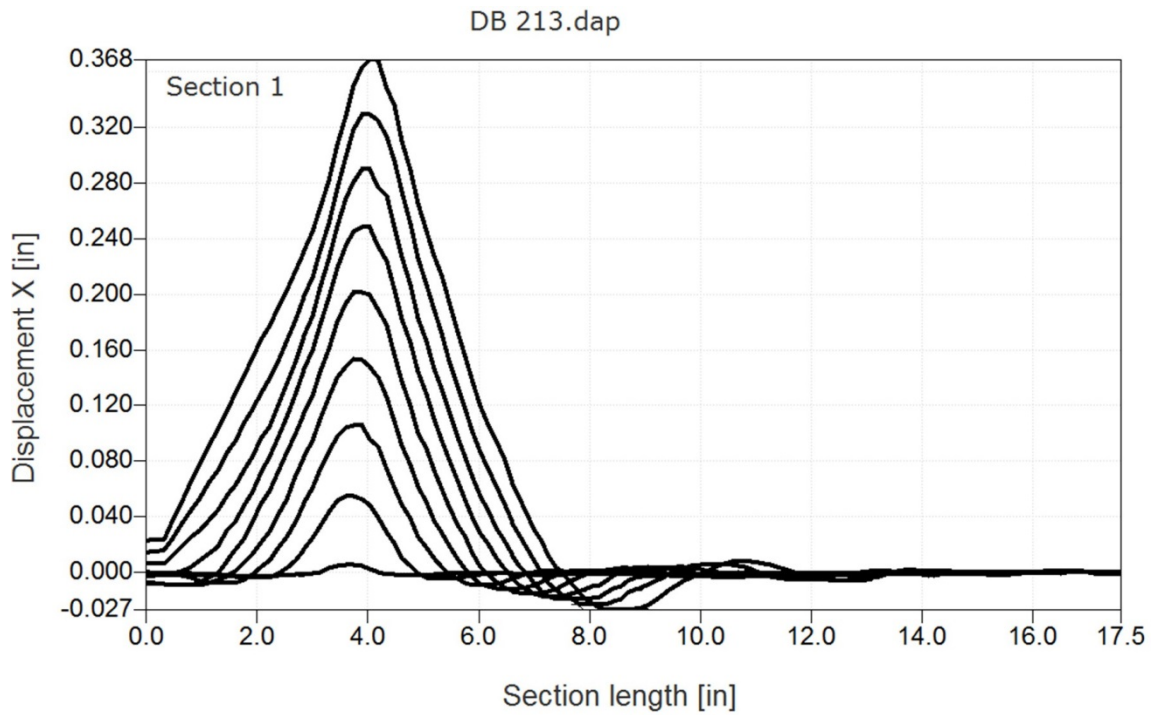


Figure A59.—Test DB213. Out-of-plane deformation along section line indicated in Figure A53 for a series of time steps up until the time of initial failure (frame rate 27000 frames/sec).

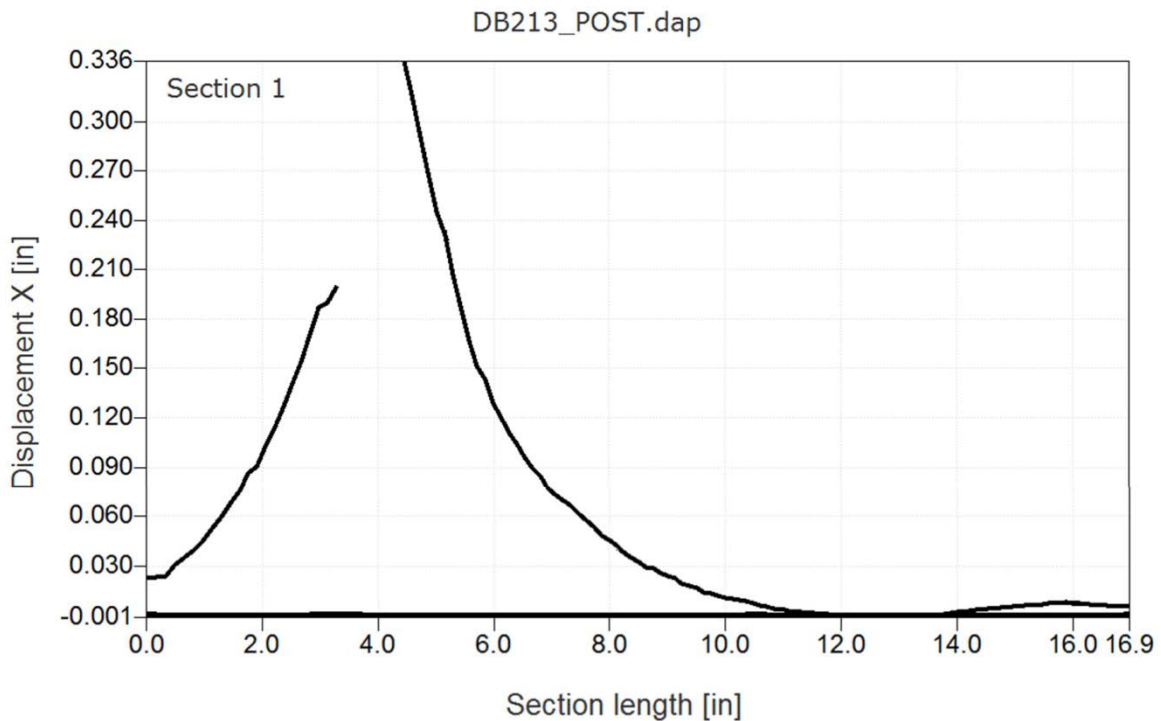


Figure A60.—Test DB213. Out-of-plane deformation along section line indicated in Figure A54. This indicates the plastic deformation along the section line after all movement has stopped.

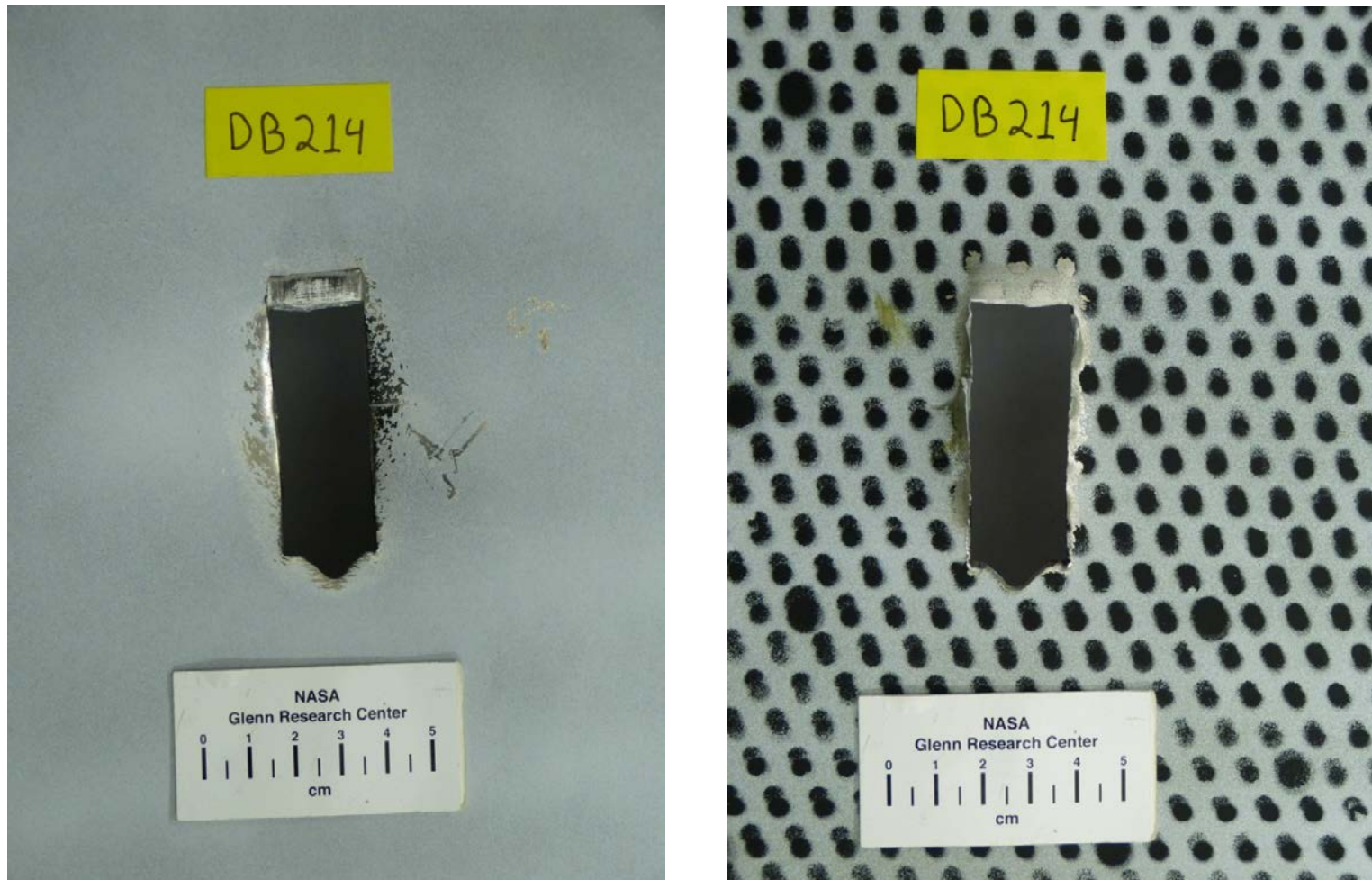


Figure A61.—Front (left) and back side views of impacted panel in test DB214.



Figure A62.—Front (left) and back side views of impacted panel in test DB215.

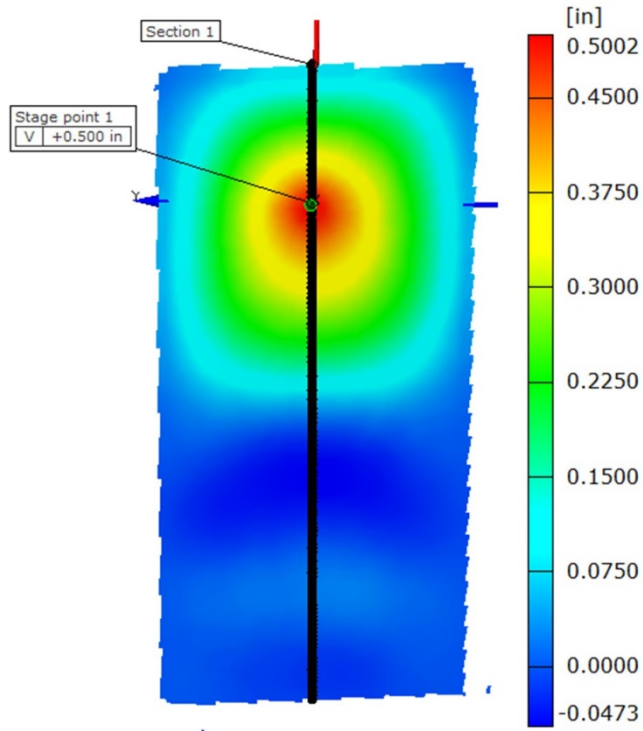


Figure A63.—Out-of-plane deformation map of panel in test DB215 at the point of maximum deflection.

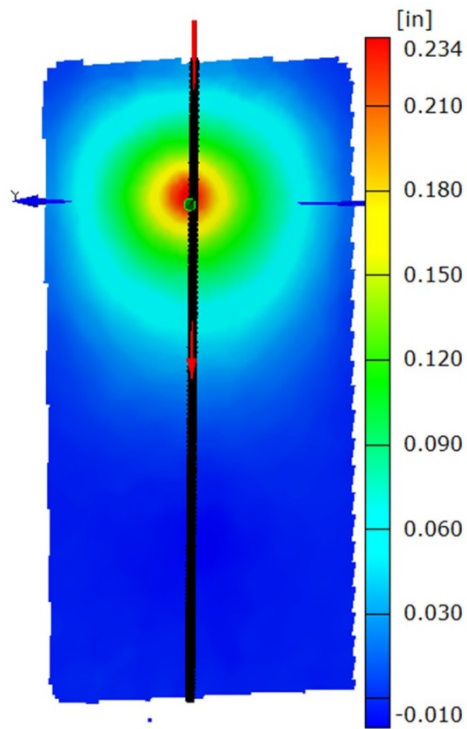


Figure A64.—Out-of-plane deformation map of panel in test DB215 after test is completed and all movement has stopped. This indicates the permanent deformation field.

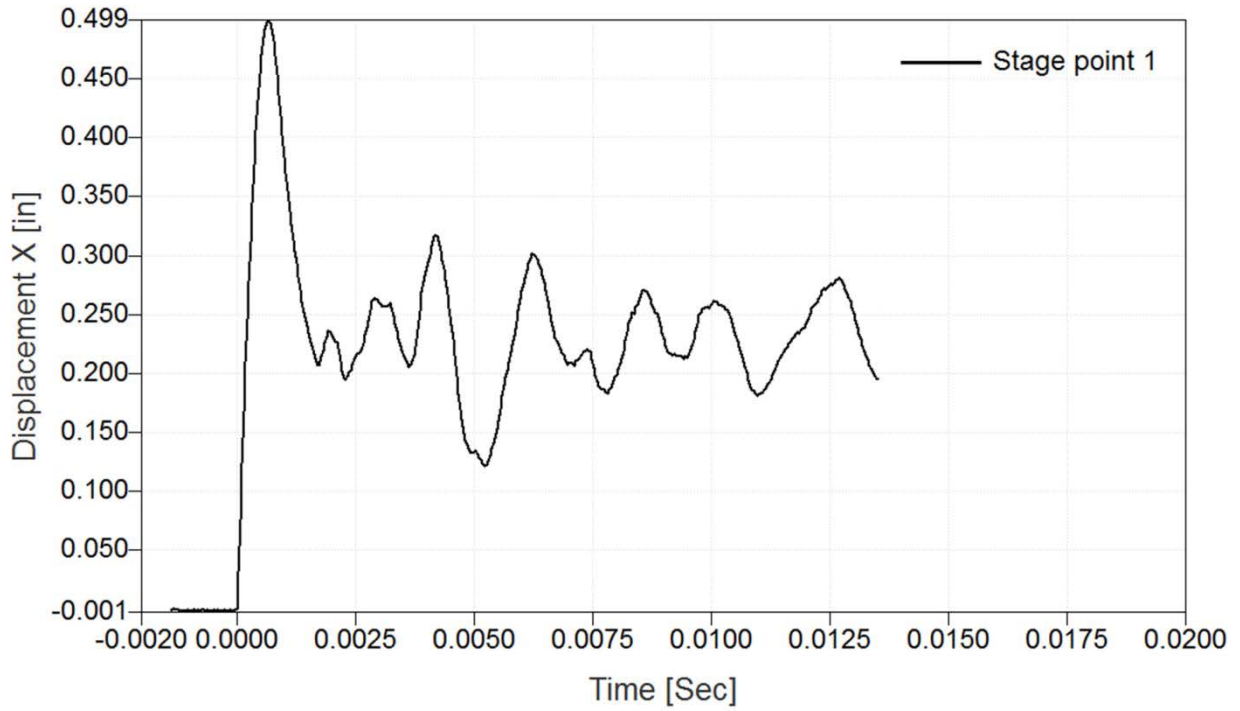


Figure A65.—Out-of-plane deformation as a function of time of point indicated in Figure A59 for test DB215.

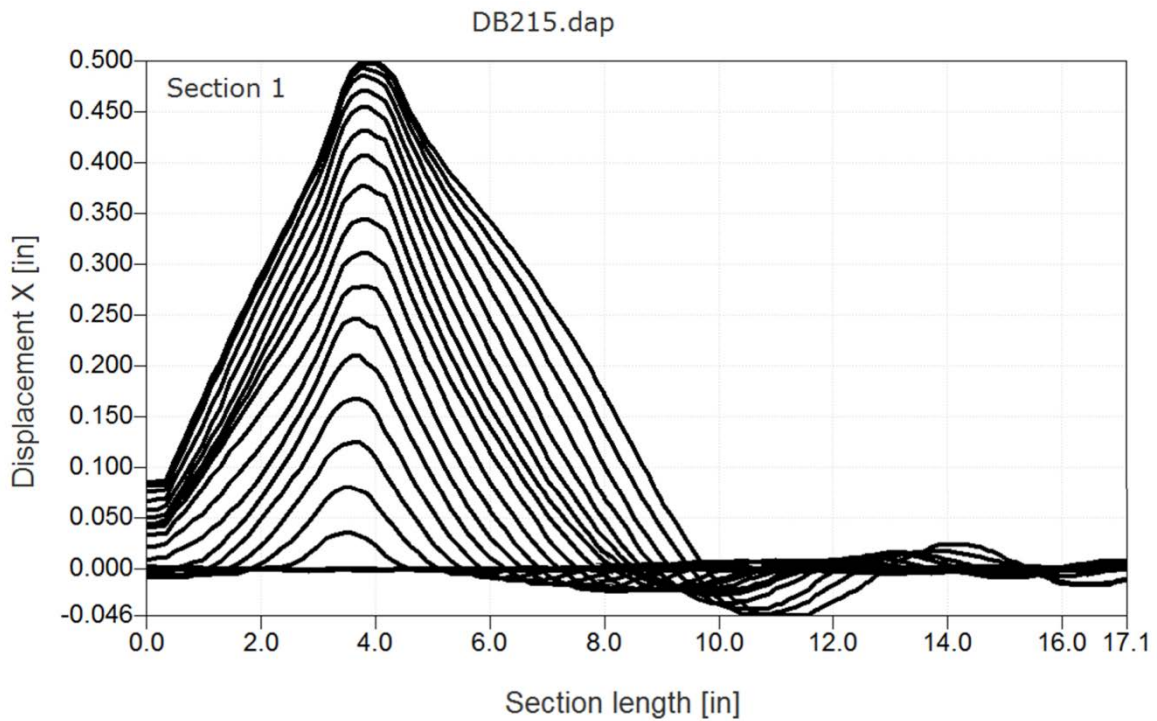


Figure A66.—Test DB215. Out-of-plane deformation along section line indicated in Figure A59 for a series of time steps up until the time of maximum deformation (frame rate 27000 frames/sec).

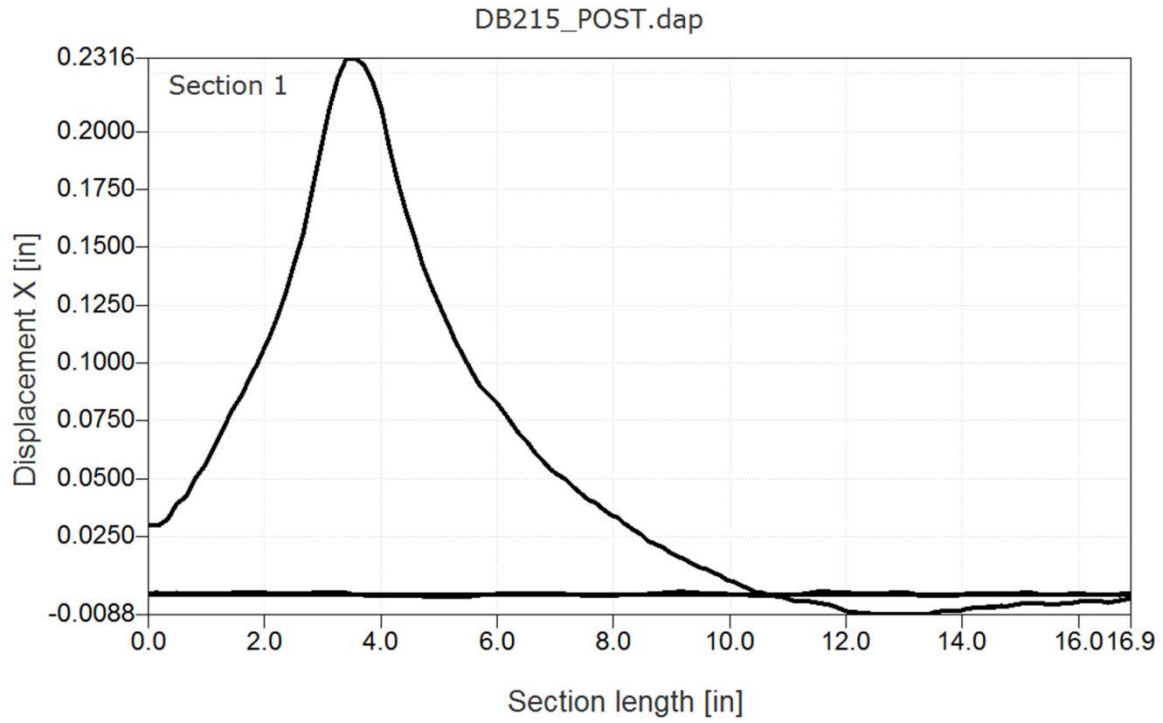


Figure A67.—Test DB215. Out-of-plane deformation along section line indicated in Figure A60. This indicates the plastic deformation along the section line after all movement has stopped.

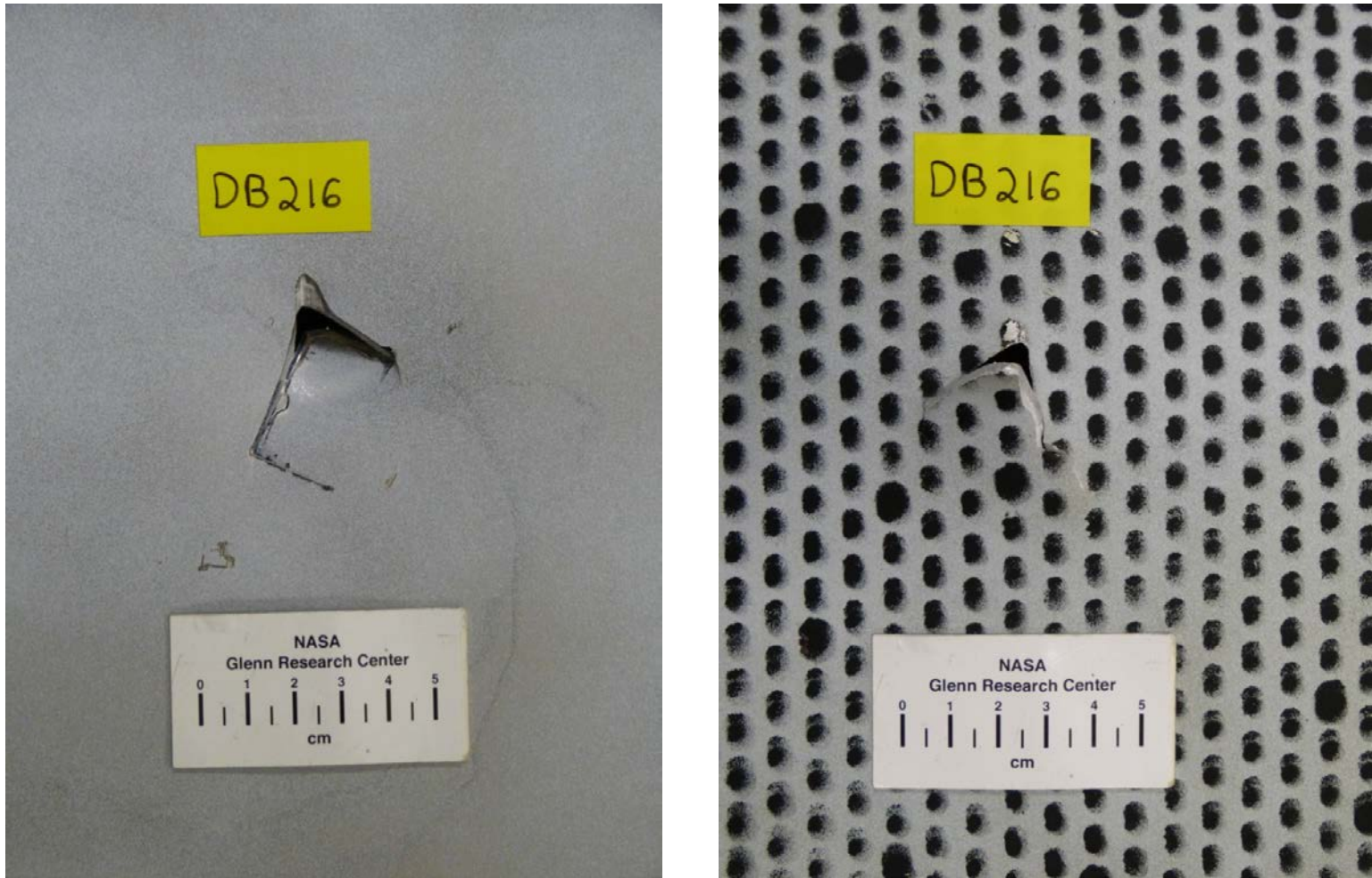


Figure A68.—Front (left) and back side views of impacted panel in test DB216.

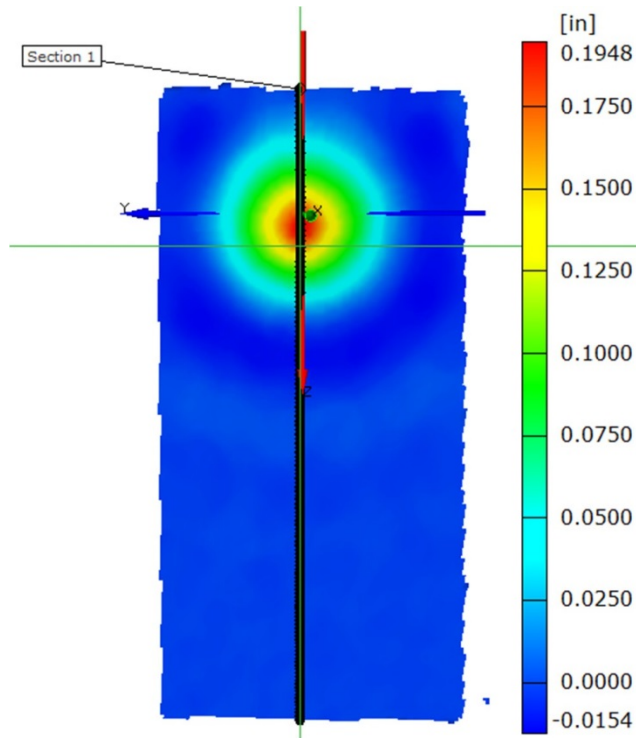


Figure A69.—Out-of-plane deformation map of panel in test DB216 at the point of maximum deflection prior to failure.

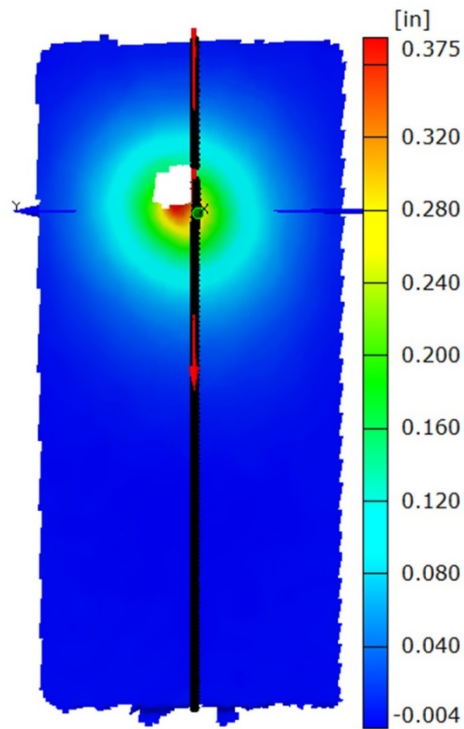


Figure A70.—Out-of-plane deformation map of panel in test DB216 after test is completed and all movement has stopped. This indicates the permanent deformation field.

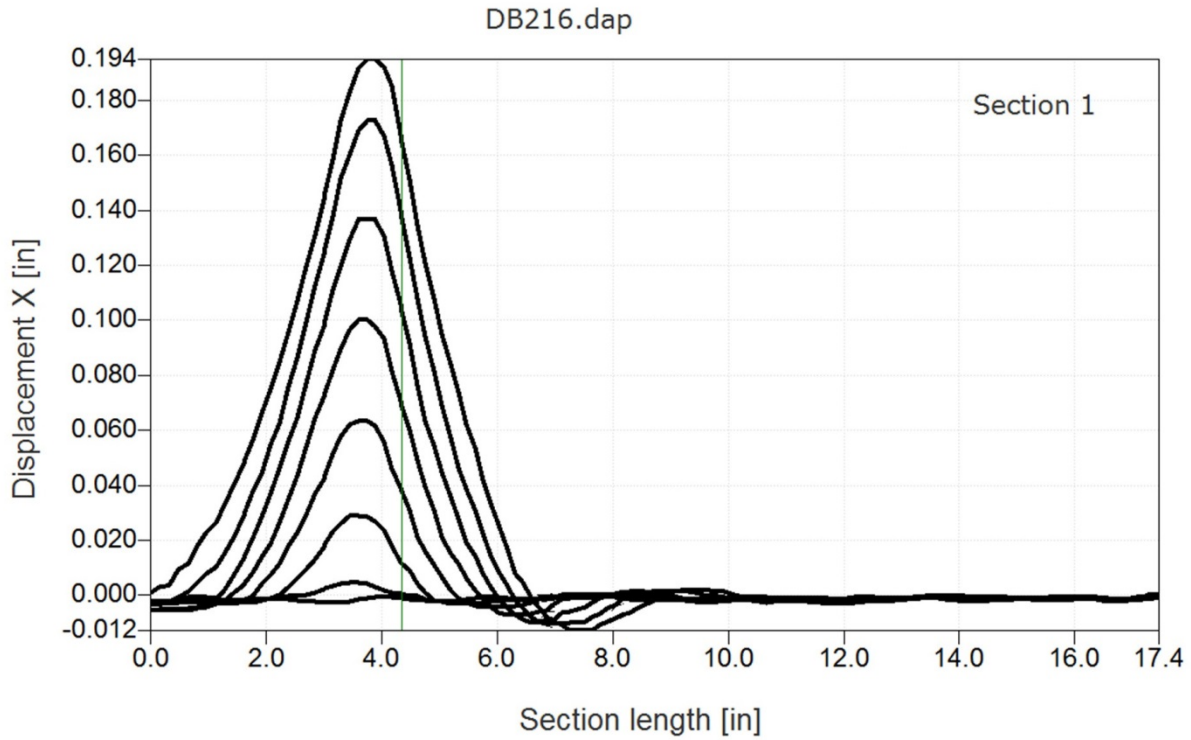


Figure A71.—Test DB216. Out-of-plane deformation along section line indicated in Figure A66 for a series of time steps up until the time of maximum deformation (frame rate 27000 frames/sec).

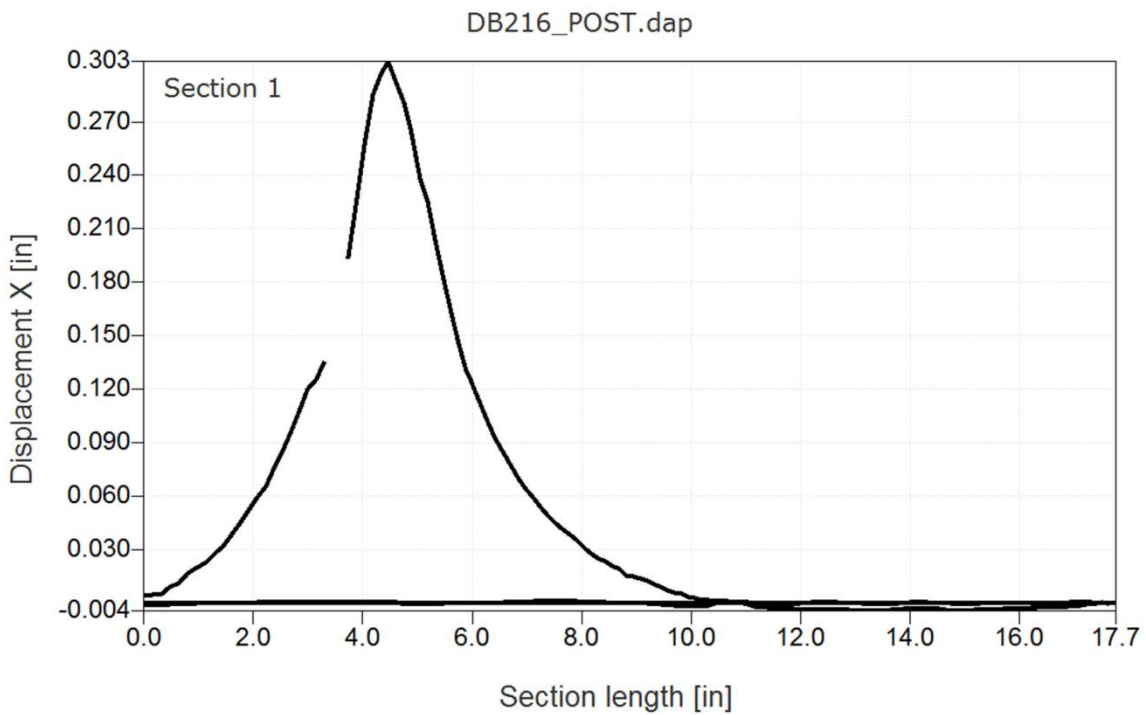


Figure A72.—Test DB216. Out-of-plane deformation along section line indicated in Figure A66. This indicates the plastic deformation along the section line after all movement has stopped.

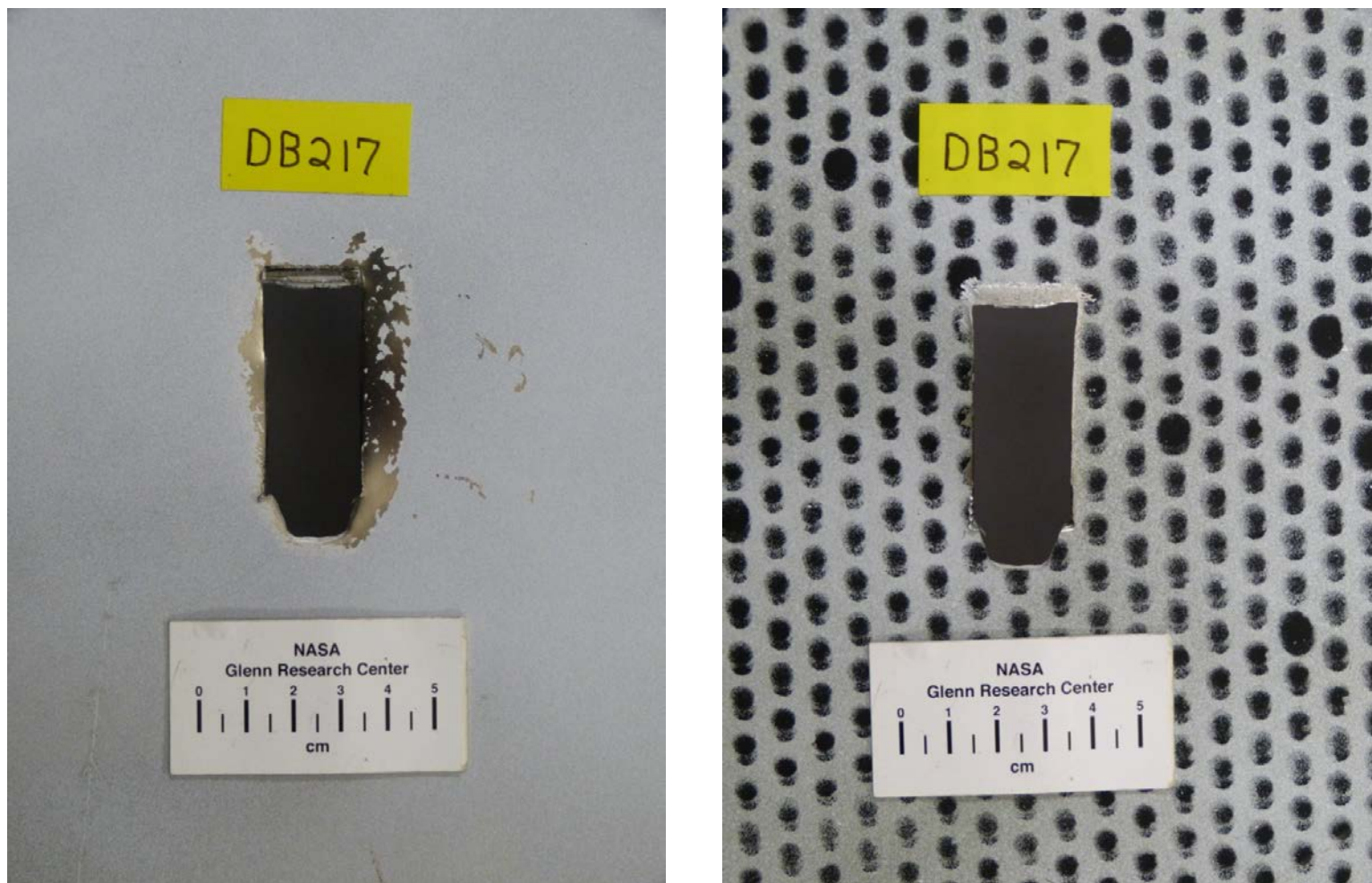


Figure A73.—Front (left) and back side views of impacted panel in test DB217.

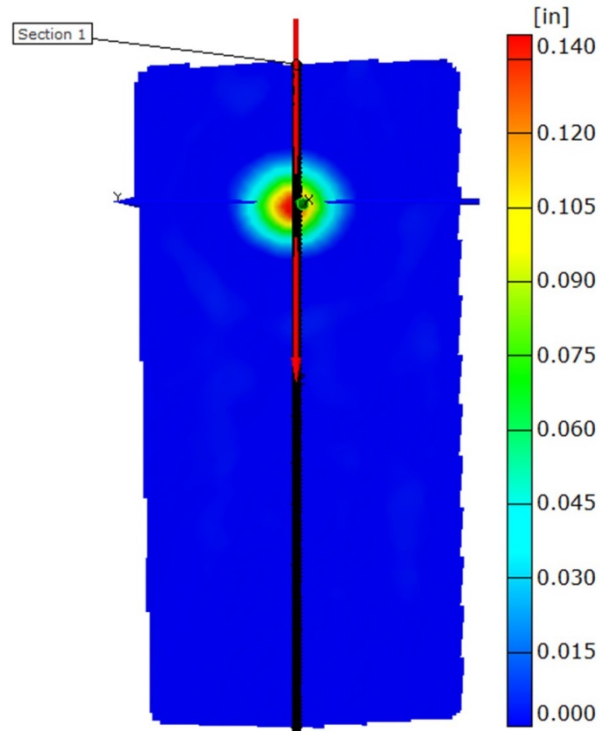


Figure A74.—Out-of-plane deformation map of panel in test DB217 at the point of maximum deflection prior to failure.

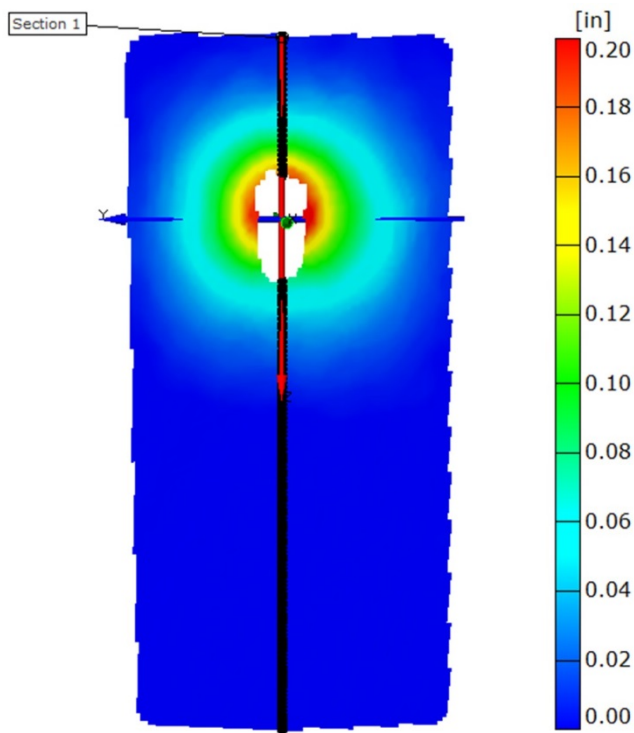


Figure A75.—Out-of-plane deformation map of panel in test DB217 after test is completed and all movement has stopped. This indicates the permanent deformation field.

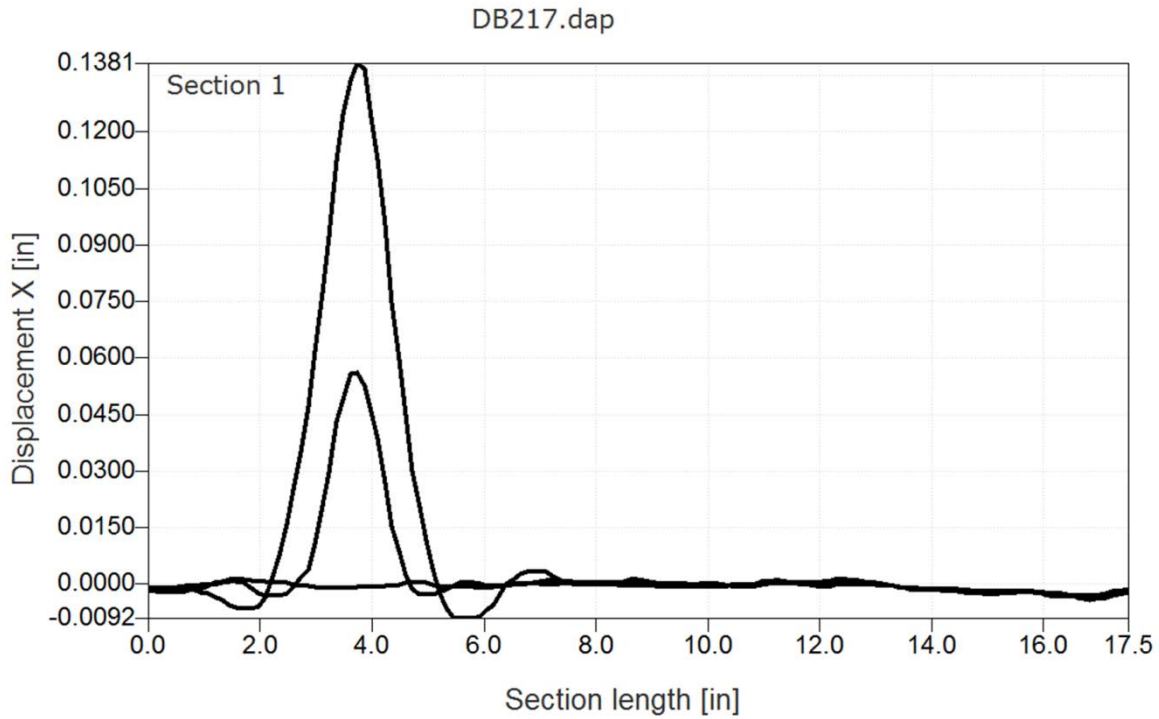


Figure A76.—Test DB217. Out-of-plane deformation along section line indicated in Figure A70 for a series of time steps up until the time of maximum deformation prior to failure (frame rate 27000 frames/sec).

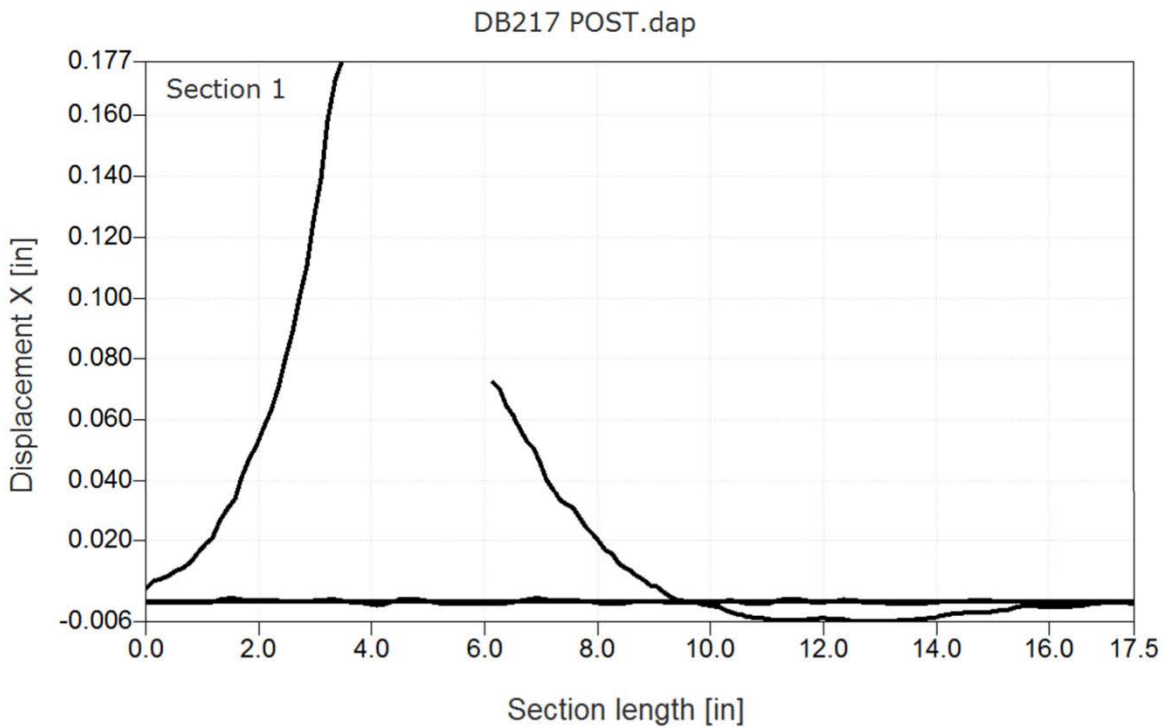


Figure A77.—Test DB217. Out-of-plane deformation along section line indicated in Figure A71. This indicates the plastic deformation along the section line after all movement has stopped.

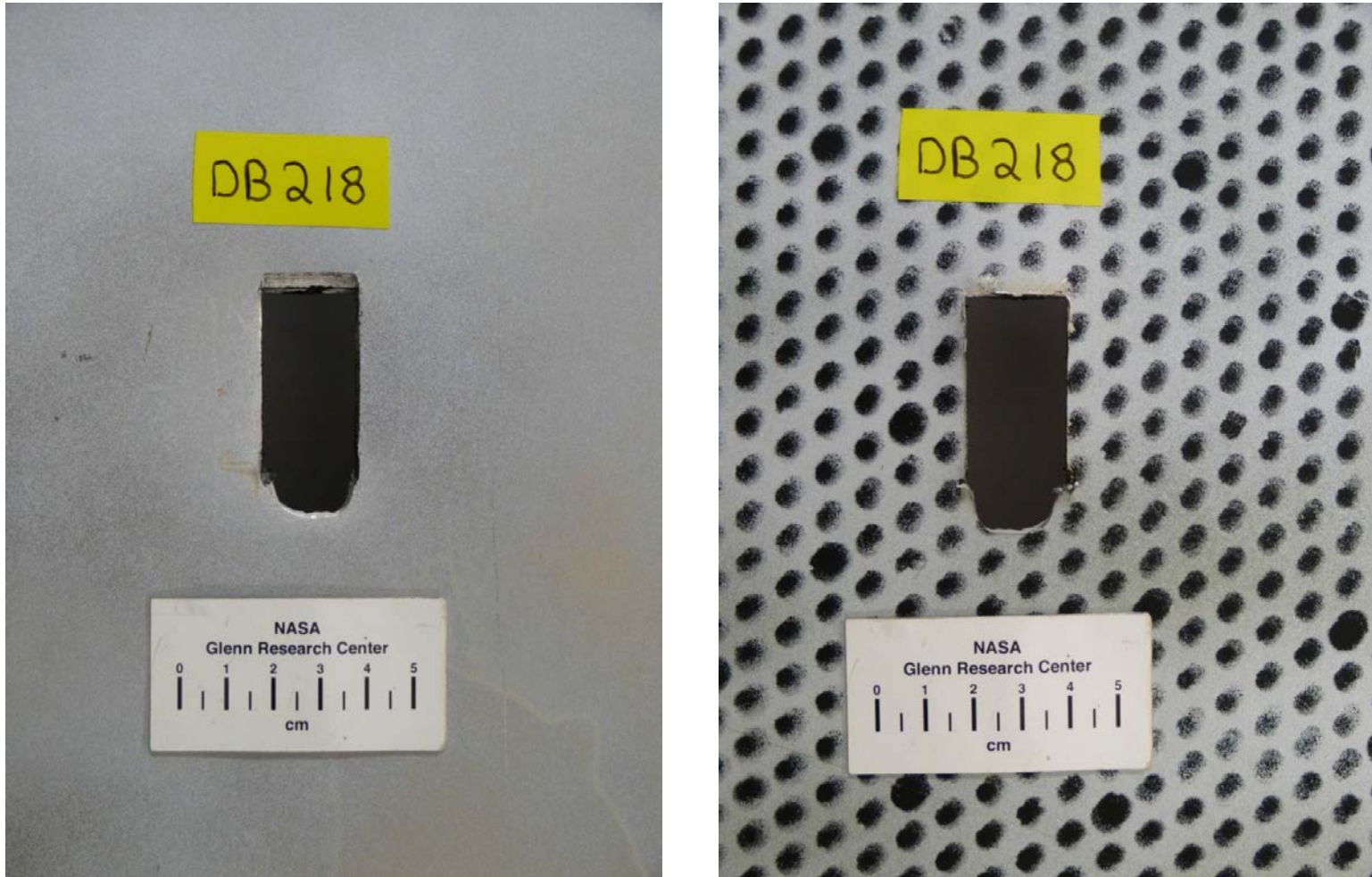


Figure A78.—Front (left) and back side views of impacted panel in test DB218.

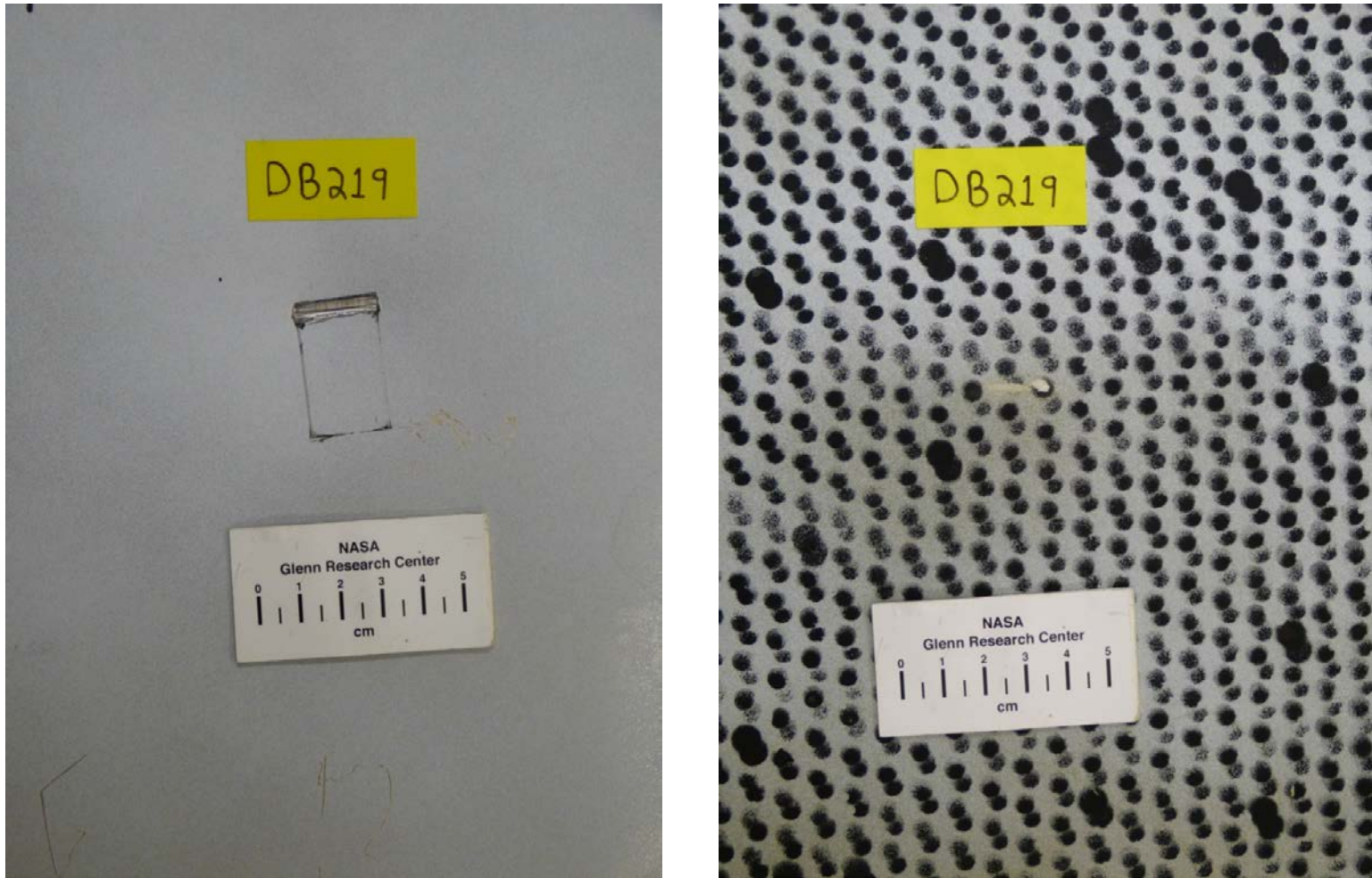


Figure A79.—Front (left) and back side views of impacted panel in test DB219.

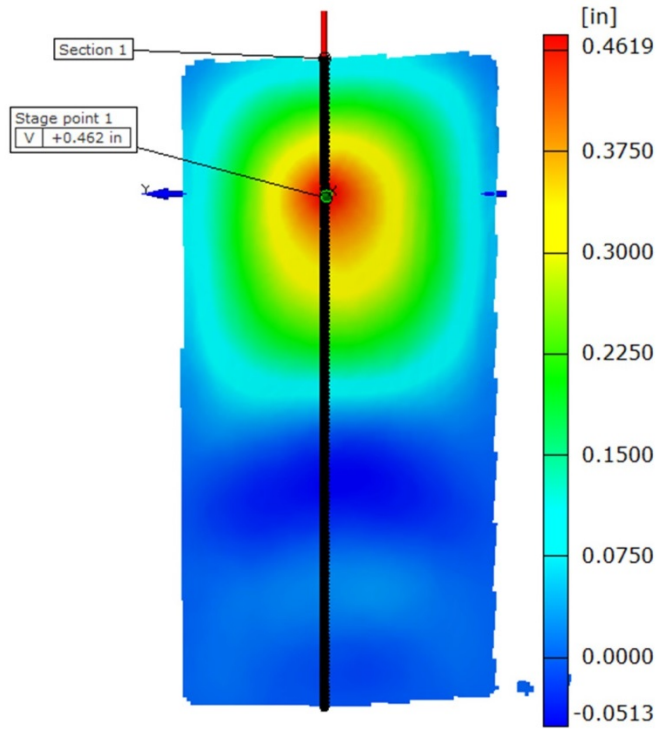


Figure A80.—Out-of-plane deformation map of panel in test DB217 at the point of maximum deflection.

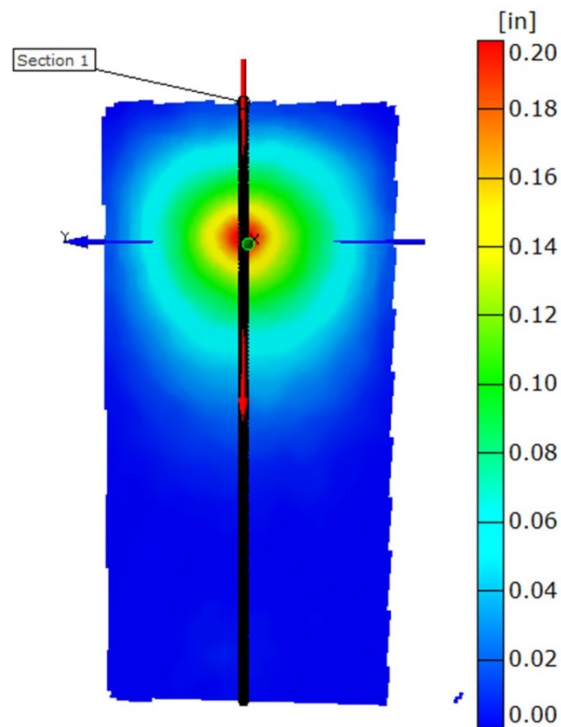


Figure A81.—Out-of-plane deformation map of panel in test DB219 after test is completed and all movement has stopped. This indicates the permanent deformation field.

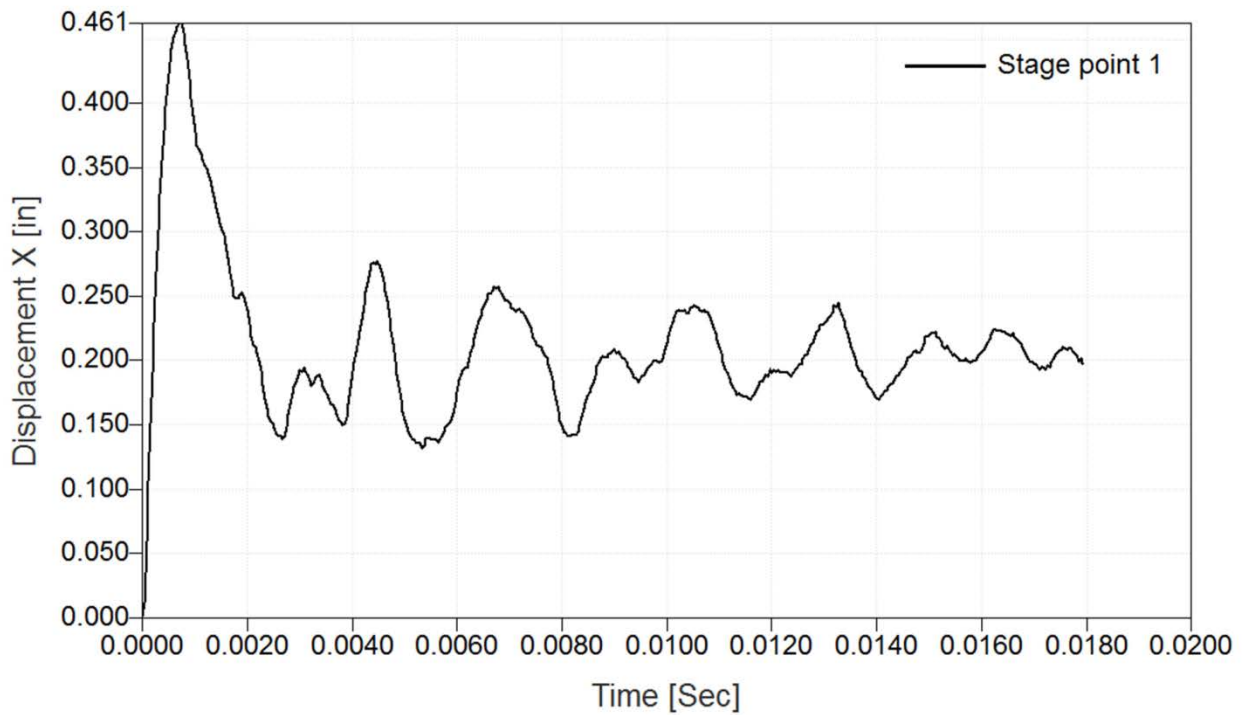


Figure A82.—Out-of-plane deformation as a function of time of point indicated in Figure A76 for test DB219.

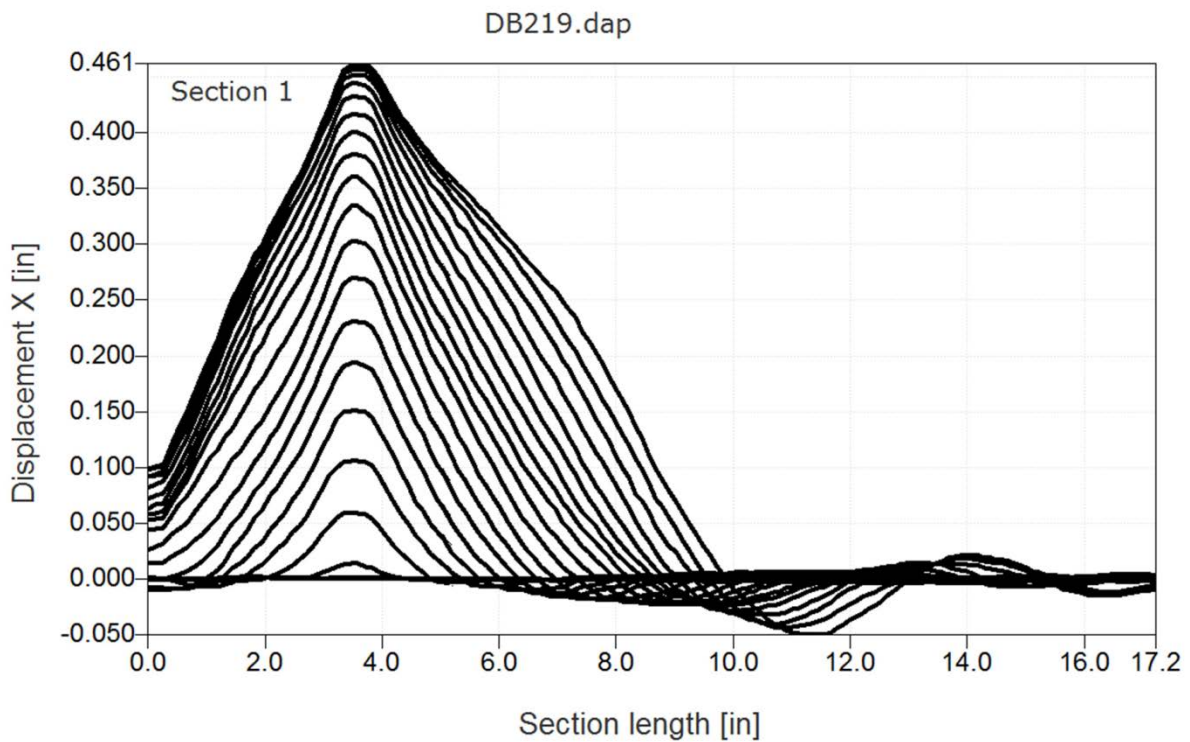


Figure A83.—Test DB219. Out-of-plane deformation along section line indicated in Figure A76 for a series of time steps up until the time of maximum deformation (frame rate 27000 frames/sec).

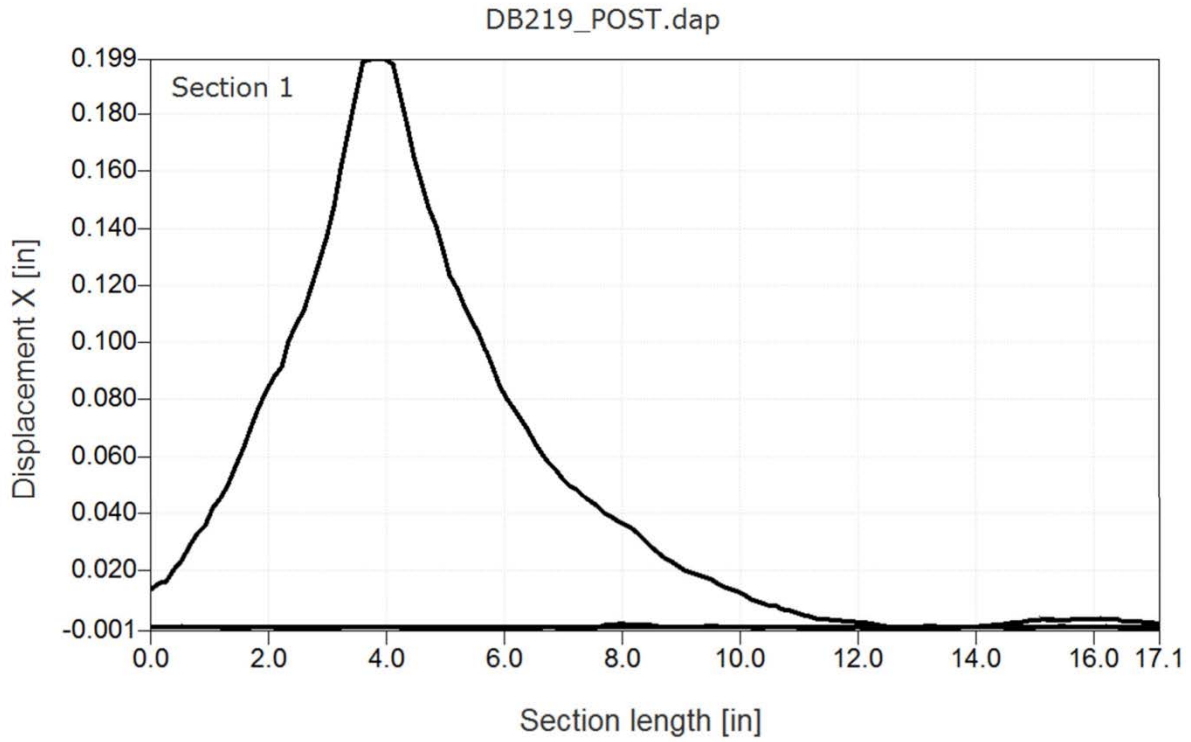


Figure A84.—Test DB219. Out-of-plane deformation along section line indicated in Figure A77. This indicates the plastic deformation along the section line after all movement has stopped.

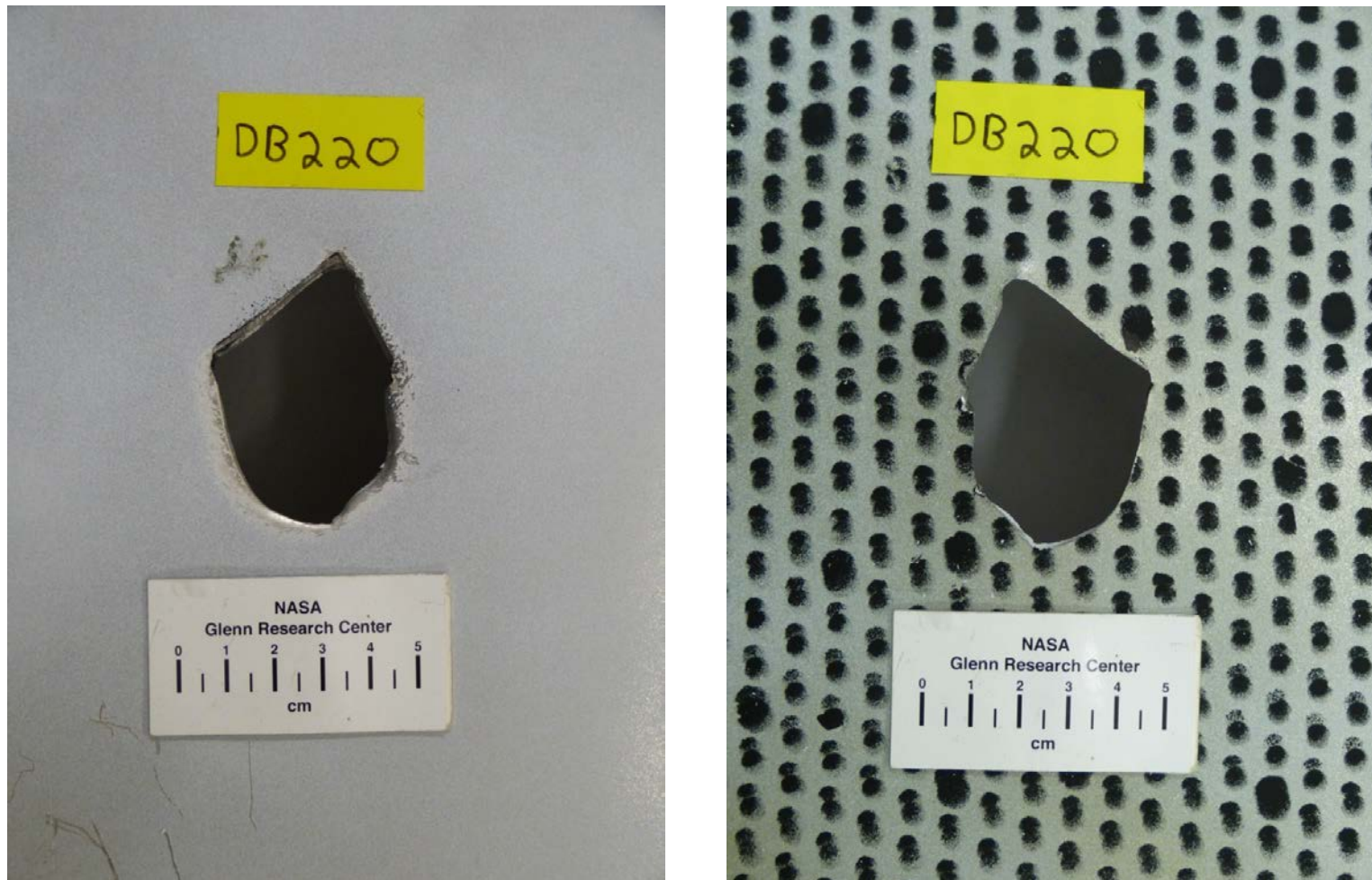


Figure A85.—Front (left) and back side views of impacted panel in test DB220.

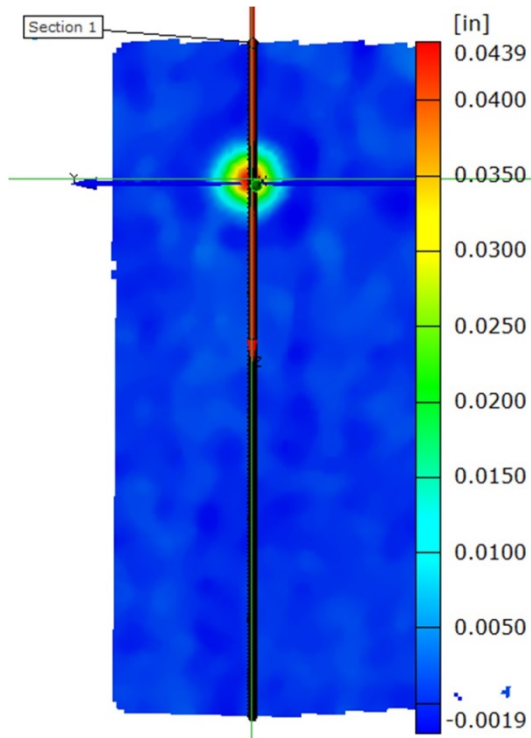


Figure A86.—Out-of-plane deformation map of panel in test DB220 at the point of maximum deflection prior to failure.

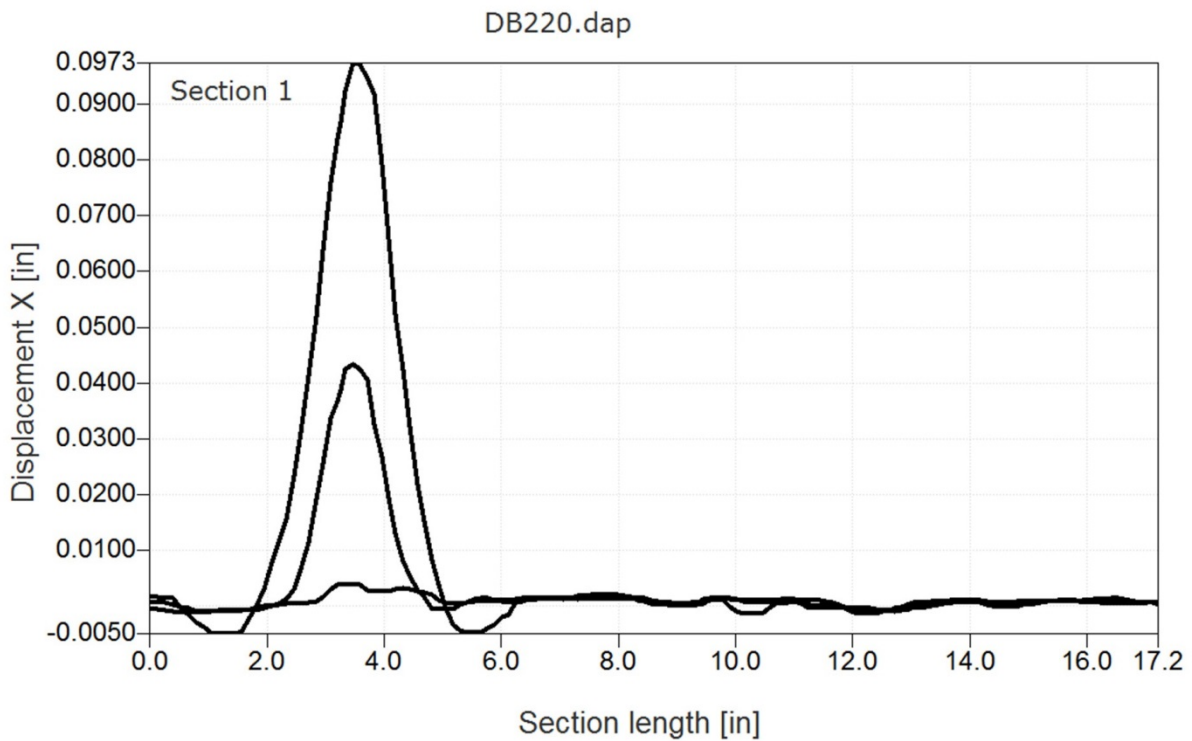


Figure A87.—Test DB220. Out-of-plane deformation along section line indicated in Figure A82 for a series of time steps up until the time of maximum deformation prior to failure (frame rate 27000 frames/sec).

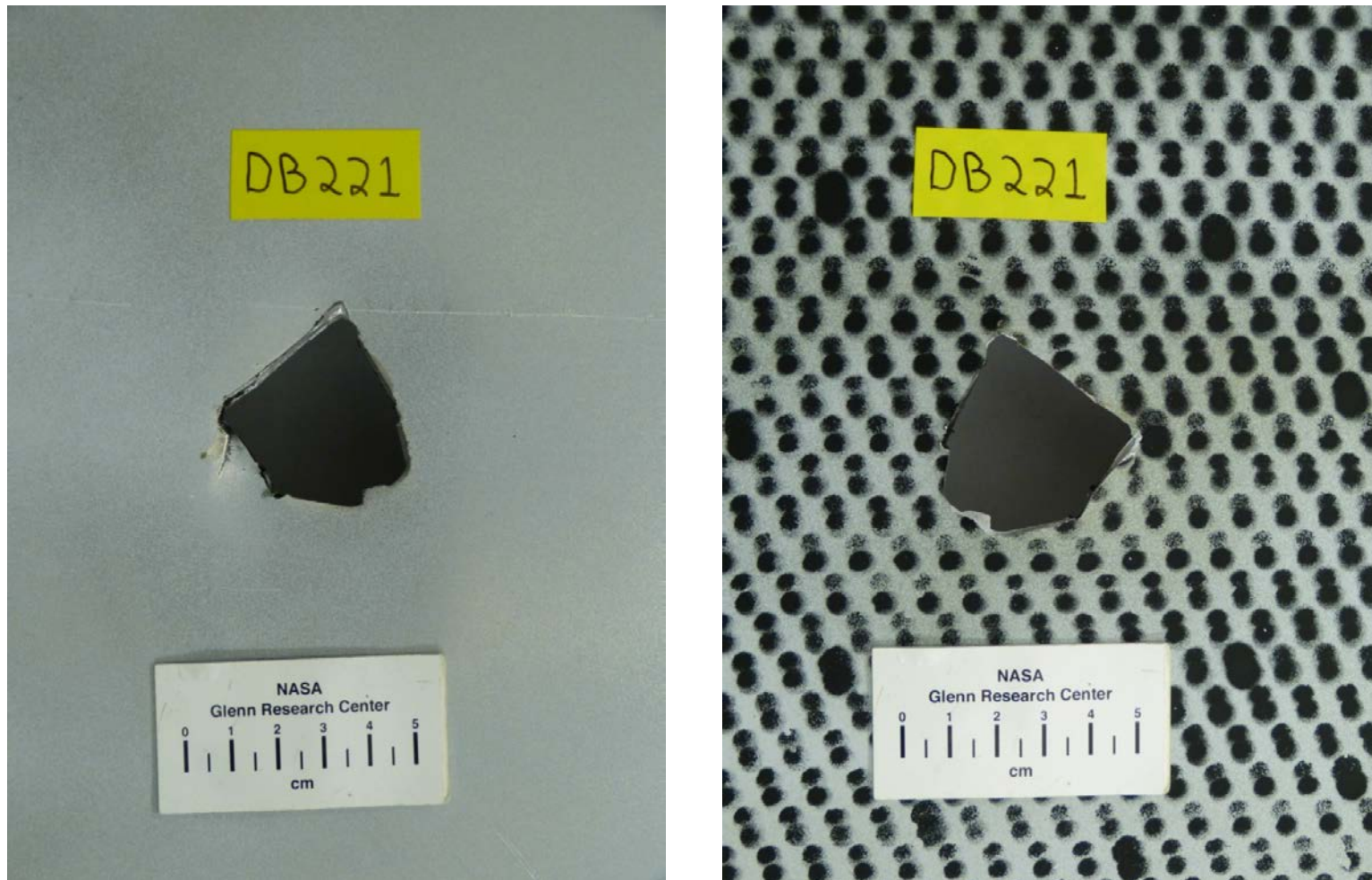


Figure A88.—Front (left) and back side views of impacted panel in test DB221.

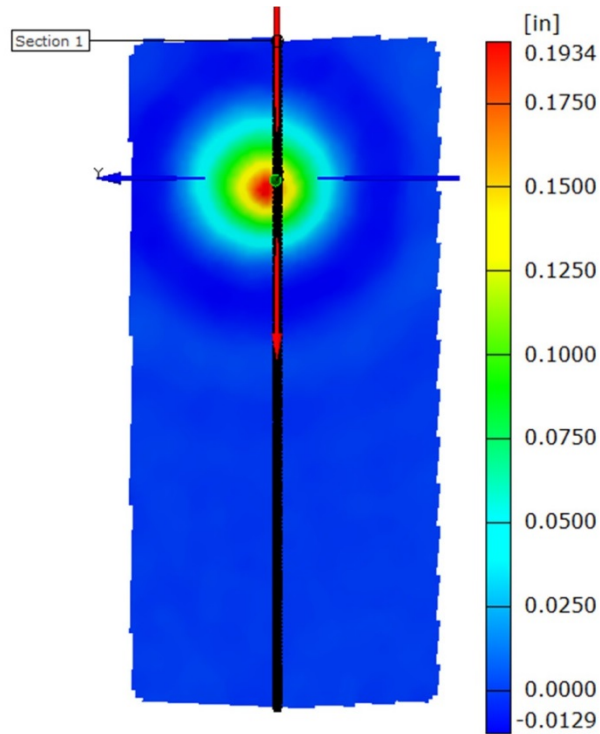


Figure A89.—Out-of-plane deformation map of panel in test DB221 at the point of maximum deflection prior to failure.

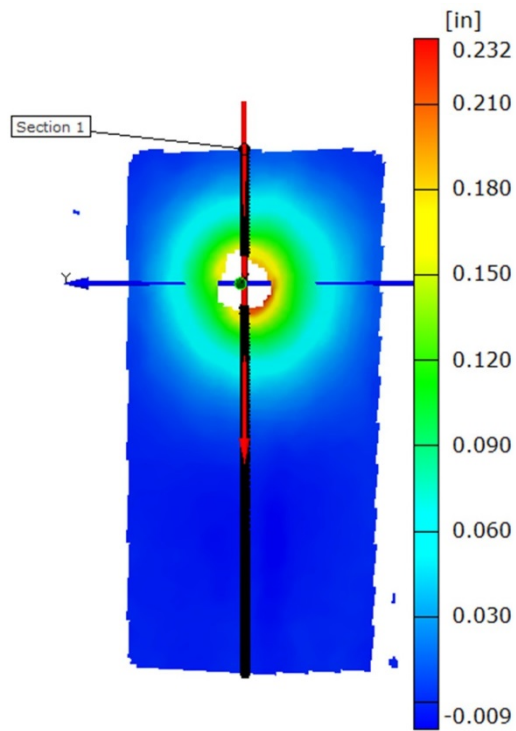


Figure A90.—Out-of-plane deformation map of panel in test DB221 after test is completed and all movement has stopped. This indicates the permanent deformation field.

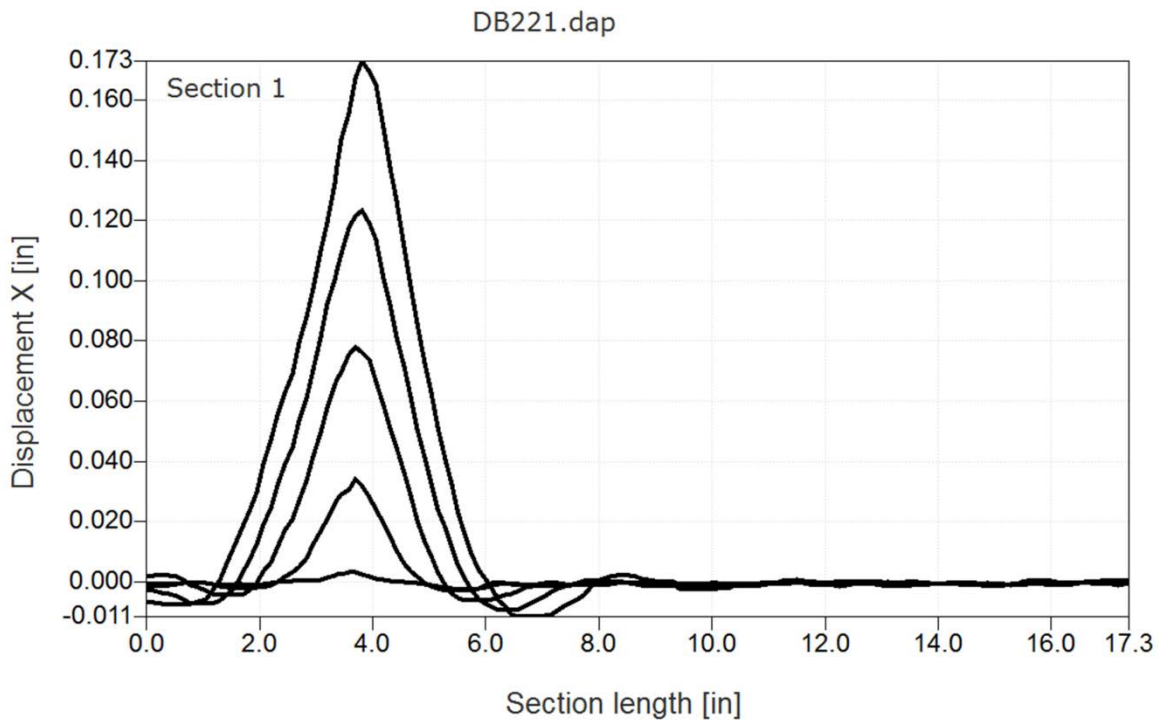


Figure A91.—Test DB221. Out-of-plane deformation along section line indicated in Figure A85 for a series of time steps up until the time of maximum deformation prior to failure (frame rate 27000 frames/sec).

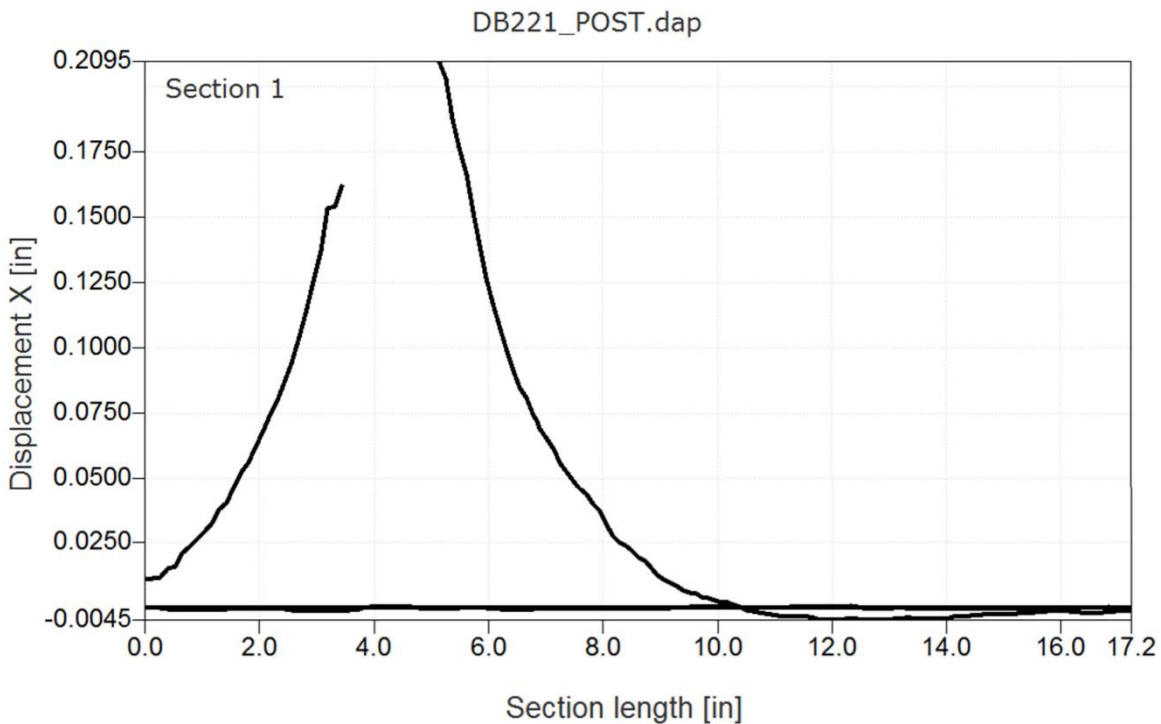


Figure A92.—Test DB221. Out-of-plane deformation along section line indicated in Figure A86. This indicates the plastic deformation along the section line after all movement has stopped.



Figure A93.—Front (left) and back side views of impacted panel in test DB222.

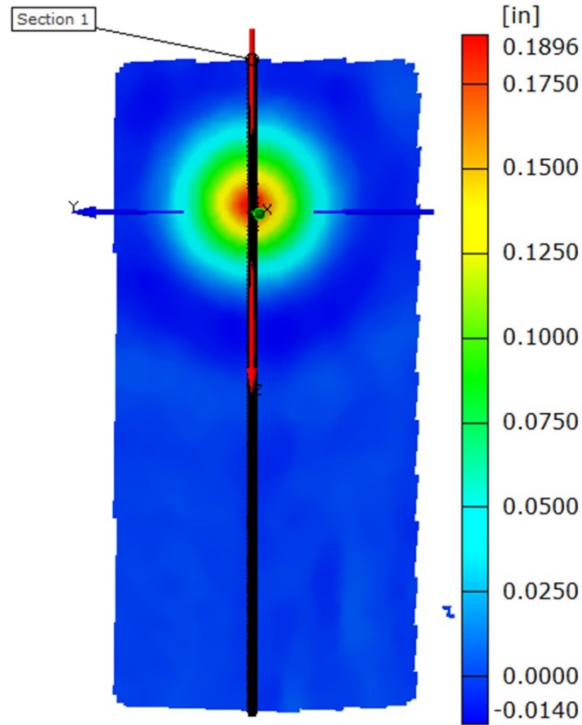


Figure A94.—Out-of-plane deformation map of panel in test DB222 at the point of maximum deflection prior to failure.

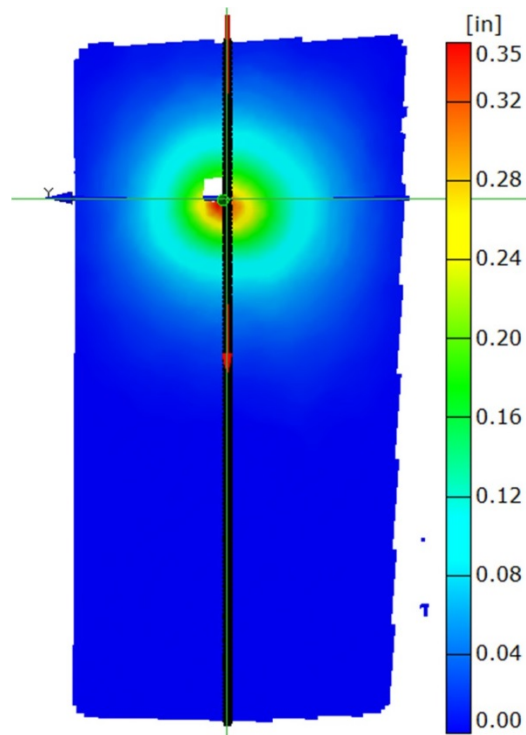


Figure A95.—Out-of-plane deformation map of panel in test DB222 after test is completed and all movement has stopped. This indicates the permanent deformation field.

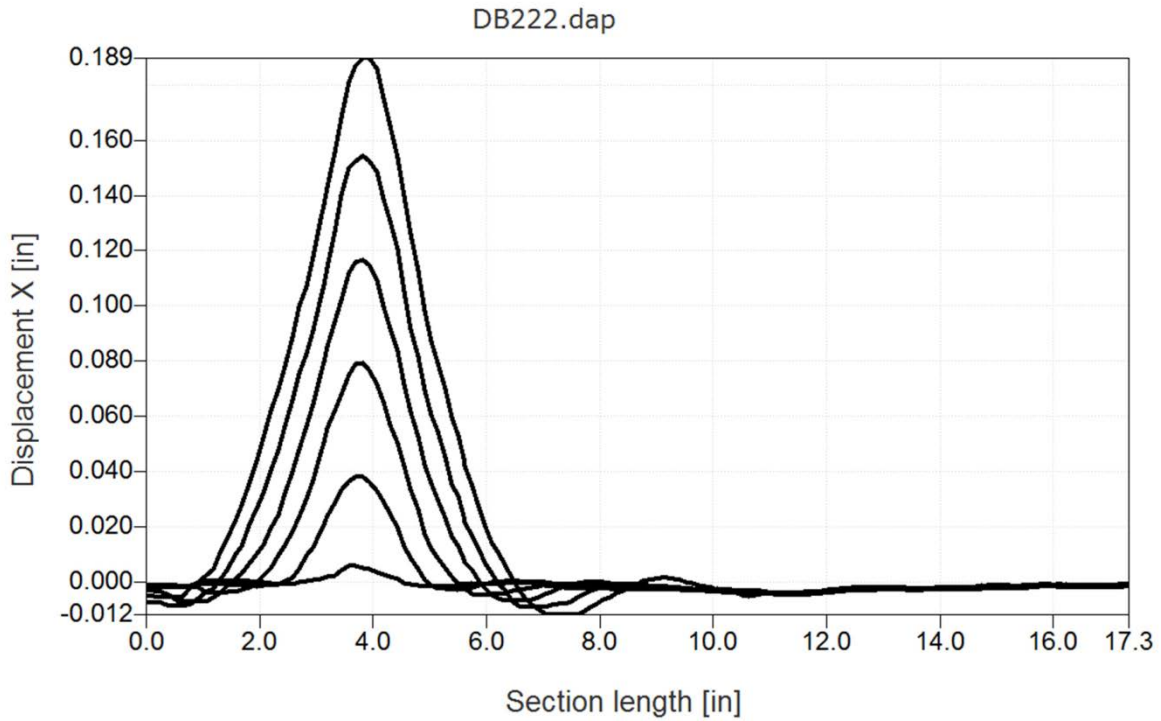


Figure A96.—Test DB222. Out-of-plane deformation along section line indicated in Figure A90 for a series of time steps up until the time of maximum deformation prior to failure (frame rate 27000 frames/sec).

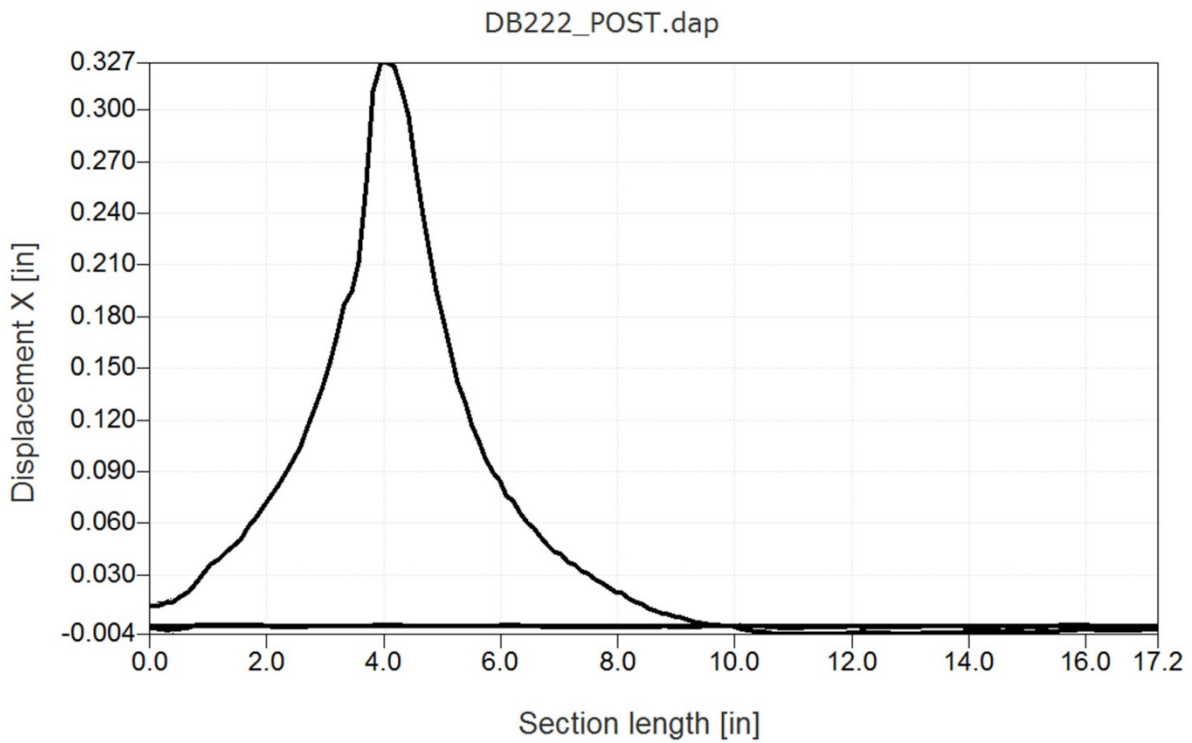


Figure A97.—Test DB222. Out-of-plane deformation along section line indicated in Figure A91. This indicates the plastic deformation along the section line after all movement has stopped.

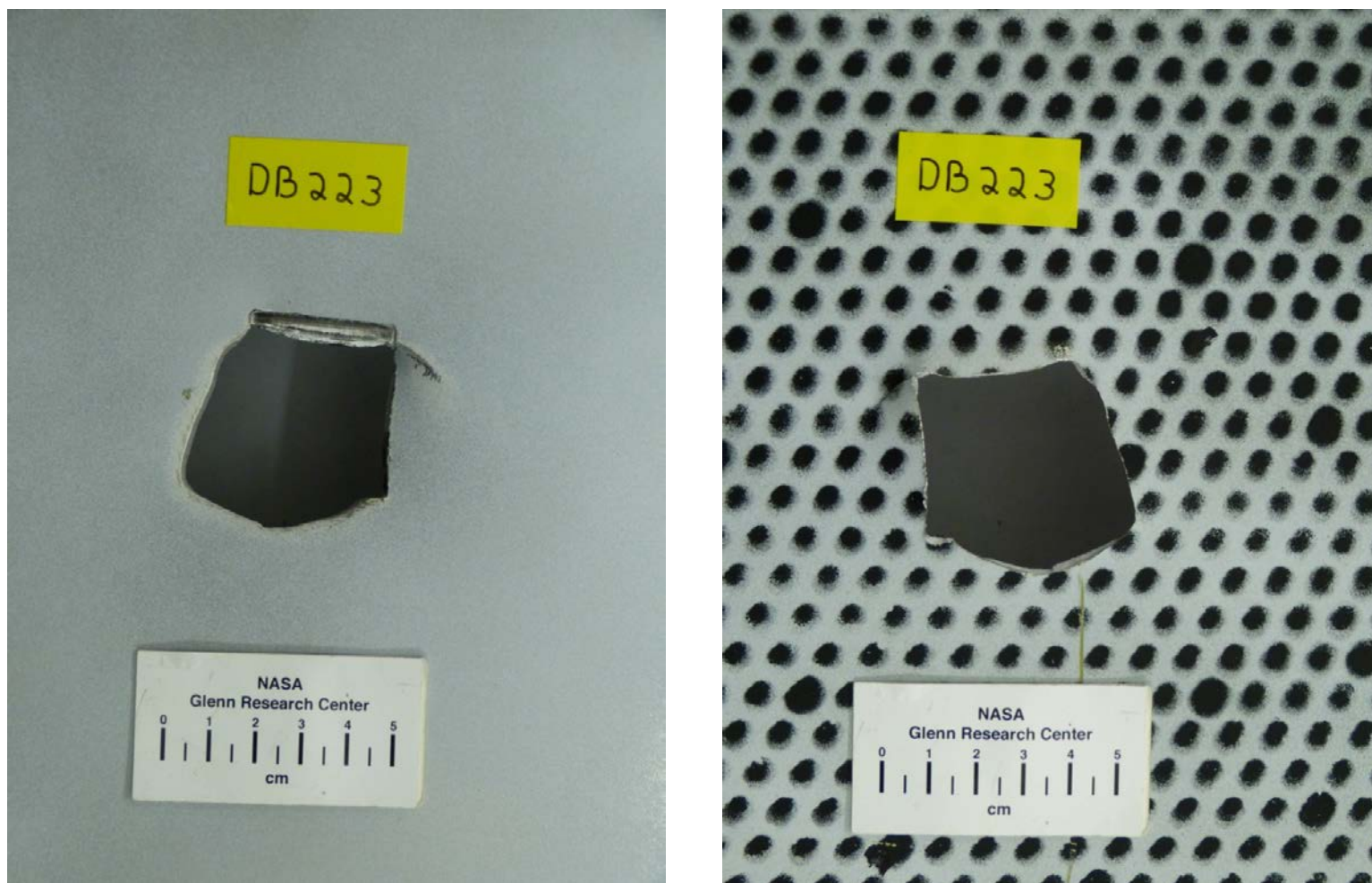


Figure A98.—Front (left) and back side views of impacted panel in test DB223.

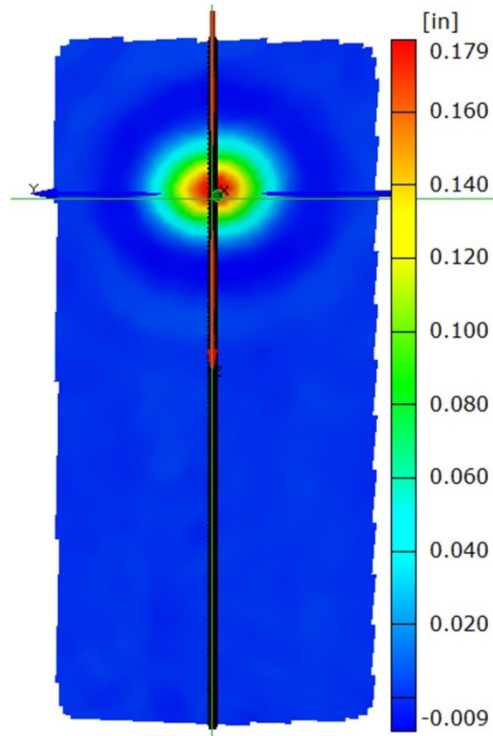


Figure A99.—Out-of-plane deformation map of panel in test DB223 at the point of maximum deflection prior to failure.

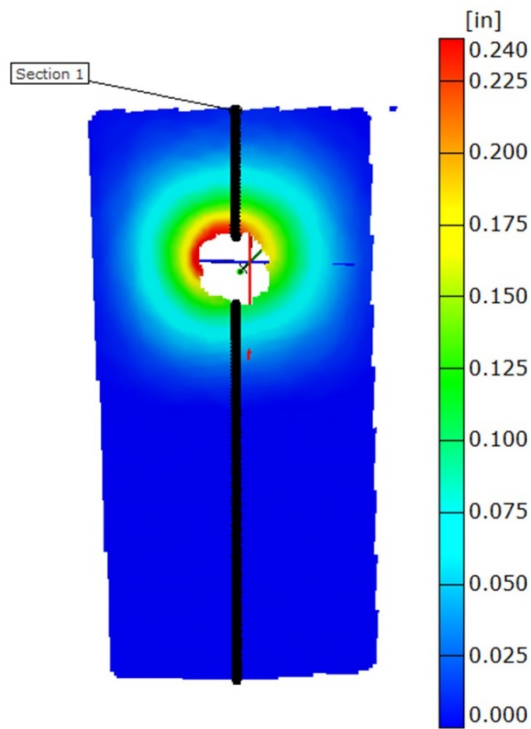


Figure A100.—Out-of-plane deformation map of panel in test DB223 after test is completed and all movement has stopped. This indicates the permanent deformation field.

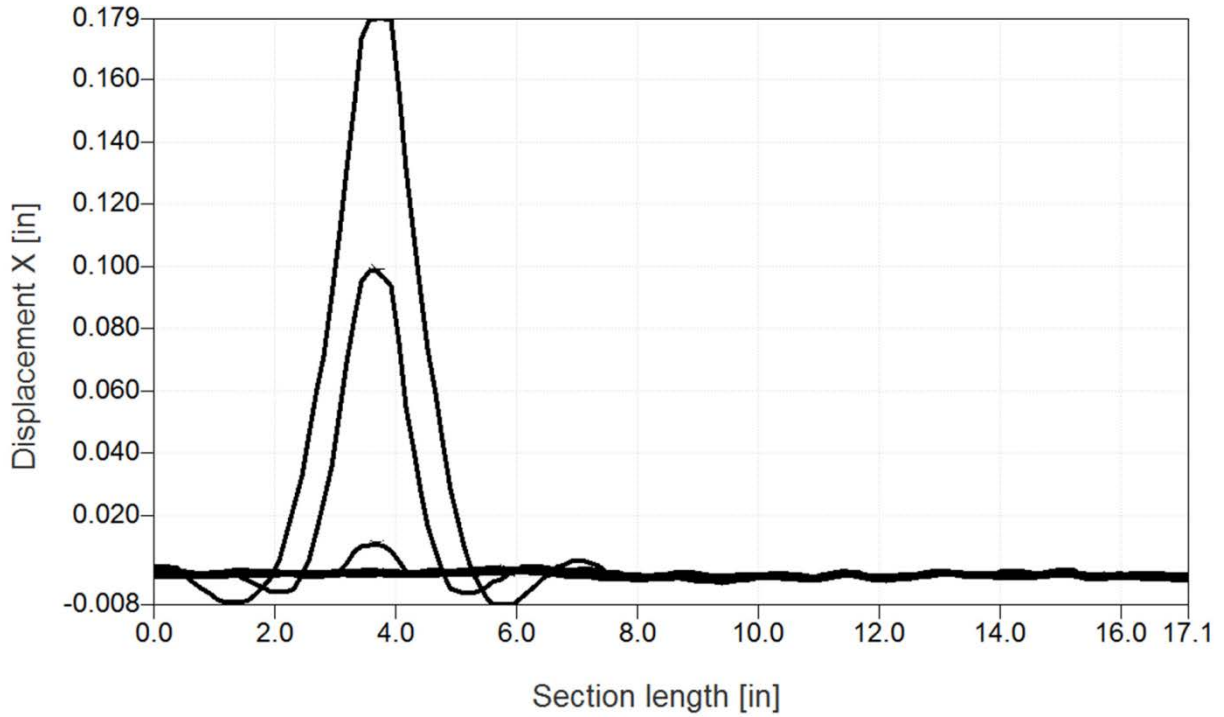


Figure A101.—Test DB223. Out-of-plane deformation along section line indicated in Figure A95 for a series of time steps up until the time of maximum deformation prior to failure (frame rate 27000 frames/sec).

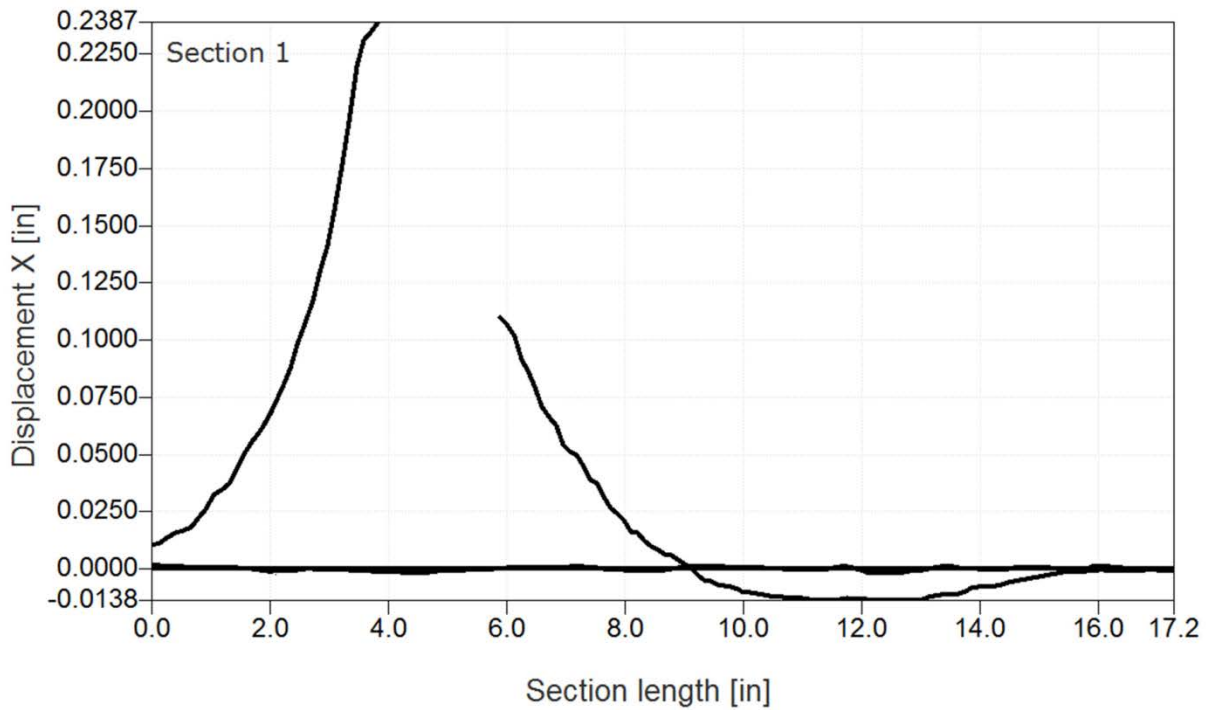


Figure A102.—Test DB223. Out-of-plane deformation along section line indicated in Figure A96. This indicates the plastic deformation along the section line after all movement has stopped.

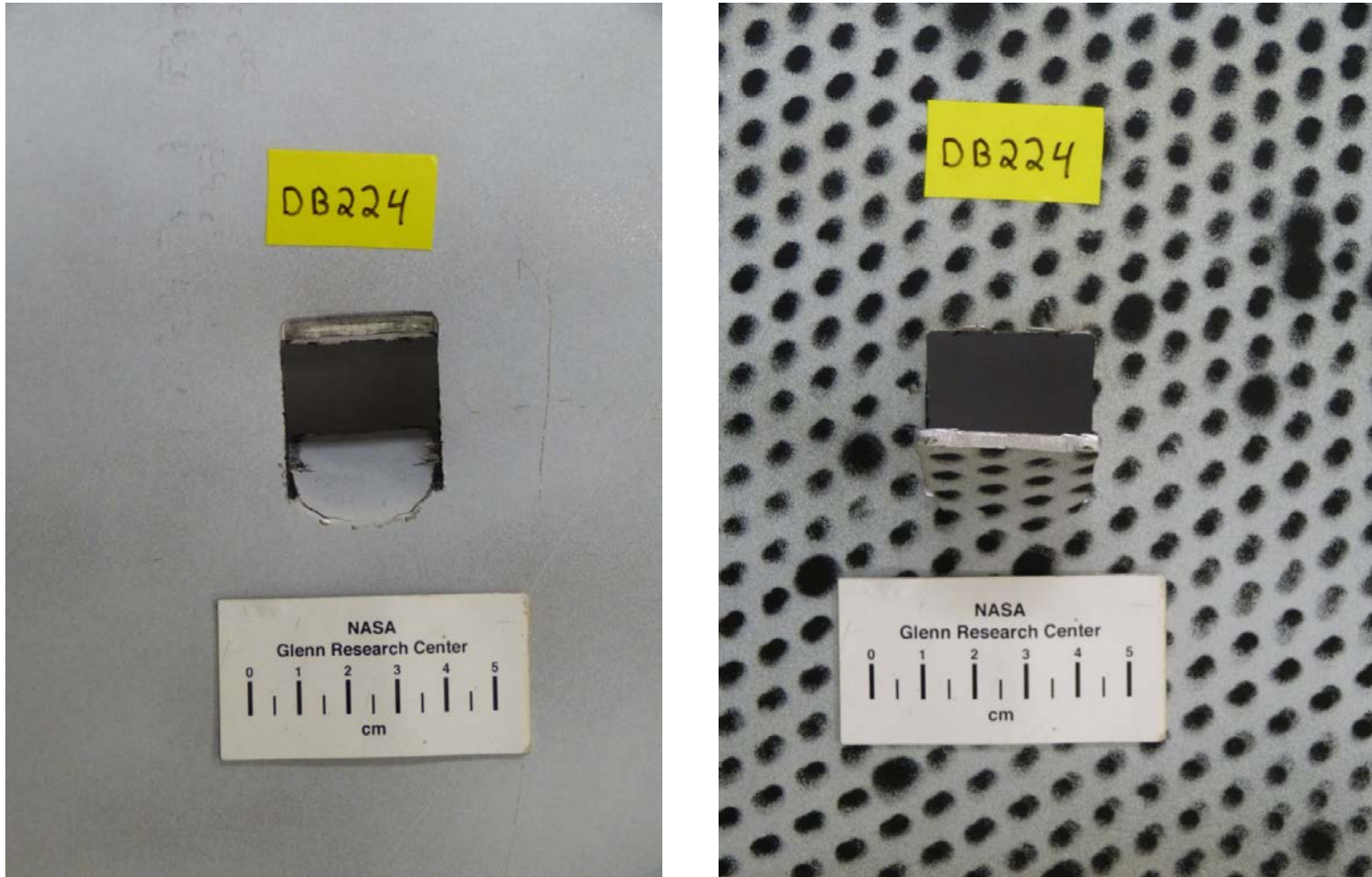


Figure A103.—Front (left) and back side views of impacted panel in test DB224.

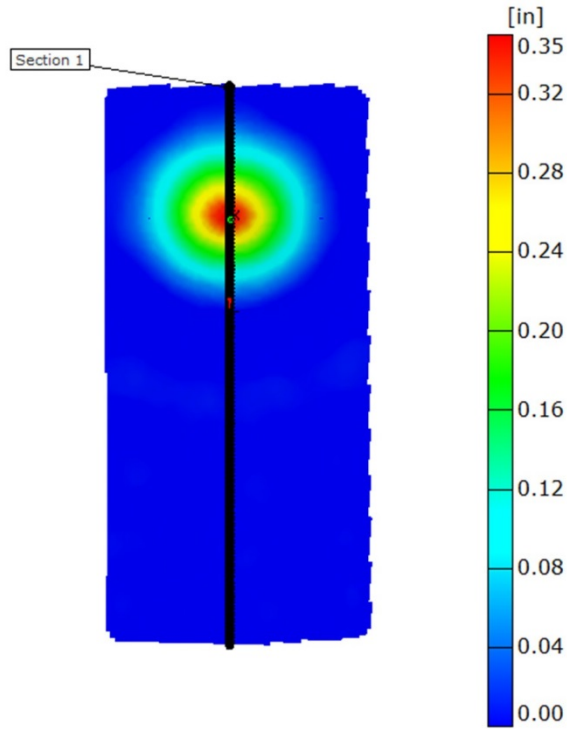


Figure A104.—Out-of-plane deformation map of panel in test DB224 at the point of maximum deflection prior to failure.

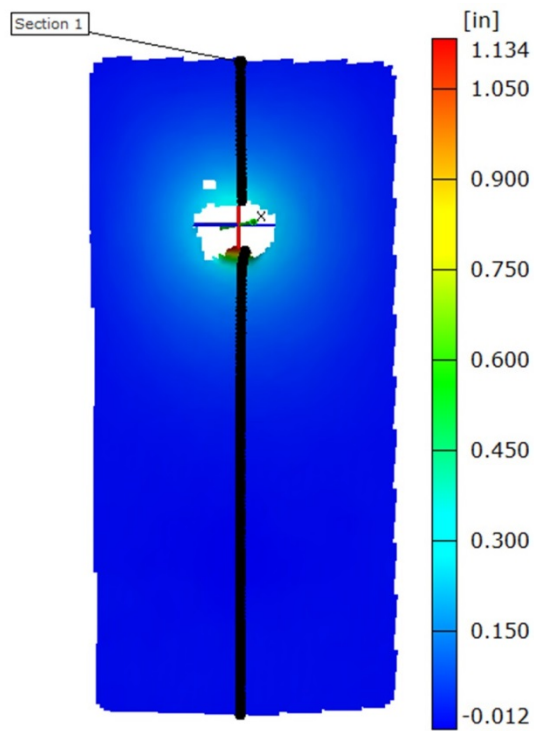


Figure A105.—Out-of-plane deformation map of panel in test DB224 after test is completed and all movement has stopped. This indicates the permanent deformation field.

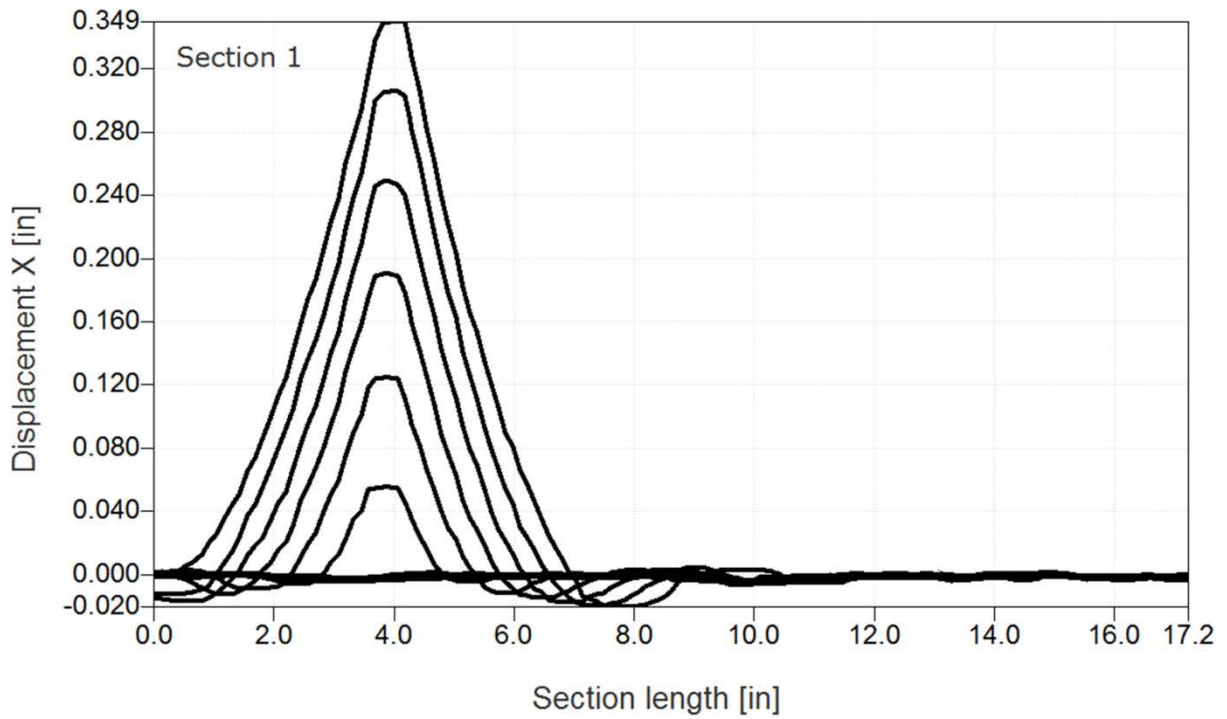


Figure A106.—Test DB224. Out-of-plane deformation along section line indicated in Figure A100 for a series of time steps up until the time of maximum deformation prior to failure (frame rate 27000 frames/sec).

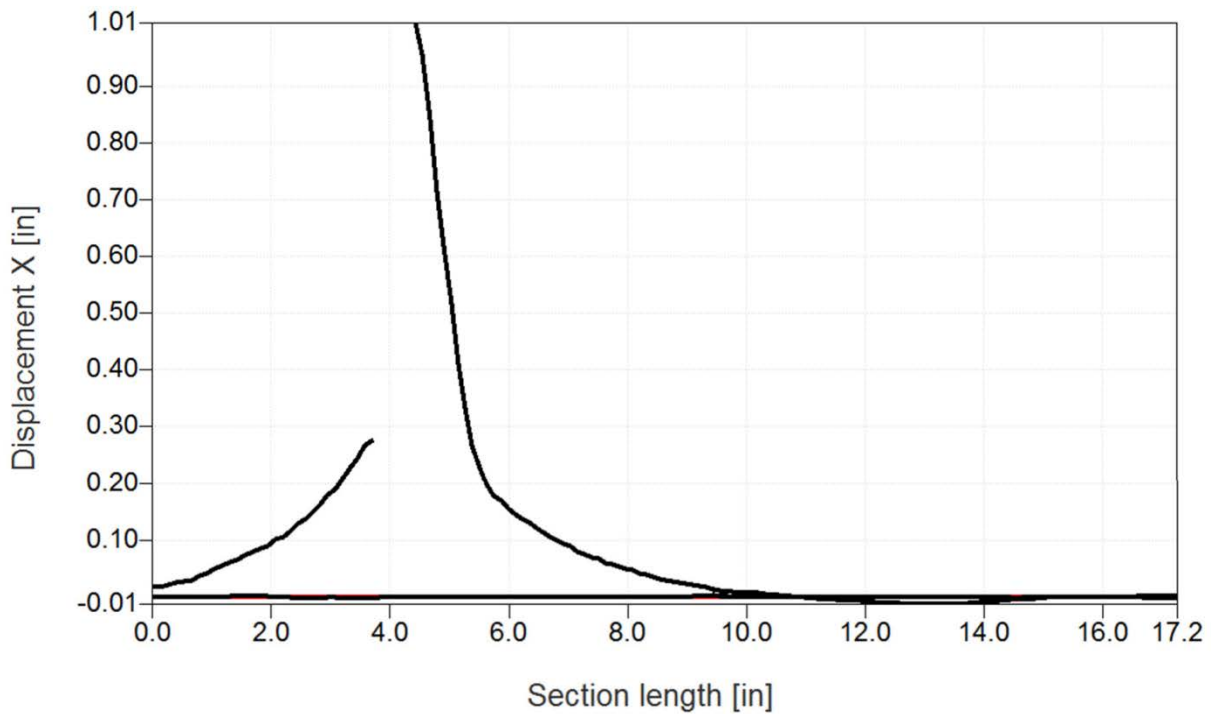


Figure A107.—Test DB224. Out-of-plane deformation along section line indicated in Figure A101. This indicates the plastic deformation along the section line after all movement has stopped.

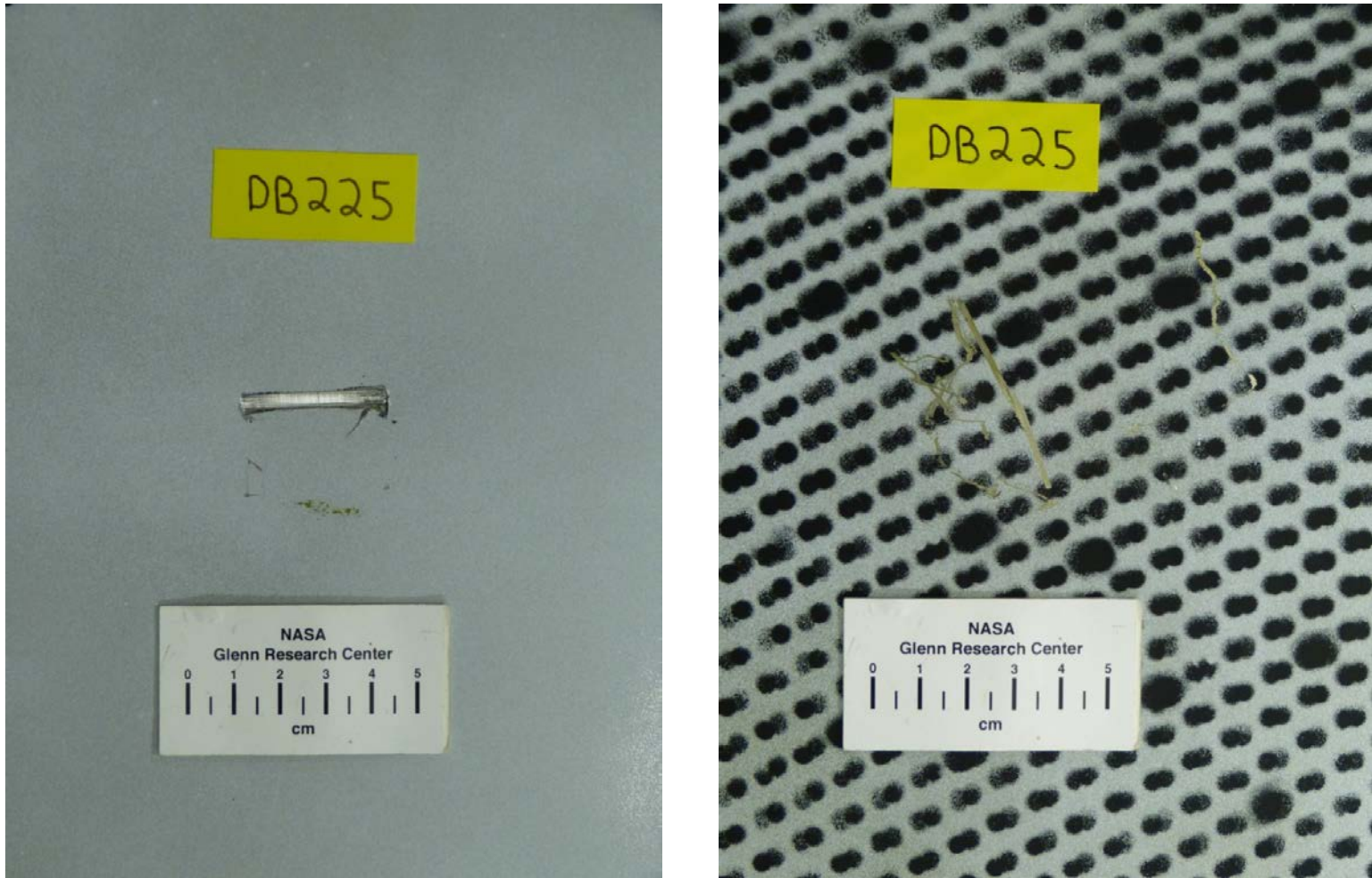


Figure A108.—Front (left) and back side views of impacted panel in test DB225.

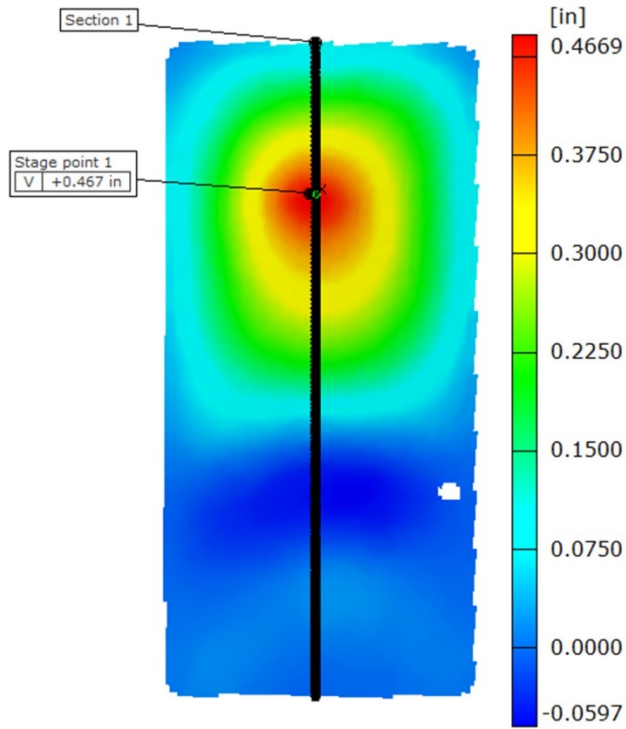


Figure A109.—Out-of-plane deformation map of panel in test DB225 at the point of maximum deflection.

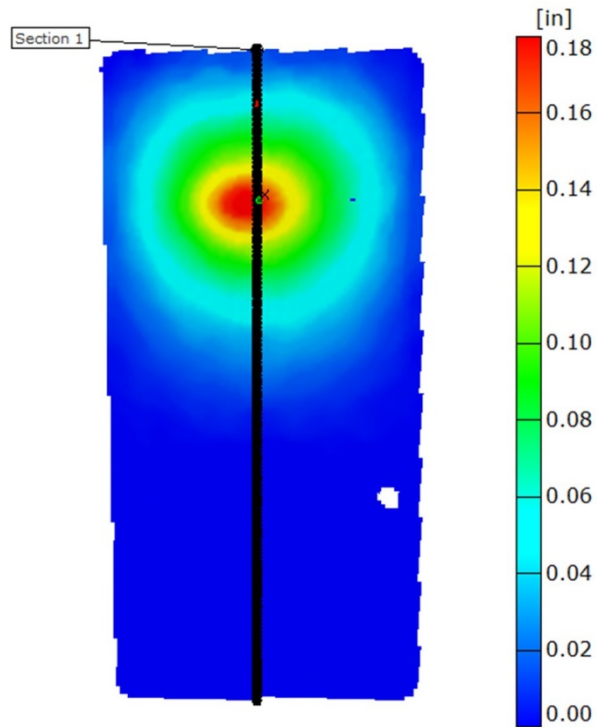


Figure A110.—Out-of-plane deformation map of panel in test DB225 after test is completed and all movement has stopped. This indicates the permanent deformation field.

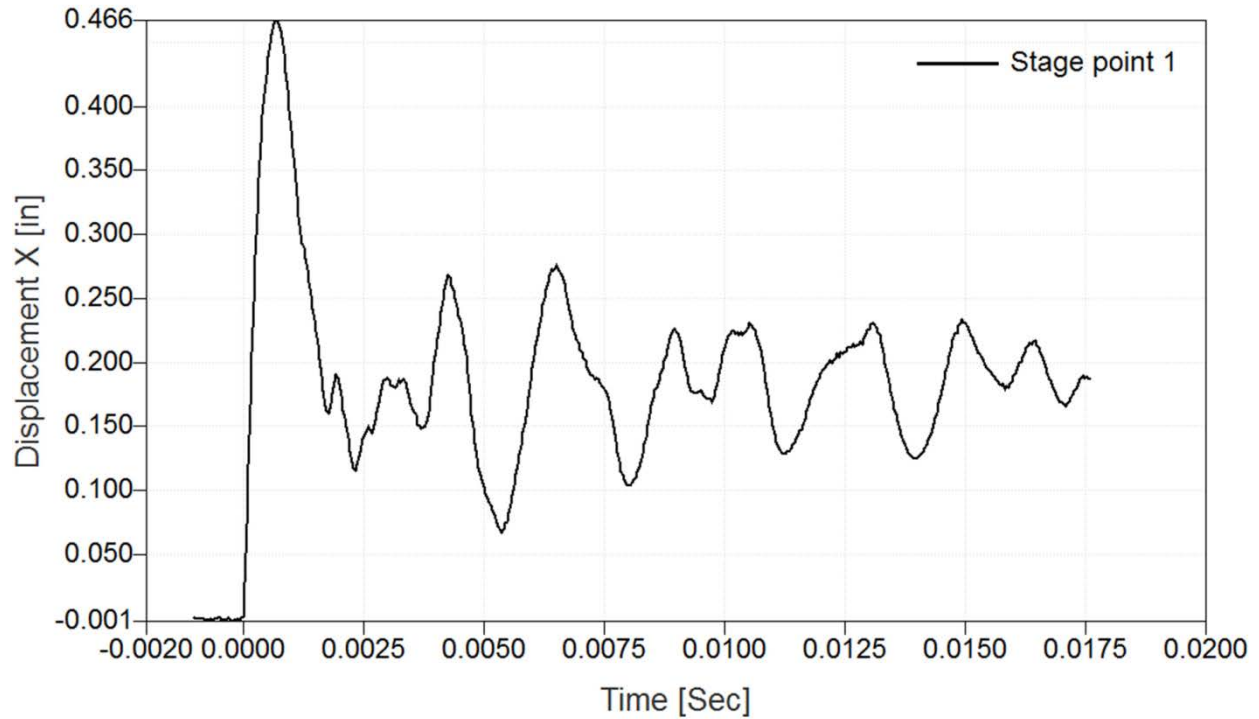


Figure A111.—Out-of-plane deformation as a function of time of point indicated in Figure A105 for test DB225.

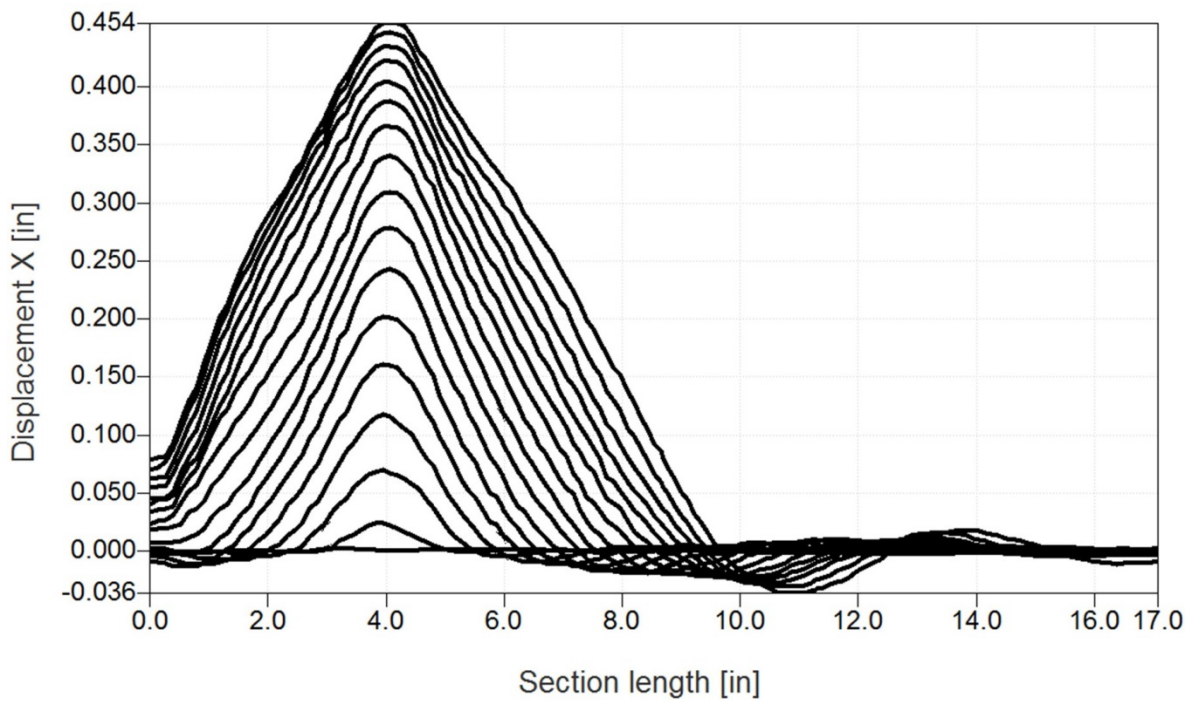


Figure A112.—Test DB225. Out-of-plane deformation along section line indicated in Figure A105 for a series of time steps up until the time of maximum deformation (frame rate 27000 frames/sec).

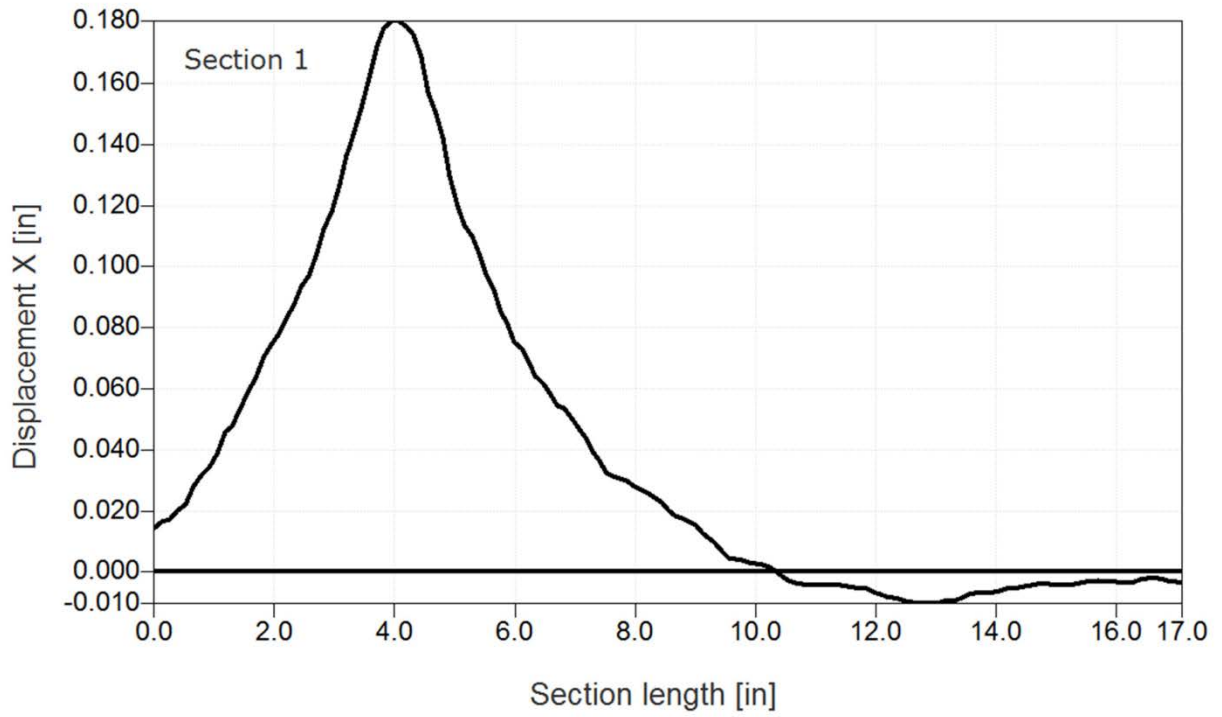


Figure A113.—Test DB225. Out-of-plane deformation along section line indicated in Figure A106. This indicates the plastic deformation along the section line after all movement has stopped.

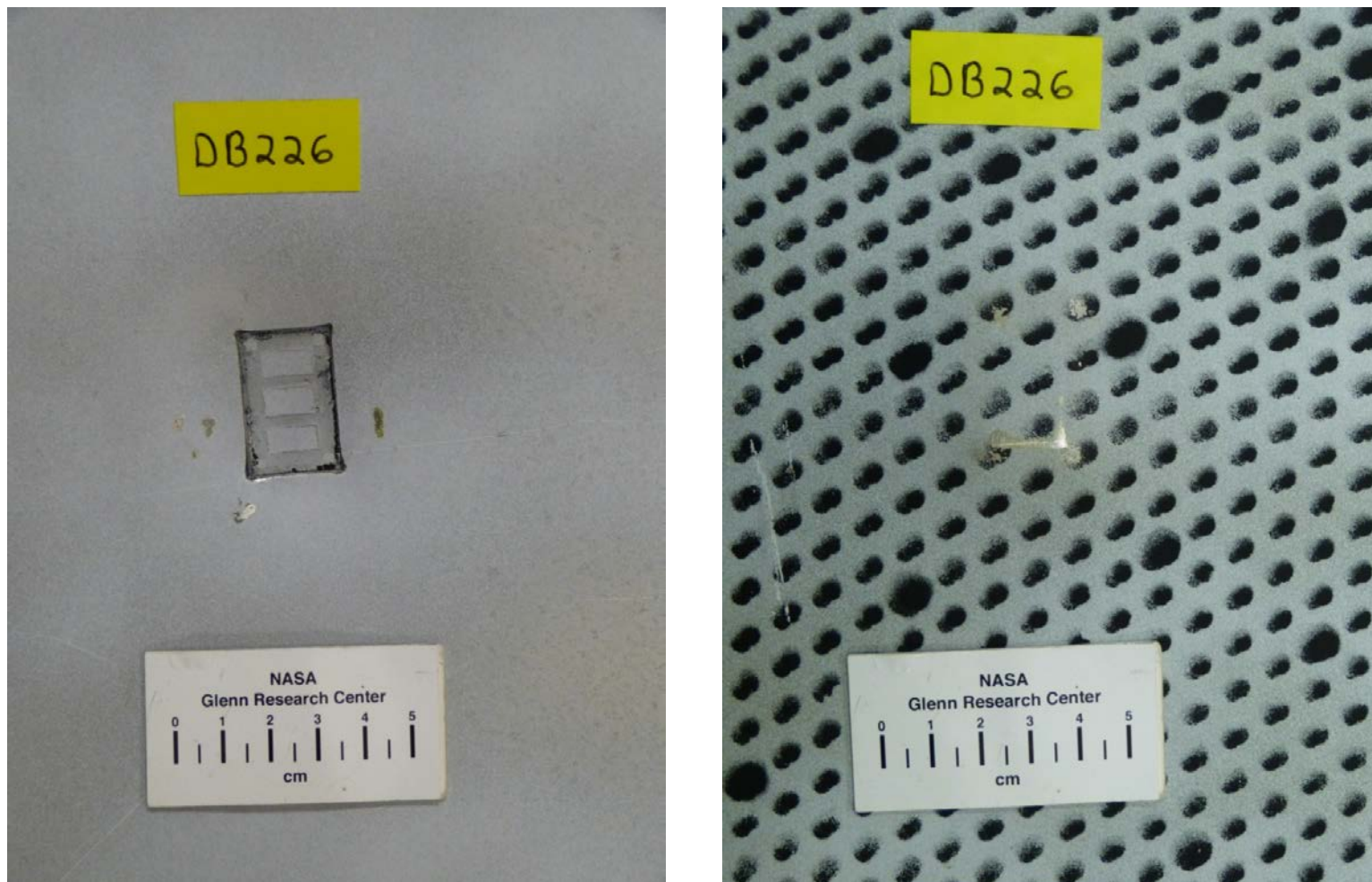


Figure A114.—Front (left) and back side views of impacted panel in test DB226.

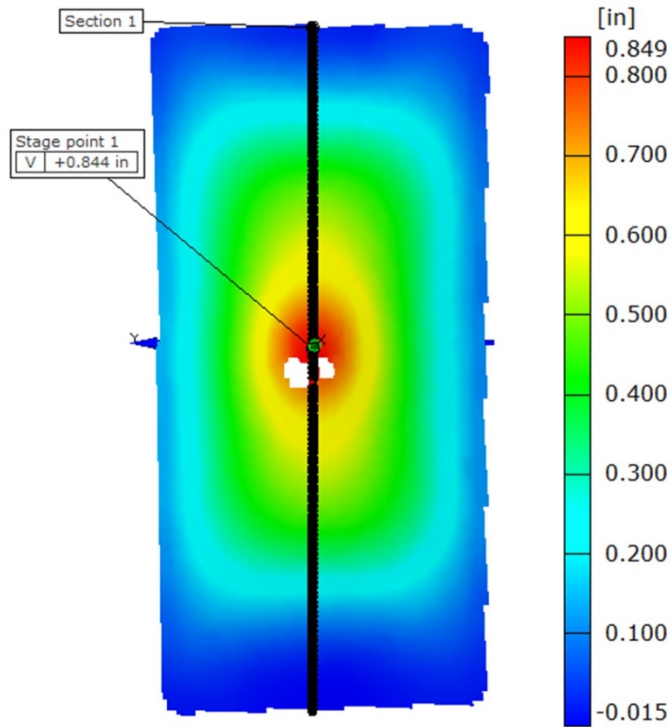


Figure A115.—Out-of-plane deformation map of panel in test DB226 at the point of maximum deflection.

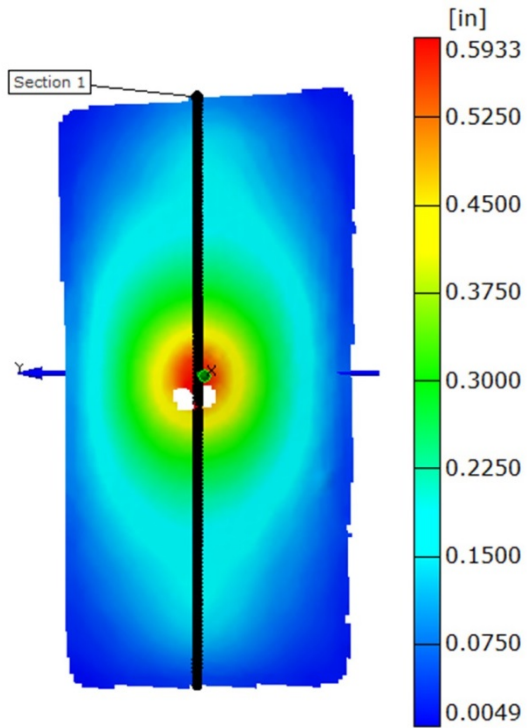


Figure A116.—Out-of-plane deformation map of panel in test DB226 after test is completed and all movement has stopped. This indicates the permanent deformation field.

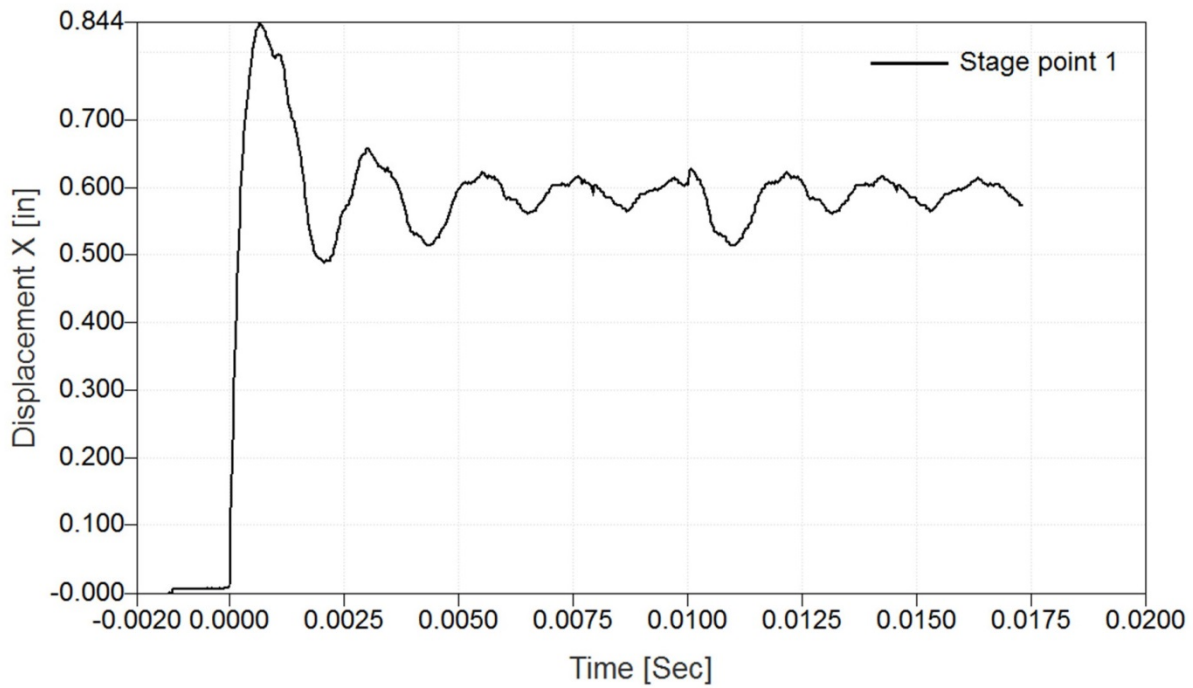


Figure A117.—Out-of-plane deformation as a function of time of point indicated in Figure A111 for test DB226.

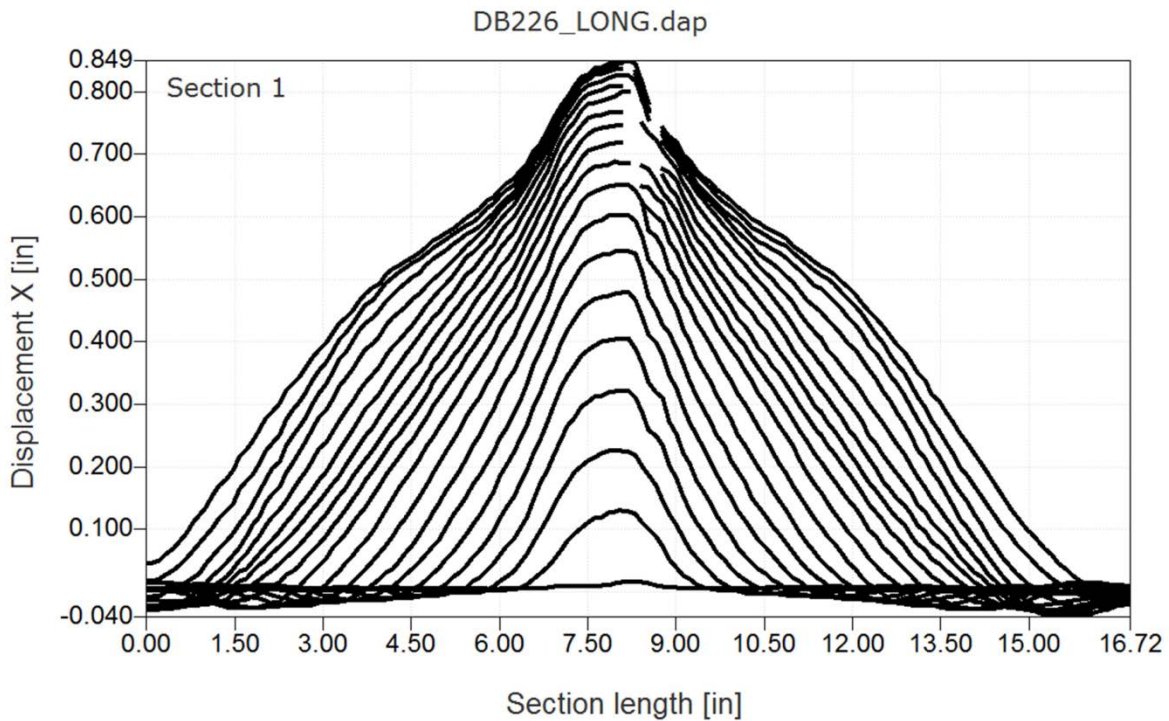


Figure A118.—Test DB226. Out-of-plane deformation along section line indicated in Figure A111 for a series of time steps up until the time of maximum deformation (frame rate 27000 frames/sec).

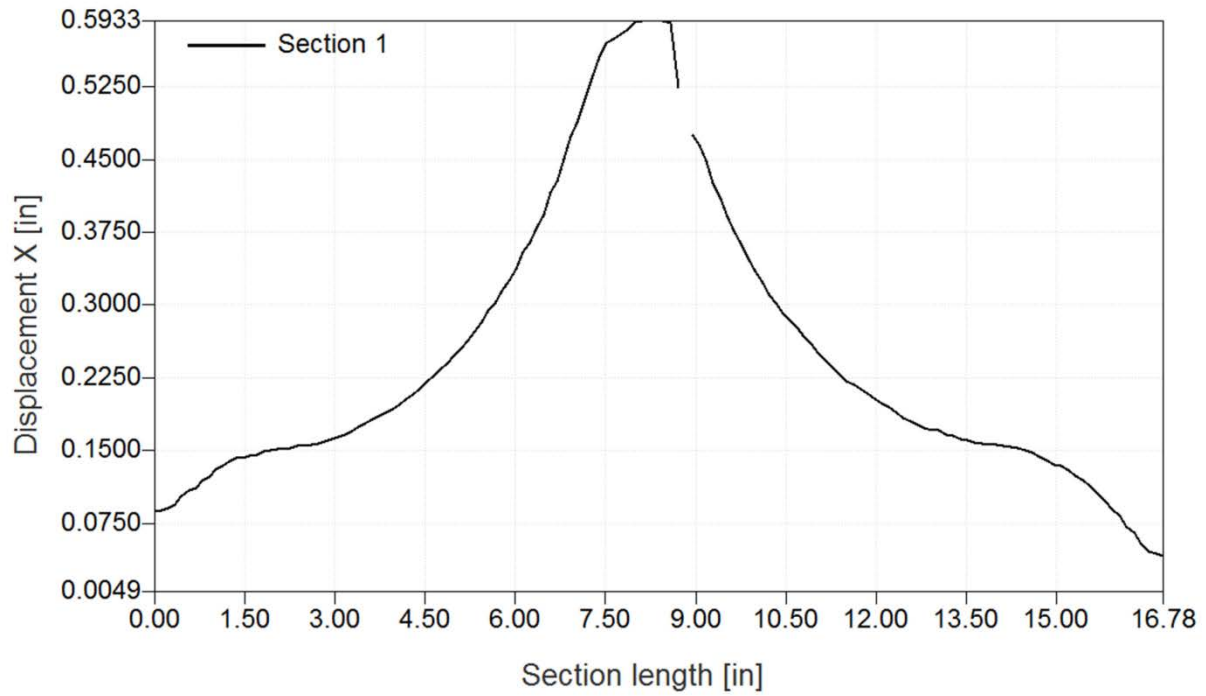


Figure A119.—Test DB226. Out-of-plane deformation along section line indicated in Figure A112. This indicates the plastic deformation along the section line after all movement has stopped.



Figure A120.—Front (left) and back side views of impacted panel in test DB227.

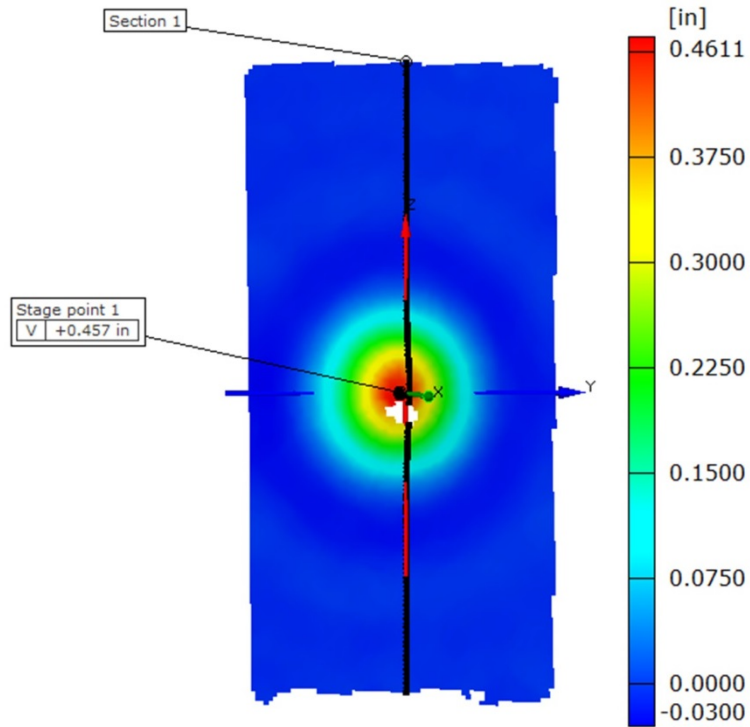


Figure A121.—Out-of-plane deformation map of panel in test DB227 at the point of maximum deflection prior to failure.

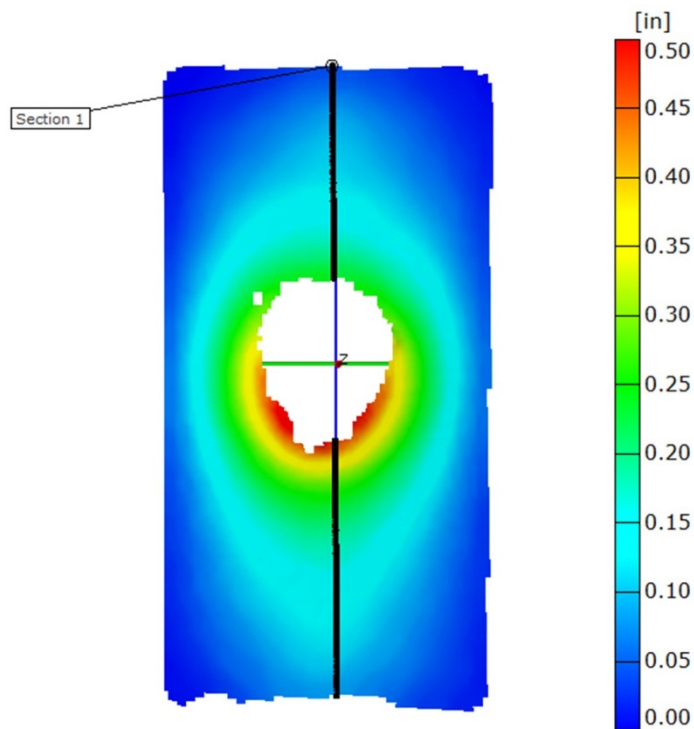


Figure A122.—Out-of-plane deformation map of panel in test DB227 after test is completed and all movement has stopped. This indicates the permanent deformation field.

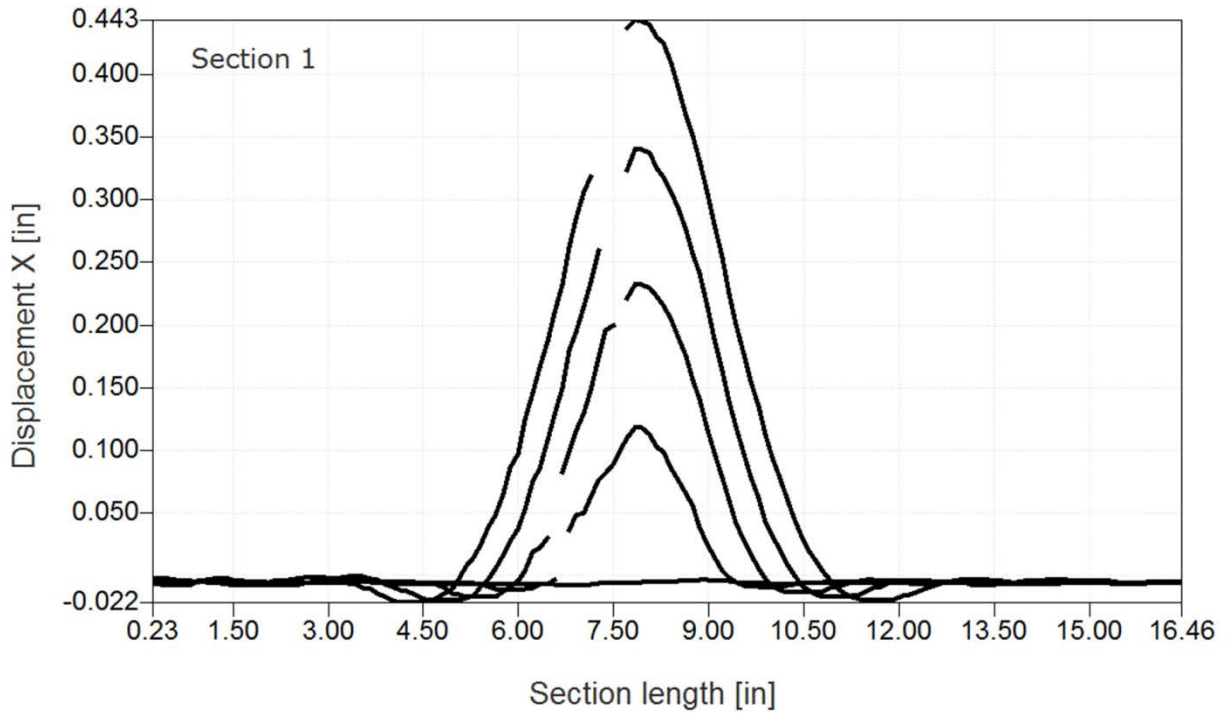


Figure A123.—Test DB227. Out-of-plane deformation along section line indicated in Figure A117 for a series of time steps up until the time of maximum deformation prior to failure (frame rate 27000 frames/sec).

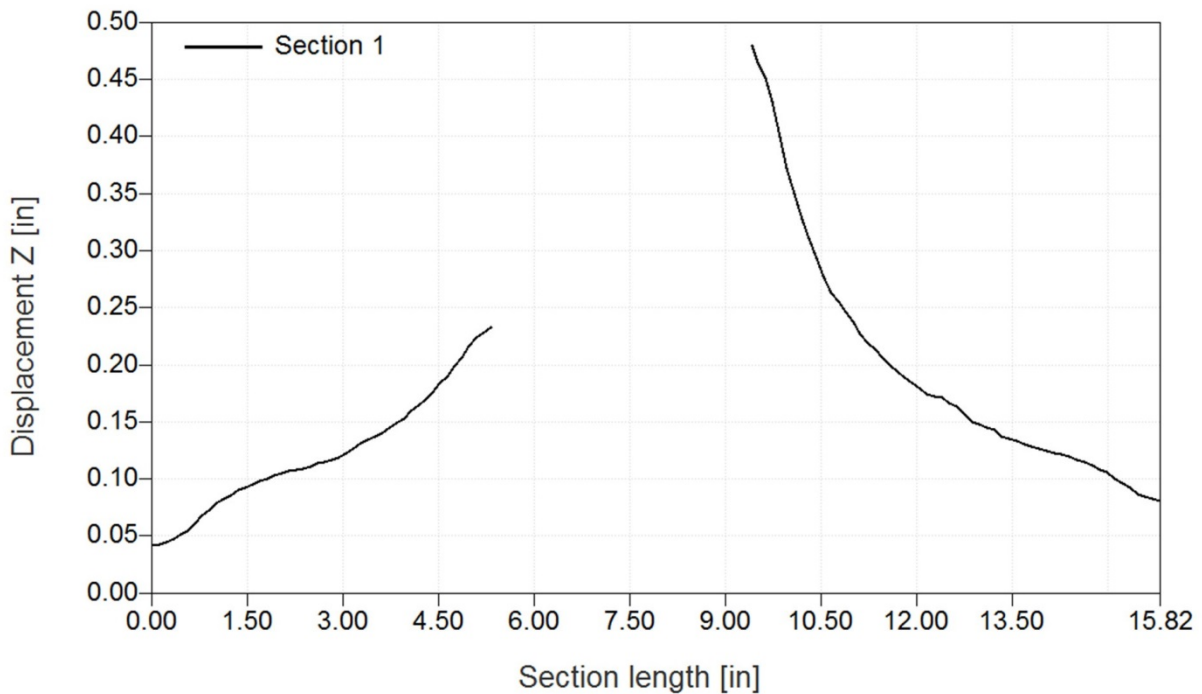


Figure A124.—Test DB227. Out-of-plane deformation along section line indicated in Figure A118. This indicates the plastic deformation along the section line after all movement has stopped.

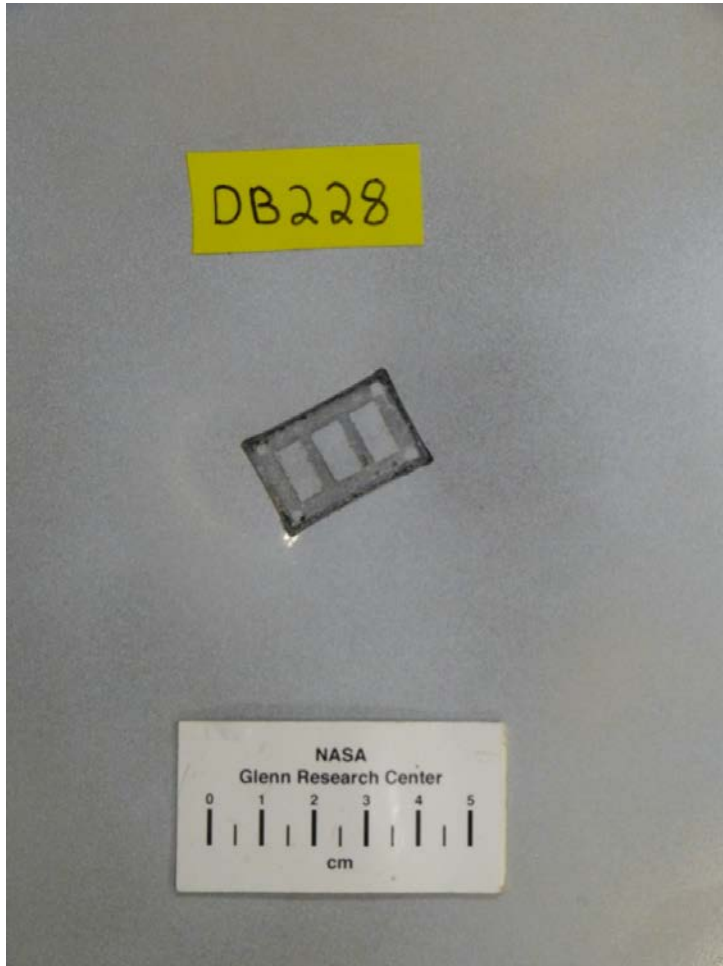


Figure A125.—Front (left) and back side views of impacted panel in test DB228.

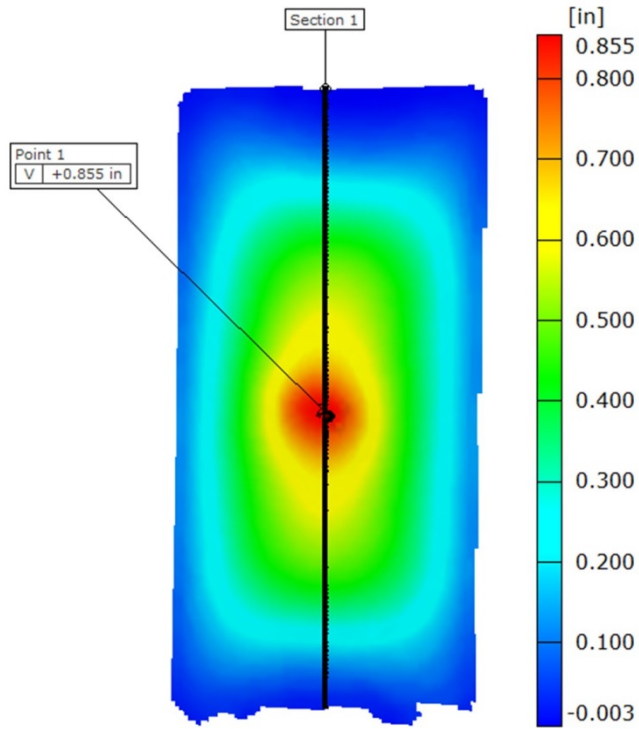


Figure A126.—Out-of-plane deformation map of panel in test DB228 at the point of maximum deflection.

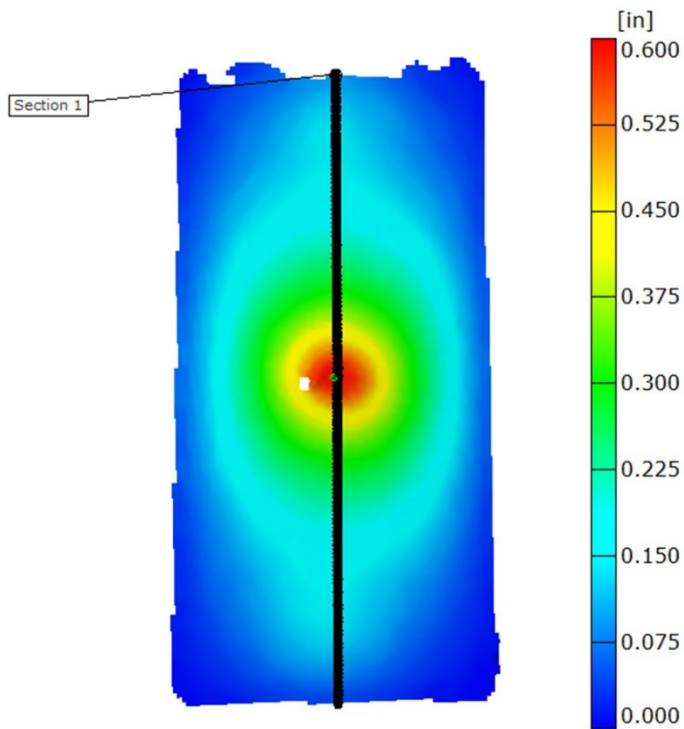


Figure A127.—Out-of-plane deformation map of panel in test DB228 after test is completed and all movement has stopped. This indicates the permanent deformation field.

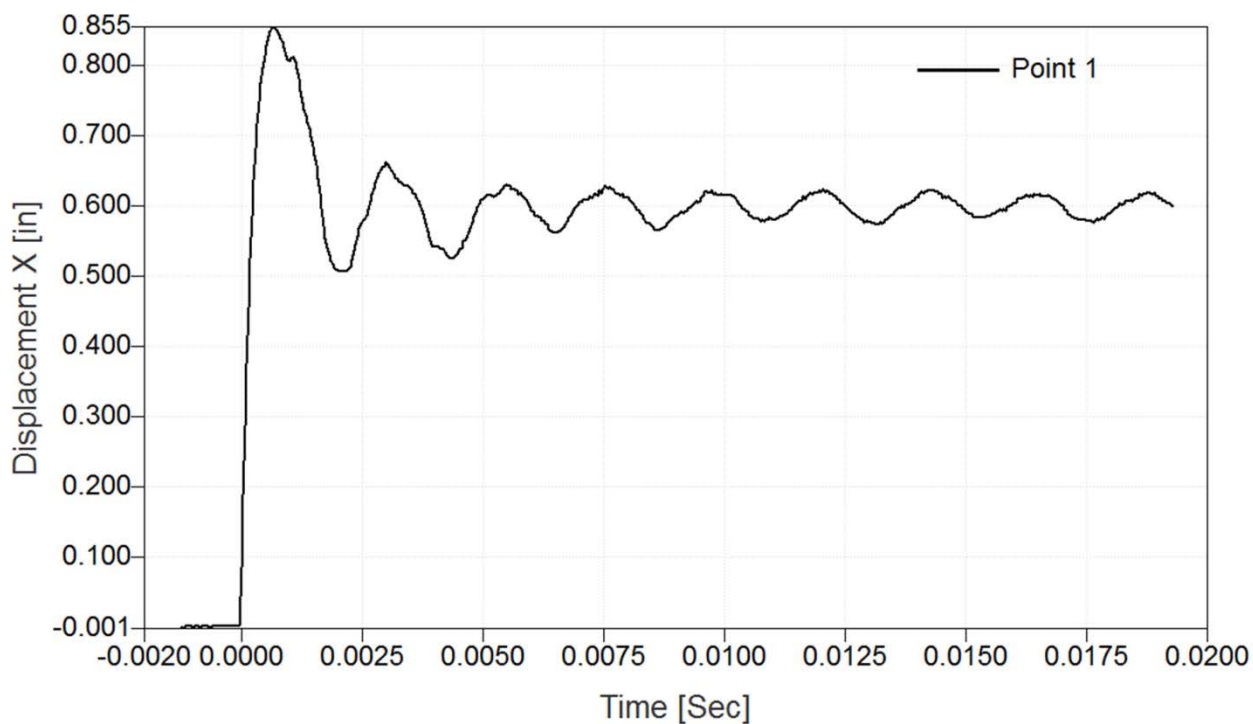


Figure A128.—Out-of-plane deformation as a function of time of point indicated in Figure A111 for test DB228.

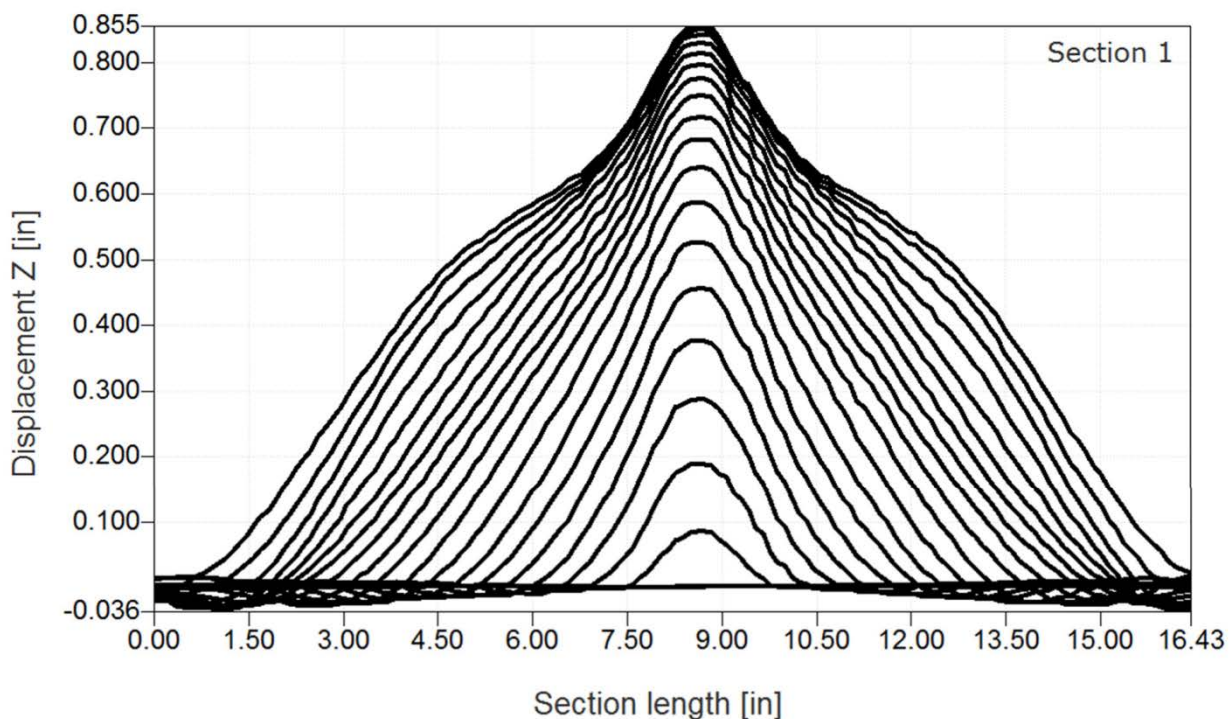


Figure A129.—Test DB228. Out-of-plane deformation along section line indicated in Figure A122 for a series of time steps up until the time of maximum deformation (frame rate 27000 frames/sec).

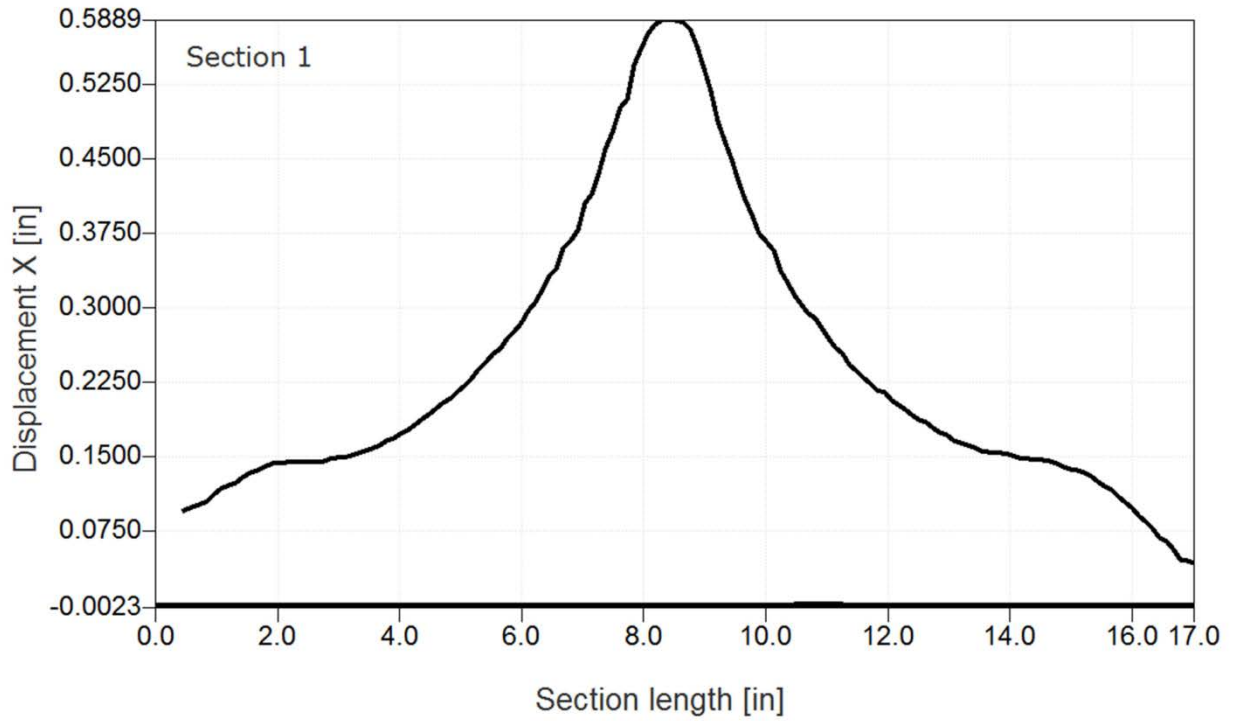


Figure A130.—Test DB228. Out-of-plane deformation along section line indicated in Figure A123. This indicates the plastic deformation along the section line after all movement has stopped.

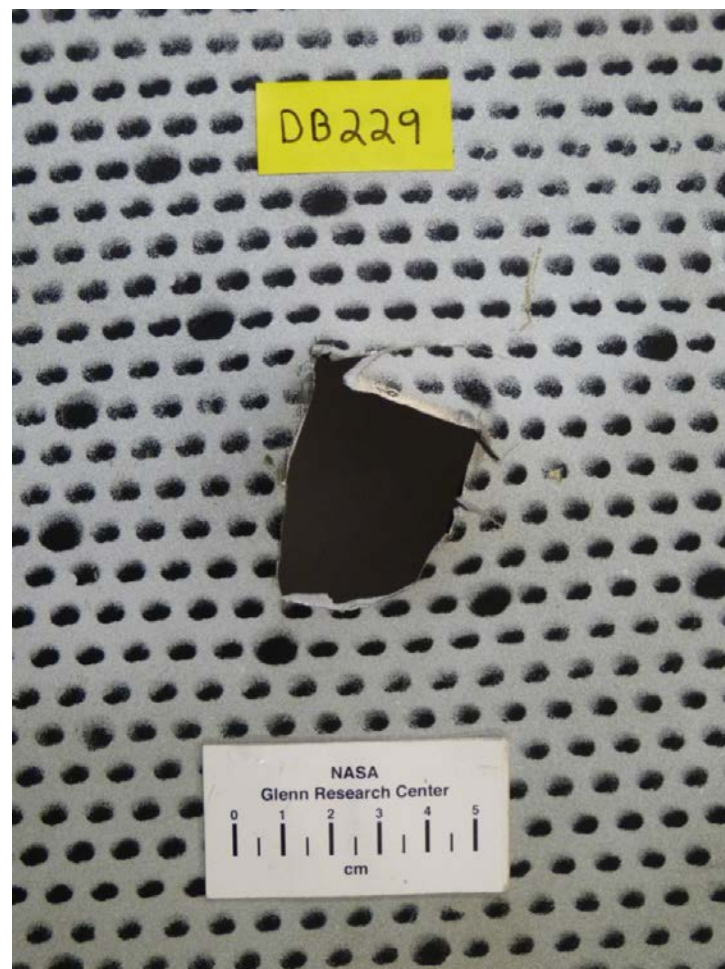
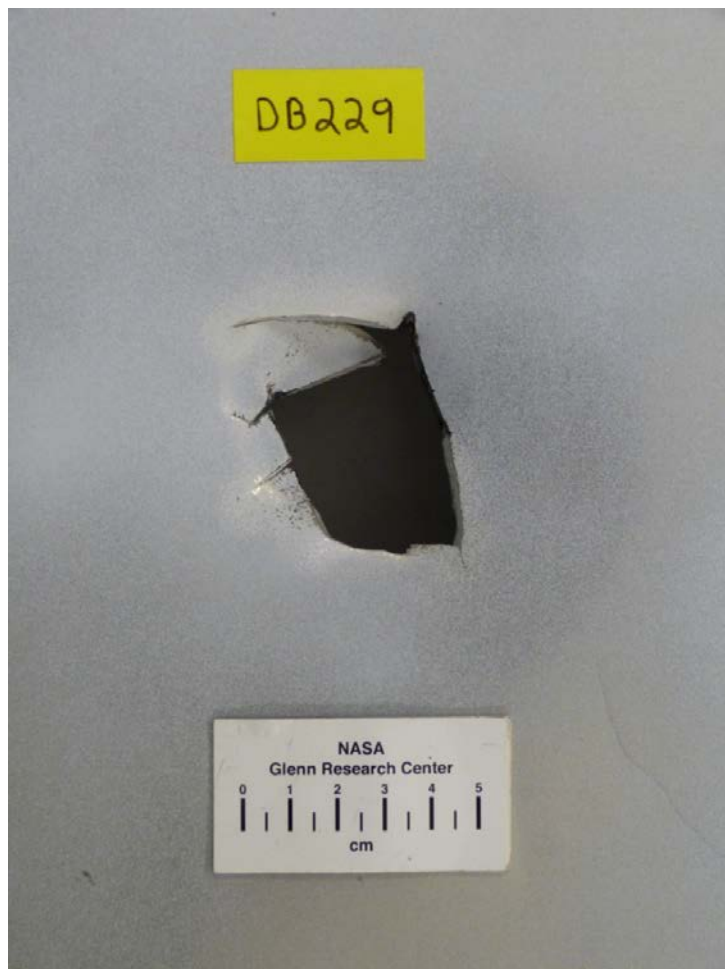


Figure A131.—Front (left) and back side views of impacted panel in test DB229.

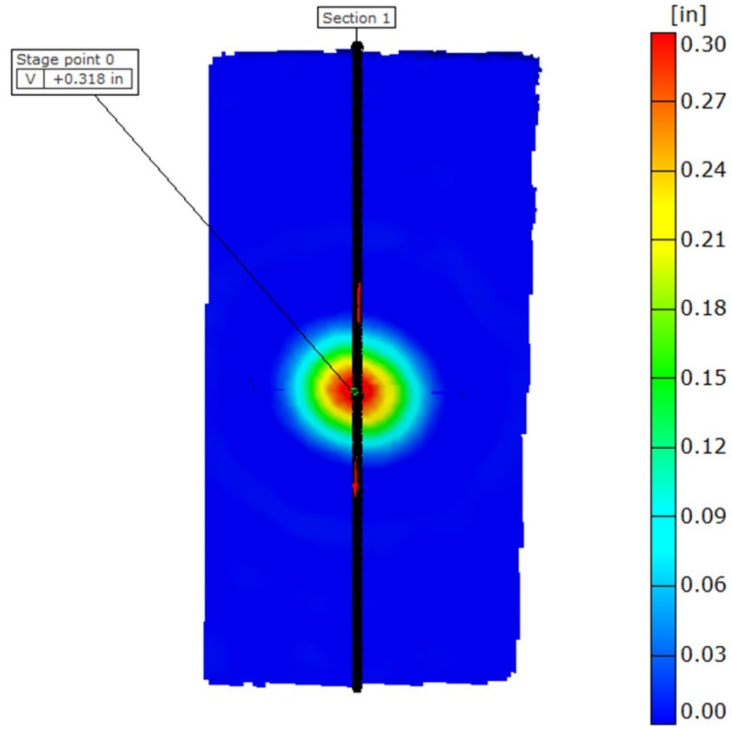


Figure A132.—Out-of-plane deformation map of panel in test DB229 at the point of maximum deflection prior to failure.

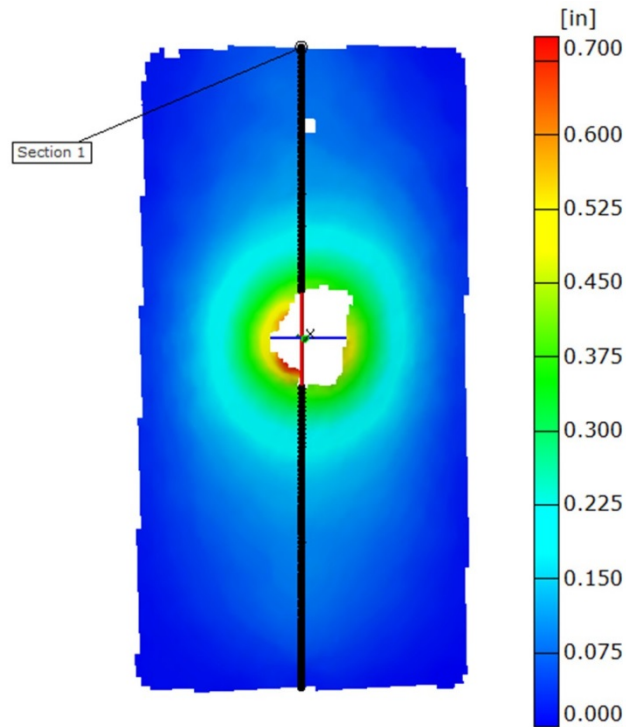


Figure A133.—Out-of-plane deformation map of panel in test DB229 after test is completed and all movement has stopped. This indicates the permanent deformation field.

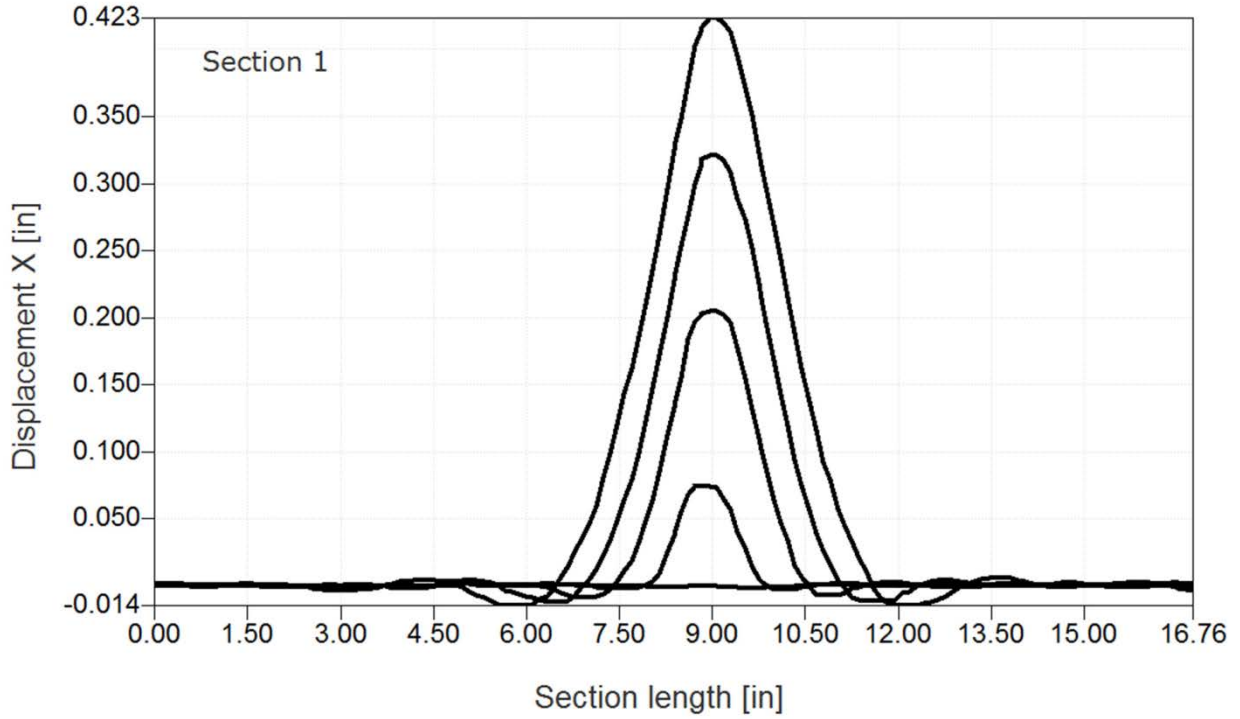


Figure A134.—Test DB229. Out-of-plane deformation along section line indicated in Figure A128 for a series of time steps up until the time of maximum deformation prior to failure (frame rate 27000 frames/sec).

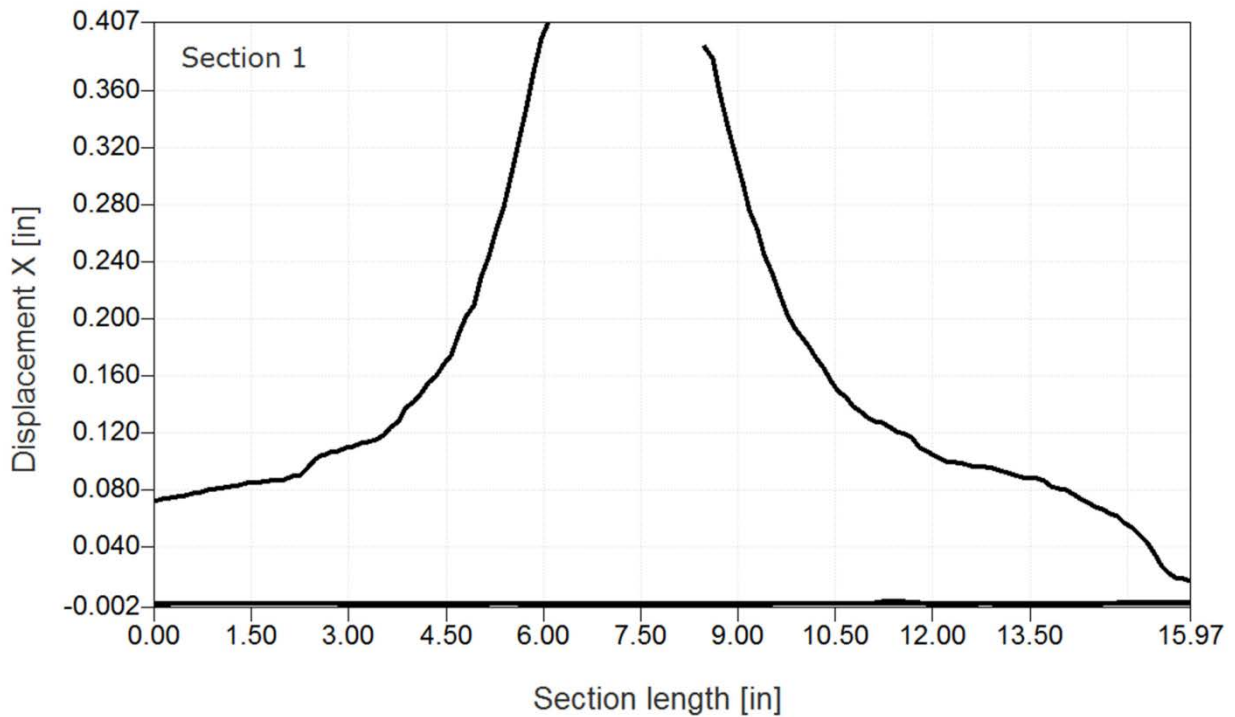


Figure A135.—Test DB229. Out-of-plane deformation along section line indicated in Figure A129. This indicates the plastic deformation along the section line after all movement has stopped.

References

1. Buyuk, M., “Development of a New Metal Material Model in LS-DYNA. Part 2: Development of A Tabulated Thermo-Viscoplastic Material Model with Regularized Failure for Dynamic Ductile Failure Prediction of Structures under Impact Loading,” DOT/FAA/TC-13/25, P2, (Date needed).
2. Seidt, J.D., “Plastic Deformation and Ductile Fracture of 2024-T351 Aluminum under Various Loading Condition,” Dissertation, The Ohio State University, 2010.
3. Pereira, J.M., Revilock, D.M., Lerch, B.A. and Ruggeri, C.R., “Impact Testing of Aluminum 2024 and Titanium 6Al-4V for Material Model Development,” NASA/TM—2013-217869 (DOT/FAA/TC-12/58), May, 2013.

